

UNCLASSIFIED

AD NUMBER	
ADC029546	
CLASSIFICATION CHANGES	
TO:	unclassified
FROM:	confidential
LIMITATION CHANGES	
TO:	Approved for public release, distribution unlimited
FROM:	Distribution: Further dissemination only as directed by Director, Long Range Acoustics Propagation Project, NSTL Station, MI 39529, MAR 1980, or higher DoD authority.
AUTHORITY	
ONR ltr, 15 Jun 2006; ONR ltr, 15 Jun 2006	

THIS PAGE IS UNCLASSIFIED

**CONFIDENTIAL**

**NORDA Report 23**  
**March 1980**

OCEAN ACOUSTICS DIVISION  
OCEAN SCIENCE AND TECHNOLOGY LABORATORY

**Sound Speed Structure of the Northeast Atlantic  
Ocean in Summer 1973 During the SQUARE DEAL  
Exercise (U)**

*Prepared for Long Range Acoustics Propagation Project*

**Don F. Fenner**



DTIC  
ELECTE  
OCT 18 1982  
A

...tion only as directed by

approval of the Director, Long Range Acoustics  
Propagation Project, NSTL Station, Mississippi 39529

Classified by: OPNAVINST 5513.5 ENCL. 42  
Review on 31 January 1999

**NAVAL OCEAN RESEARCH AND DEVELOPMENT ACTIVITY**  
**NSTL Station, Mississippi 39529**

**UNCLASSIFIED SECURITY INFORMATION**  
Unauthorized Disclosure Subject to Criminal  
Penalties

82 10 18 802  
**CONFIDENTIAL**

AD C029546

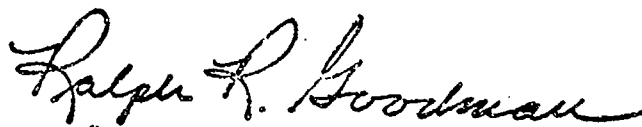
FILE COPY

CONFIDENTIAL

## Foreword (U)

---

(U) The SQUARE DEAL Exercise was a program of acoustic and environmental measurements conducted in the northeast Atlantic Ocean between July and September 1973. The exercise was sponsored by the Long Range Acoustic Propagation Project (LRAPP), and included participation of several U.S. Navy Laboratories, the United Kingdom Admiralty Research Laboratory, and several private contractors. Personnel from the Naval Ocean Research and Development Activity (NORDA), then of the Naval Oceanographic Office (NAVOCEANO), managed the environmental data collection program, participated in the exercise, and analyzed most resulting environmental data. This report summarizes environmental findings from SQUARE DEAL and represents a major contribution to the exercise. Much of the information contained herein has appeared in the SQUARE DEAL Synopsis and Environmental Acoustics Summary Reports, previously published in 1974 and 1975 by the Maury Center for Ocean Science.



Ralph R. Goodman  
Technical Director  
NORDA

CONFIDENTIAL

CONFIDENTIAL

## Executive Summary (U)

---

(U) This report contains an interpretation of oceanographic (sound velocity, temperature, and salinity), meteorological, and bathymetric data collected during summer 1973 in the northeast Atlantic Ocean as part of the SQUARE DEAL Exercise.

### Environmental Findings

(U) The total exercise sound velocity data base was extremely well-distributed (both temporally and spatially), and was more than adequate to describe environmental effects on acoustic propagation.

(U) Sound velocity structures were extremely complex and variable throughout most of the exercise area owing to internal waves and mixing between intrusions of Mediterranean Intermediate Water, Labrador Sea Water, and Norwegian Sea Overflow Water.

(U) The interplay of various water masses created a bichannel sound velocity profile in the eastern half of the exercise area (east of 20°-25°W), where the upper and deep sound channels were separated by an intermediate-depth sound velocity maximum.

(U) The greatest spatial sound velocity variability was found across the crest of the Faeroe-Iceland Ridge associated with intrusions of Norwegian Sea Overflow Water.

(U) Significant temporal sound velocity variability was found at all exercise acoustic receiver sites associated with internal waves and mixing of intrusive water masses.

### Acoustic Implications

(C) The sonic layer was too shallow for effective low frequency propagation throughout the exercise area.

(C) The upper channel apparently acted as a reliable acoustic path in most of the eastern half of the exercise area (east of 20°-25°W), including the shallow regions over the Rockall Plateau, Porcupine Bank, and the northern Rockall Trough.

(C) The deep sound channel apparently was the most effective sound propagation path throughout most of the exercise area, and was uninterrupted in most of the West European Basin, southern Rockall Trough, and Maury Trough.

(C) Depth excess was adequate for convergence zone propagation from a near-surface source throughout most of the West European Basin and the Maury Trough.

(C) Throughout the exercise, the Acoustic Data Capsule (ACODAC) receiver sites were separated by zones of intensive oceanographic mixing that should have degraded all modes of sound propagation along the three major exercise baselines.

(C) Internal waves and mixing (interleaving) could be partially responsible for the diurnal and semidiurnal periods observed in the spectral ambient noise intensities at several acoustic receiver sites.

(C) Two major storms led to increased ambient noise intensities at ACODAC 1C and Western Electric Company (WECO) Survey Array 1A (phase I), and at ACODAC 1C (end of phase III).

CONFIDENTIAL

**CONFIDENTIAL**

## Preface (U)

(U) This report was originally written during the summer of 1974 while the author was a member of the Undersea Surveillance Oceanographic Center (USOC) of NAVOCEANO. At that time the term "sound velocity" was still in widespread use rather than the presently accepted term "sound speed." Rather than redraft the numerous figures of this report, the term "sound velocity" has been retained throughout, in the figures, the tables, and the text. Only in the title does the term "sound speed" appear.

(U) At the time this report was originally prepared, kilometers were not widely used to measure range in the Navy community. Therefore, all range-dependent figures were prepared and drafted using nautical miles rather than kilometers. Ranges cited in the text also are reported only in nautical miles.

(U) Similarly, throughout the text and in all the figures, wind speed is reported in knots (rather than meters per second), and sea/swell heights are reported in feet (rather than meters).

## Acknowledgements (U)

(U) The author acknowledges the excellent performance of all field personnel involved in the collection of environmental data, and gives special acknowledgement to the NAVOCEANO SQUARE DEAL Coordinator, Benjamin A. Watrous. Without his perseverance throughout all phases of the exercise, the environmental data used in this report would not have been collected.

(U) Grateful thanks are extended to the many members of NORDA involved in the preparation of this report. William C. Lippert and William J. Cronin (presently with NAVOCEANO) made valuable contributions to the report, including reduction of most environmental data and preparation of many analytical figures. Reuben J. Busch provided the bathymetric profiles and depth difference/depth excess chart used herein. All illustrations were prepared by Joanne V. Lackie, and the original manuscript was typed by Judith A. Albright. The section on meteorology was prepared largely by George L. Hansen of NAVOCEANO.

[illegible]

**COPIES DESTROYED**

# CONFIDENTIAL

## Contents (U)

LIST OF ILLUSTRATIONS (U)	iv	E. Deep Sound Channel (DSC) Axis (U)	38
LIST OF TABLES (U)	vi	F. Critical Depth (U)	42
I. INTRODUCTION (U)	1	G. Depth Difference/Depth Excess (U)	42
II. DISCUSSION OF ENVIRONMENTAL DATA (U)	1	VI. SPATIAL VARIABILITY IN SOUND VELOCITY ALONG SQUARE DEAL BASELINES (U)	47
A. Data Availability (U)	1	A. Point 1E to Point 3B Track (Phase I) (U)	47
B. Treatment of Data (U)	2	B. Point 2L to Point 2K Track (Phase II) (U)	47
C. Data Accuracy (U)	2	C. Point 2BB to Point 3AB Track (Phase II) (U)	50
III. GENERAL OCEANOGRAPHY OF THE SQUARE DEAL AREA (U)	9	D. Point 3F to Point 3ZZ Track (Phase III) (U)	50
A. Generalized Circulation and Water Masses (U)	9	E. Summary of Spatial Sound Velocity Variability Along the Three Major SQUARE DEAL Baselines (U)	54
B. Temperature-Salinity (T-S) Relations Along the SQUARE DEAL Baselines (U)	12	VII. METEOROLOGY (U)	56
C. Temperature at 10 m Depth (U)	12	A. Phase I (25 Jul-10 Aug) (U)	56
IV. TEMPORAL VARIABILITY (U)	15	B. Phase II (15-27 Aug) (U)	59
A. Long-Term Variability Throughout the Exercise Area (U)	15	C. Phase III (2-16 Sep) (U)	59
B. Time-Series Studies (U)	15	VIII. SUMMARY (U)	64
C. Summary of SQUARE DEAL Temporal Variability (U)	24	IX. REFERENCES (U)	69
V. SPATIAL VARIABILITY OF SELECTED SOUND VELOCITY PARAMETERS (U)	24	APPENDICES (U)	
A. Sonic Layer Depth (U)	24	APPENDIX A: Temperature-Salinity-Sound Velocity Relations at Selected SQUARE DEAL Reference Points (U)	71
B. Upper Sound Channel (USC) Axis (U)	27	APPENDIX B: Data Identification Tables (U)	87
C. Intermediate Sound Velocity Maximum (U)	31	APPENDIX C: Glossary (U)	99
D. "Strength" of Upper Sound Channel (U)	31		

# CONFIDENTIAL

## Illustrations (U)

Figure 1. Location of All Oceanographic Observations (U)	4	Figure 13. Time-Series Plot of Sound Velocity at Point 2C During Phase II (U)	18
Figure 2. Location of Oceanographic Observations Extending to Within 100 m of the Bottom (U)	5	Figure 14. Time-Series Plot of Sound Velocity at Point 2D During Phase II (U)	19
Figure 3. Location of Oceanographic Observations Deeper than 1000 m (U).	6	Figure 15. Time-Series Plot of Sound Velocity at Point 2FA During Phase II (U)	20
Figure 4. Location of Oceanographic Observations Deeper than 400 m but Shallower than 1000 m (U)	7	Figure 16. Time-Series Plot of Sound Velocity at Point 3Z During Phase III (U)	21
Figure 5. Location of Oceanographic Observations Deeper than 100 m but Shallower than 400 m (U)	8	Figure 17. Time-Series Plot of Sound Velocity at Point 3ZZ During Phase III (U)	22
Figure 6. General Circulation Diagram and Location of Selected SQUARE DEAL Reference Points (U)	10	Figure 18. Time-Series Plot of Sound Velocity West of Porcupine Bank During Phase I (U)	23
Figure 7. Generalized Northeast Atlantic T-S Diagram (U)	11	Figure 19. Time-Series Plot of Sound Velocity West of Porcupine Bank During Phase II (U)	23
Figure 8. T-S Diagram Composites Along the Three Major SQUARE DEAL Baselines (U)	13	Figure 20. Regions With Similar Average Sonic Layer Depth (U)	25
Figure 9. Average Temperature at 10 m Depth (U)	14	Figure 21. Persistence of Sonic Layer (U)	26
Figure 10. Standard Deviation in Average Temperature at 10 m Depth (U)	16	Figure 22. Average Depth of Upper Sound Channel Axis (U)	28
Figure 11. Temporal Variability at Selected Reference Points (U)	17	Figure 23. Standard Deviation in Average Depth of Upper Sound Channel Axis (U)	29
Figure 12. Time-Series Plot of Sound Velocity at Point 1C During Phase I (U)	18	Figure 24. Average Sound Velocity at Upper Sound Channel Axis (U)	30
		Figure 25. Standard Deviation in Average Sound Velocity at Upper Sound Channel Axis (U)	32

# CONFIDENTIAL

Figure 26. Average Depth of Intermediate Maximum (U)	33	Figure 42. Sound Velocity Variability Along the Three Major SQUARE DEAL Baselines (U)	55
Figure 27. Standard Deviation in Average Depth of Intermediate Maximum (U)	34	Figure 43. Major Storm Tracks During Phase I (25 Jul-10 Aug) (U)	57
Figure 28. Average Sound Velocity at Intermediate Maximum (U)	35	Figure 44. Meteorological Conditions Near Phase I ACODAC Sites (U)	58
Figure 29. Standard Deviation in Average Sound Velocity at Intermediate Maximum (U)	36	Figure 45. Major Storm Tracks During Phase II (15-27 Aug) (U)	60
Figure 30. "Strength" of Upper Sound Channel (U)	37	Figure 46. Meteorological Conditions Near Phase II ACODAC Sites (U)	61
Figure 31. Average Depth of Deep Sound Channel Axis (U)	39	Figure 47. Major Storm Tracks During Phase III (2-16 Sep) (U)	62
Figure 32. Standard Deviation in Average Depth to Deep Sound Channel Axis (U)	40	Figure 48. Meteorological Conditions Near Phase III ACODAC Sites (U)	63
Figure 33. Average Sound Velocity at Deep Sound Channel Axis (U)	41	Figure 49. Temperature-Salinity-Sound Velocity Profiles and T-S Diagram at Point 1C (U)	72
Figure 34. Standard Deviation in Average Sound Velocity at Deep Sound Channel Axis (U)	43	Figure 50. Temperature-Salinity-Sound Velocity Profiles and T-S Diagram at Point 1E (U)	73
Figure 35. Average Critical Depth (U)	44	Figure 51. Temperature-Salinity-Sound Velocity Profiles and T-S Diagram at Point 2C (U)	74
Figure 36. Standard Deviation in Average Critical Depth (U)	45	Figure 52. Temperature-Salinity-Sound Velocity Profiles and T-S Diagram at Point 2D (U)	75
Figure 37. Regions Shallower and Deeper than Average Critical Depth (U)	46	Figure 53. Temperature-Salinity-Sound Velocity Profiles and T-S Diagram at Point 2F (U)	76
Figure 38. Sound Velocity Cross Section from Point 1E to Point 3B During Phase I (U)	48	Figure 54. Temperature-Salinity-Sound Velocity Profiles and T-S Diagram at Point 2L (U)	77
Figure 39. Sound Velocity Cross Section from Point 2L to Point 2K During Phase II (U)	49	Figure 55. Temperature-Salinity-Sound Velocity Profiles and T-S Diagram at Point 3B(U)	78
Figure 40. Sound Velocity Cross Section from Point 2BB to Point 3AB During Phase II (U)	51	Figure 56. Temperature-Salinity-Sound Velocity Profiles and T-S Diagram at Point 3D (U)	79
Figure 41. Sound Velocity Cross Section from Point 3F to Point 3Z During Phase III (U)	52		



# CONFIDENTIAL

Figure 57. Temperature-Salinity-Sound Velocity Profiles and T-S Diagram at Point 3F (U)	81	Table 9. Identification of Data Used in Phase I Porcupine Bank Time-Series Study (U)	92
Figure 58. Temperature-Salinity-Sound Velocity Profiles and T-S Diagram on Faeroe-Iceland Ridge Near Point 3Z (U)	82	Table 10. Identification of Data Used in Phase II Porcupine Bank Time-Series Study (U)	92
Figure 59. Temperature-Salinity-Sound Velocity Profiles and T-S Diagram at Point 3ZZ (U)	83	Table 11. Identification of Data Used in Point 1E to Point 3B Cross Section (U)	93
Figure 60. Temperature-Salinity-Sound Velocity Profiles and T-S Diagram Off Porcupine Bank (Phase I) (U)	84	Table 12. Identification of Data Used in Point 2L to Point 2K Cross Section (U)	94
Figure 61. Temperature-Salinity-Sound Velocity Profiles and T-S Diagram Off Porcupine Bank (Phase II) (U)	85	Table 13. Identification of Data Used in Point 2BB to Point 3AB Cross Section (U)	95
		Table 14. Identification of Data Used in Point 3F to Point 3ZZ Cross Section (U)	96

## Tables (U)

Table 1. SQUARE DEAL Environmental Data Summary (U)	2
Table 2. Identification of Temporal Sound Velocity Comparison Data (U)	87
Table 3. Identification of Data Used in Phase I Time-Series Study at Point 1C (U)	88
Table 4. Identification of Data Used in Phase II Time-Series Study at Point 2C (U)	88
Table 5. Identification of Data Used in Phase II Time-Series Study at Point 2D (U)	89
Table 6. Identification of Data Used in Phase II Time-Series Study at Point 2FA (U)	89
Table 7. Identification of Data Used in Phase III Time-Series Study at Point 3Z (U)	90
Table 8. Identification of Data Used in Phase III Time-Series Study at Point 3ZZ (U)	91

# CONFIDENTIAL

## Sound Speed Structure of the Northeast Atlantic Ocean in Summer 1973 During the SQUARE DEAL Exercise (U)

Don F. Fenner

### I. Introduction (U)

(C) The SQUARE DEAL Exercise was conducted from July through September 1973 in the northeast Atlantic Ocean north of about 48°N in the region between the continental shelf of the United Kingdom and the crests of the Reykjanes and Mid-Atlantic Ridges. The exercise consisted of three long, narrow, overlapping basins (the Rockall Trough, the northwestern portion of the West European Basin, and the Maury Trough) that were separated in the center by the Rockall Plateau and bounded on the north by the Faeroe-Iceland Ridge. The exercise included the following three phases:

- Phase I, 25 July through 10 August
- Phase II, 15 through 27 August
- Phase III, 2 through 16 September

In addition, some acoustic and oceanographic data were collected between phases II and III. All three exercise phases were typical of oceanographic summer in the northeast Atlantic. The SQUARE DEAL Exercise was followed by the Ridge Acoustics Exercise (RAE) that was conducted across the Faeroe-Iceland Ridge in late September 1973. When applicable, RAE data have been utilized in SQUARE DEAL sound velocity analyses.

(C) The following ships took part in the SQUARE DEAL Exercise:

- USNS KANE (T-AGS-27) (KN)
- USNS LYNCH (T-AGOR-7) (LY)
- USNS WILKES (T-AGS-23) (WI)
- USNS SANDS (T-AGOR-6) (SD)
- USNS KINGSPORT (T-AG-164) (KP)
- USNS MYER (T-ARC-6) (MY)
- USS NEPTUNE (ARC-2) (NP)
- R/V CHAIN (CH)
- R/V ARTEMIS (AR)
- M/V SEISMIC EXPLORER (SE)

- RFA OLMEDA (A-124) (OL)
- RMAS ST. MARGARETS (SM)
- RMAS BULLFINCH (BF)
- HMS HECLA (A-133) (HC)

The two-letter abbreviations in parentheses following each of the above ships are those as used in the data identification tables and figures of this report. All ships collected oceanographic and/or meteorological data. However, data from ST. MARGARETS, BULLFINCH, and HECLA were not available for inclusion in this report. Continuous bathymetric records were made by KANE, LYNCH, WILKES, SANDS, KINGSPORT, CHAIN, and ARTEMIS. In addition, current meter arrays were deployed and recovered at three locations during the exercise: point 2BB (54°00'N, 12°57'W), point 2C (51°47'N, 19°38'W), and point 2D (55°25'N, 13°11'W).

(U) Many of the analyses contained in this report have appeared previously in the SQUARE DEAL Synopsis Report (Maury Center for Ocean Science, 1974) and the SQUARE DEAL Environmental Acoustics Summary (Maury Center for Ocean Science, 1975). The report supplements these two reports by providing additional areal and temporal sound velocity analyses and temperature-salinity-sound velocity comparisons. Various acronyms and oceanographic terms used in this report are defined in the glossary (Appendix C).

### II. Discussion of Environmental Data (U)

#### A. Data Availability (U)

(U) Table 1 summarizes the oceanographic data collected during SQUARE DEAL by platform and the following categories:

Ship	To Bottom	400-1000m				SV/CTDs	SVDs	SV/CTDs	Surface Meteorological Observations	Bathymetry (nm of track)
		>1000m	1000 m	400-1000m	100-400m					
KANE	17	41	75	18	70	-	-	-	463	6153
SANDS	51	37	46	14	90	-	-	-	226	3700
WILKES	11	36	108	14	58	-	-	-	431	5100
LYNCH	28	19	36	21	40	-	-	-	161	2382
ARTEMIS	10	9	41	7	-	27	-	-	183	2045
CHAIN	0	4	20	0	-	-	-	21	343	3715
KINGSPORT	40	0	152	25	-	-	-	-	435	3870
OLMEDA	5	0	76	0	-	-	-	-	68	-
NEPTUNE	0	0	51	3	-	-	-	-	73	-
SEISMIC										
EXPLORER	0	0	18	12	-	-	-	-	0	-
TOTALS	162	146	623	114	258	27	21	2383		26965

## NOTES:

- MYER made no environmental measurements other than weather observations
- Corresponding details of environmental data collected on HECLA, BULLFINCH, and ST. MARGARETS not available
- SANDS and ARTEMIS totals do not include Ridge Acoustics Exercise data
- SV/STD, SVD, and SV/CTD counts for downcasts only
- - indicates not applicable

UNCLASSIFIED

(U) Table 1. SQUARE DEAL Environmental Data Summary

# CONFIDENTIAL

- Expendable bathythermographs (XBTs)
- Sound velocity-salinity-temperature-depth (SV/CTD) profiles
- Sound velocity-depth (SVD) profiles
- Sound velocity-conductivity-temperature-depth (SV/CTD) profiles
- Surface meteorological observations
- Bathymetric tracks

The exact location of individual deep oceanographic measurements (SV/STDs, SVDs, and SV/CTDs) were listed in the SQUARE DEAL Synopsis Report (Maury Center for Ocean Science, 1974).

(U) Figure 1 shows the location of all oceanographic observations taken during SQUARE DEAL. These observations formed a roughly rectilinear grid that encompassed most of the exercise area. Figure 2 shows the locations of oceanographic observations that extended to within 100 m of the bottom. These observations were concentrated in the shallower portions of the exercise area (Porcupine Bank, Rockall Plateau, and Faeroe-Iceland Ridge). Figure 3 locates observations extending deeper than 1000 m, and includes most deep oceanographic and T-5 XBT data collected during the exercise. Figure 4 shows the location of observations that extended deeper than 400 m, but were shallower than 1000 m. Most of these observations were made with T-7 XBTs. Figure 4 also locates those T-5 XBTs that failed to reach a depth of 1000 m. Finally, Figure 5 shows the locations of observations deeper than 100 m, but shallower than 400 m (i.e., XBTs that failed above a depth of 400 m).

## B. Treatment of Data (U)

(U) Sound velocity profiles were measured directly at all 306 deep oceanographic stations using either an SV/STD, SVD, or SV/CTD system. In addition, sound velocities were calculated using the equation of Wilson (1960) for all SV/STD and SV/CTD observations. Each XBT trace was converted to sound velocity using Wilson's equation and nearby salinity measurements made during the exercise. The resulting data base was sufficient

to prepare the following sound velocity analyses:

- Time-series analyses at seven reference points during one or more exercise phases.
- Average areal contours of several parameters and their standard deviations over the course of the exercise.
- Cross sections along four SQUARE DEAL baselines for one exercise phase.

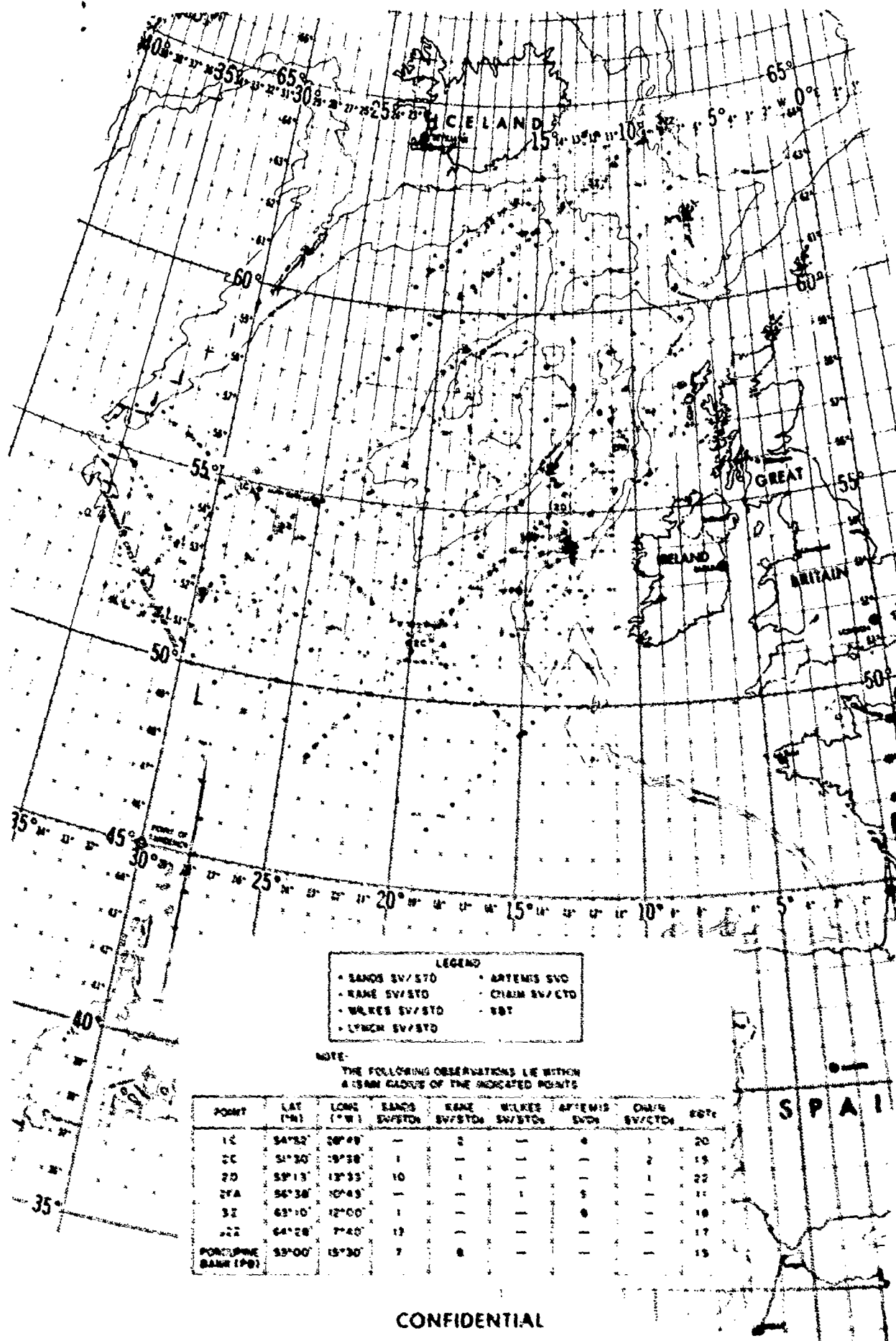
For the areal analyses, the one-degree square averages and standard deviations for the given parameter are based on all exercise data.

(U) The exercise data also were adequate to prepare areal temperature and salinity analyses at various depth levels or sigma-t surfaces. However, the only such analysis prepared for this report was a study of temperature at 10 m depth. In the opinion of the author, similar analyses might answer many perplexing questions concerning the spatial distribution of the deep sound channel (DSC) axis, the upper sound channel (USC) axis, and the intermediate sound velocity maximum that lies between the former two minima.

## C. Data Accuracy (U)

(U) Six different instrument types were used to collect environmental data during SQUARE DEAL: SV/STDs, SVDs, SV/CTDs, T-5 XBTs, T-7 XBTs, and T-4 XBTs. The first three types measured sound velocity directly with an accuracy of  $\pm 0.3$  m/sec. The SV/STD system has a temperature accuracy of  $\pm 0.02^\circ\text{C}$  and a salinity accuracy of  $\pm 0.02^\circ/\text{oo}$ , leading to an overall computed sound velocity accuracy of about  $\pm 0.2$  m/sec, disregarding any inaccuracies in Wilson's equation. The T-5, T-7, and T-4 XBTs have a temperature accuracy of about  $\pm 0.2^\circ\text{C}$ , which results in a computed sound velocity accuracy of about  $\pm 0.7$  m/sec, again assuming that there are no errors in Wilson's equation.

CONFIDENTIAL

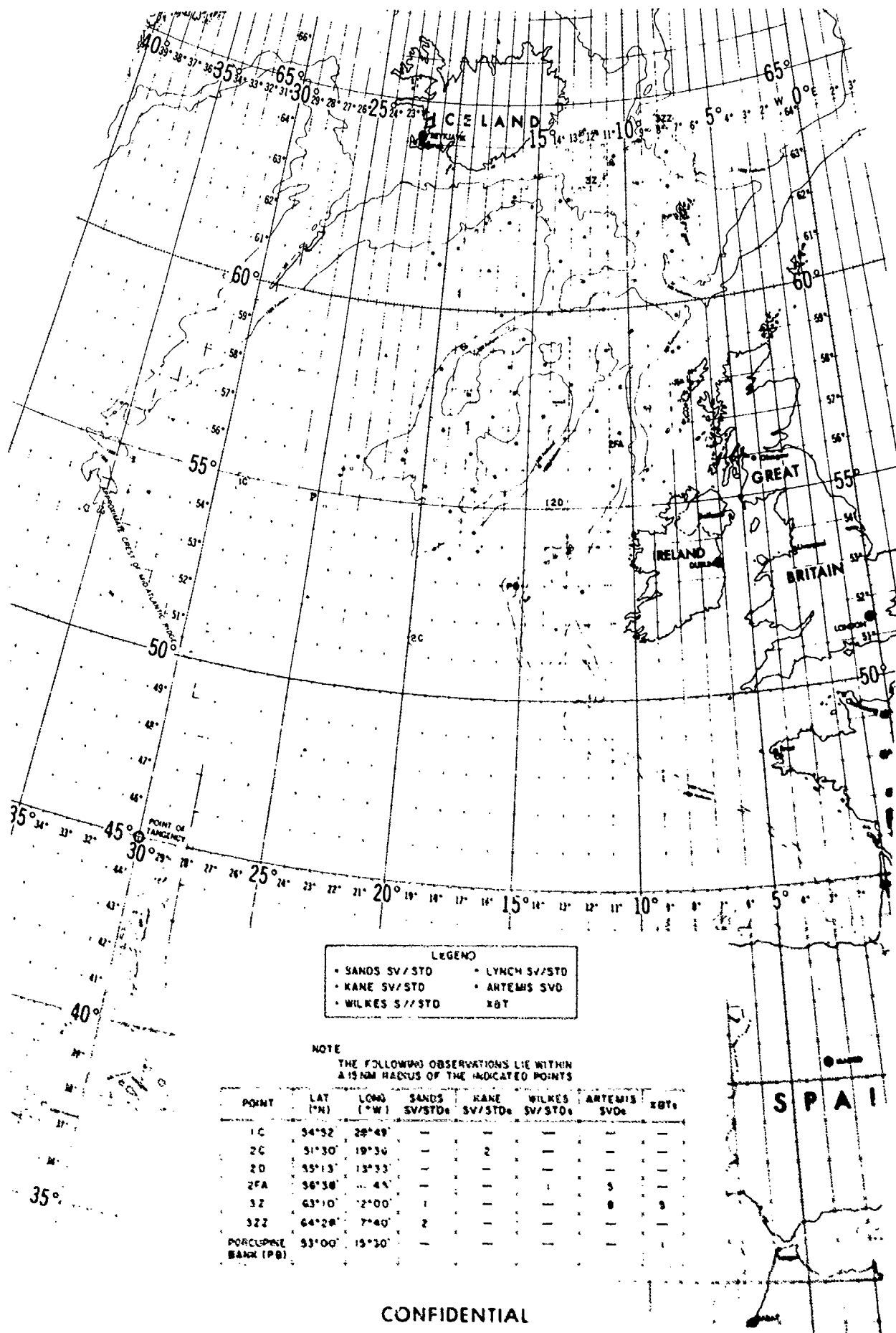


CONFIDENTIAL

(U) Figure 1. Location of All Oceanographic Observations

CONFIDENTIAL

CONFIDENTIAL

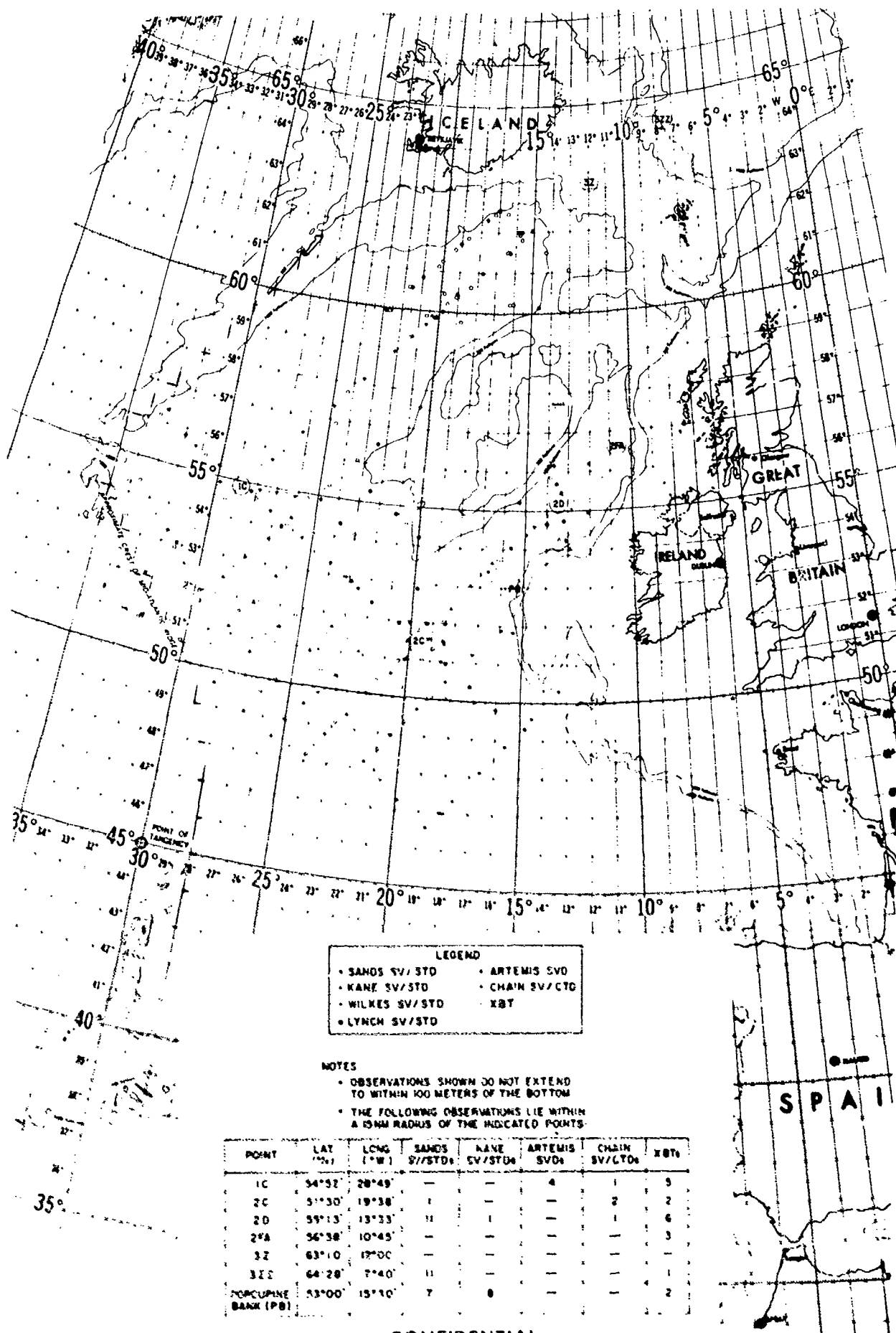


CONFIDENTIAL

(U) Figure 2. Location of Oceanographic Observations Extending to Within 100 m of the Bottom

CONFIDENTIAL

CONFIDENTIAL

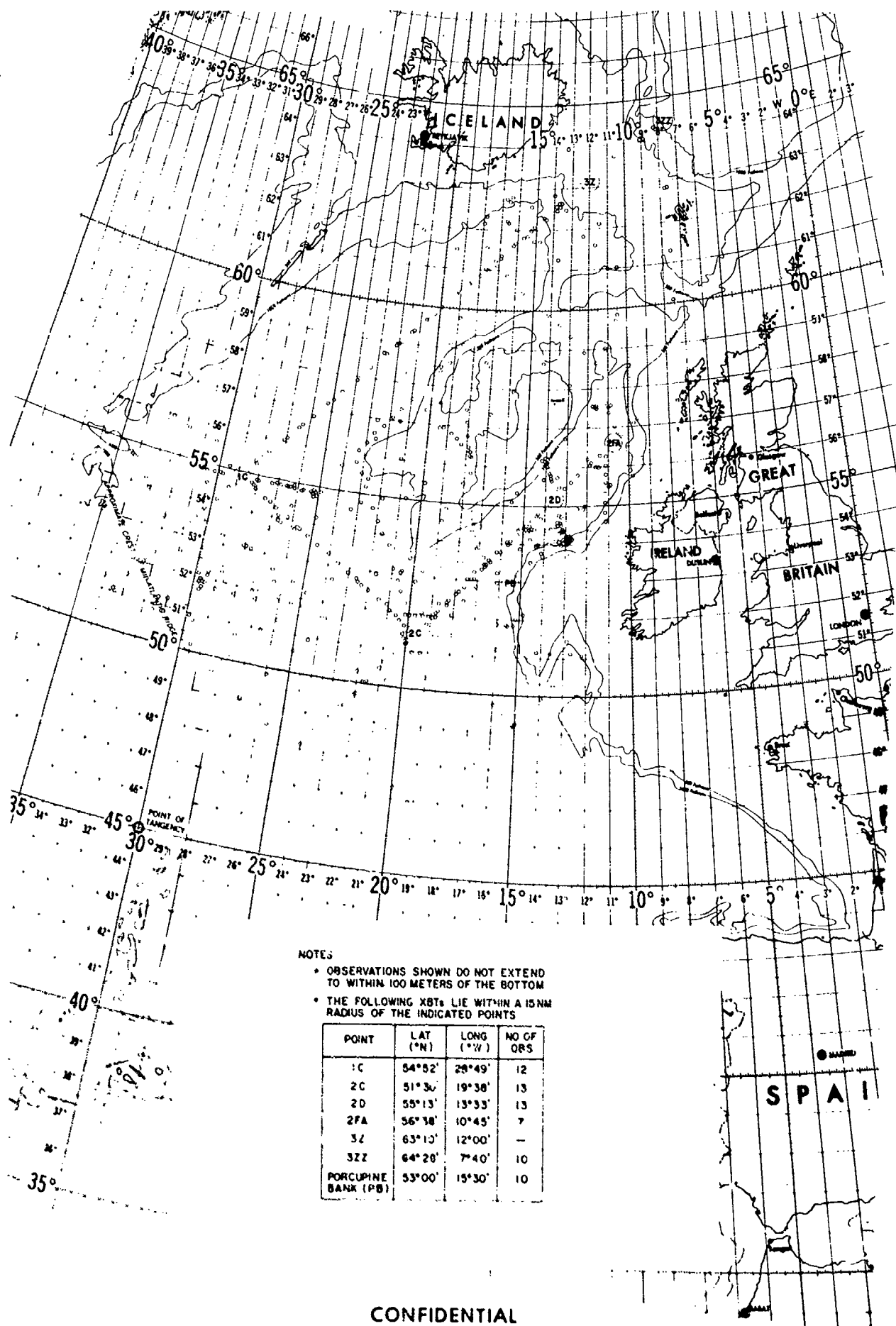


CONFIDENTIAL

(U) Figure 3. Location of Oceanographic Observations Deeper Than 1000 m

CONFIDENTIAL

CONFIDENTIAL



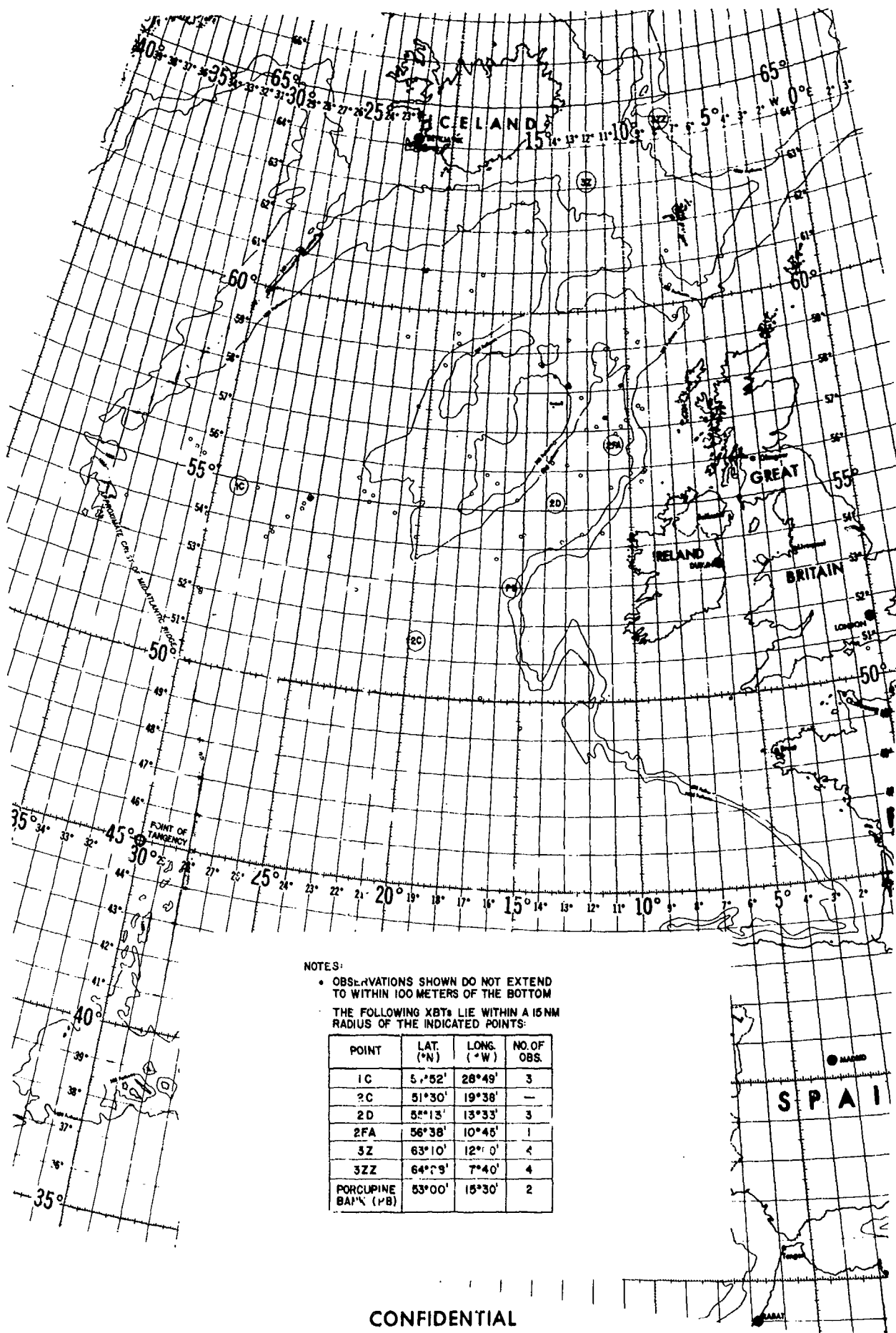
CONFIDENTIAL

(U) Figure 4. Location of Oceanographic Observations Deeper Than 400 m But Shallower Than 1000 m

CONFIDENTIAL



CONFIDENTIAL



CONFIDENTIAL

(U) Figure 5. Location of Oceanographic Observations Deeper Than 100 m But Shallower Than 400 m

CONFIDENTIAL

# CONFIDENTIAL

(U) Generally, sound velocities measured directly agreed within 0.2 to 0.5 m/sec of the computed values. This applies to both the sound velocities calculated using insitu salinities (SV/STD and SV/CTD stations) and those calculated from XBT temperatures and salinities collected at nearby locations during the exercise. Much of this error may be due to an error in Wilson's equation, as originally suggested by Carnvale et al. (1968). Because of the high percentage of XBTs in the overall data base, and in order to eliminate small disagreements between measured and calculated sound velocities, calculated sound velocities have been used in lieu of measured values whenever possible in all SQUARE DEAL sound velocity analyses.

(U) A major exception to the generally good accuracy of SQUARE DEAL data was apparent for many SANDS SV/STD stations. Below a depth of about 1800-2000 m, both measured and calculated sound velocities were sporadically 0.5 to 1.5 m/sec lower than those observed from other platforms. Therefore, no SANDS sound velocities have been used below about 1800 m. Salinities measured at all SANDS SV/STD stations were consistently lower than those measured by other platforms. Therefore, all SANDS salinities were reduced by an average correction factor of  $0.11\text{‰}$ . In addition, the SANDS SV/STD sound velocity sensor was inoperative during phases I and II of the exercise, and the salinity sensor was inoperative during most of phase III. These and other instrumentation problems have been discussed in the SQUARE DEAL Synopsis Report (Maury Center for Ocean Science, 1974).

## III. General Oceanography of the SQUARE DEAL Area (U)

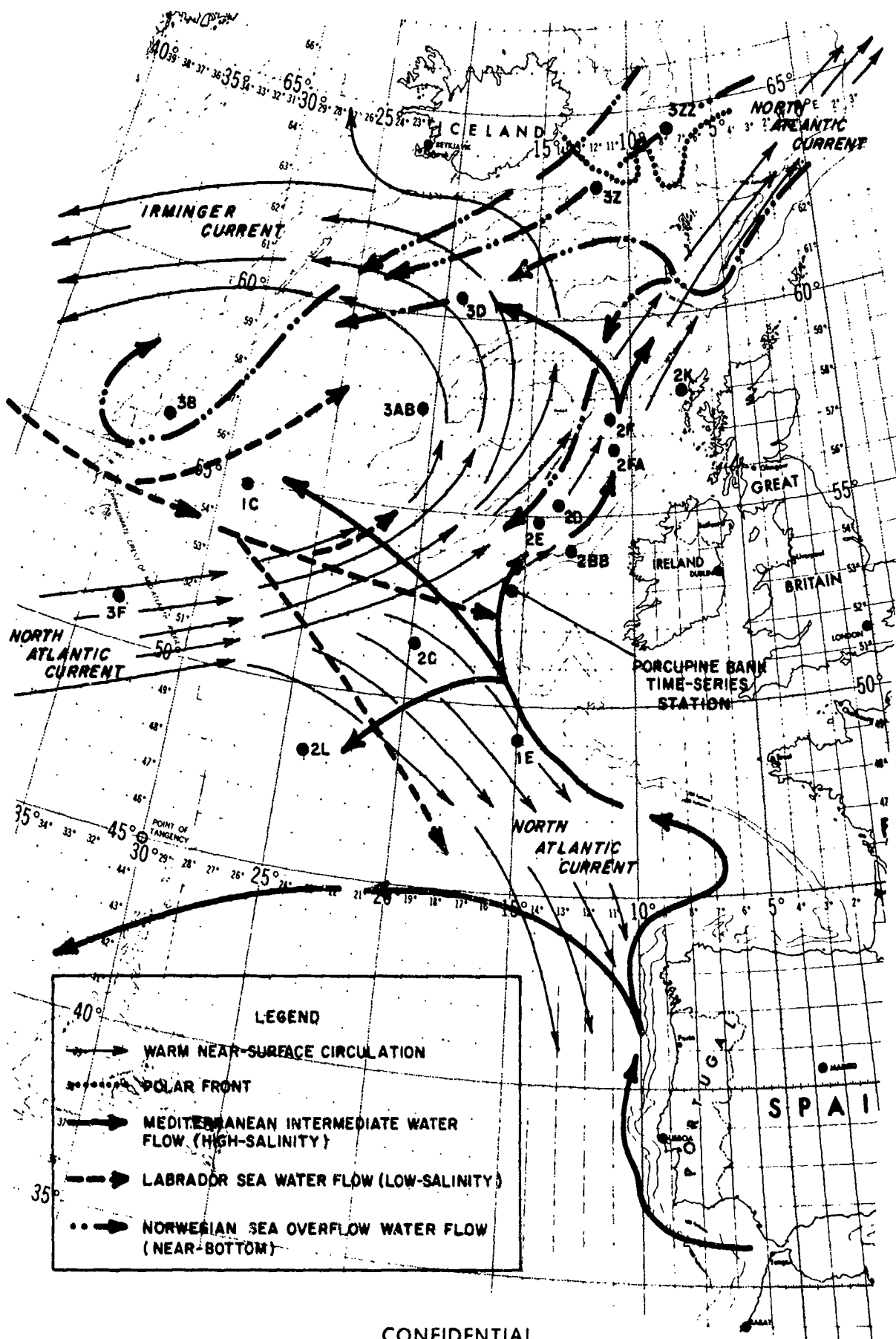
### A. Generalized Circulation and Water Masses (U)

(U) Figure 6 shows a generalized circulation diagram for both the surface and intermediate depths, and locates the reference points used in

various SQUARE DEAL sound velocity analyses. Figure 7 defines the temperature-salinity (T-S) indices of major water masses encountered in the exercise area. The most widespread of these water masses is North Atlantic Central Water (NACW) which dominates the upper 600-1000 m of the water column. This water mass is circulated throughout the exercise area by the North Atlantic and Irminger Currents, and is altered by the intrusion of two other water masses: relatively warm, high salinity Mediterranean Intermediate Water (MIW) and relatively cold, low salinity Labrador Sea Water (LSW). MIW enters the exercise area from the south after emanating from the Mediterranean Sea through the Strait of Gibraltar. This water mass has been called Upper North Atlantic Deep Water by Defant (1961). LSW enters the exercise area from the west at about  $54^{\circ}\text{N}$ ,  $35^{\circ}\text{W}$  and flows generally southeast across the West European Basin. This water mass has been called both Subarctic Intermediate Water (Bubnov, 1968) and Arctic Intermediate Water (Sverdrup et al., 1942). According to Bubnov, LSW occurs in two lobes throughout most of the western North Atlantic, one between 100 and 250 m, the other below about 900 m. Both lobes were found in the SQUARE DEAL area, where the upper LSW lobe was indistinguishable from the T-S minimum marking the bottom of the NACW layer.

(U) Throughout the northeast Atlantic, MIW and LSW mix both with each other and with NACW at depths between about 600 and 1800 m. In the region southwest of the Rockall Plateau (due west of Porcupine Bank), intensive mixing of these three water masses create a series of vertical and horizontal fronts at intermediate depths. During summer 1968, Rossof and Kislyakov (1972) found a meandering extension of the Subarctic Convergence at depths of 200, 500, and 800 m in the same general region (west of  $20^{\circ}\text{W}$  between about  $48^{\circ}\text{N}$  and  $55^{\circ}\text{N}$ ). They called this frontal zone the "Polar Front", and defined it as the boundary between sub-polar and sub-tropical waters.

CONFIDENTIAL

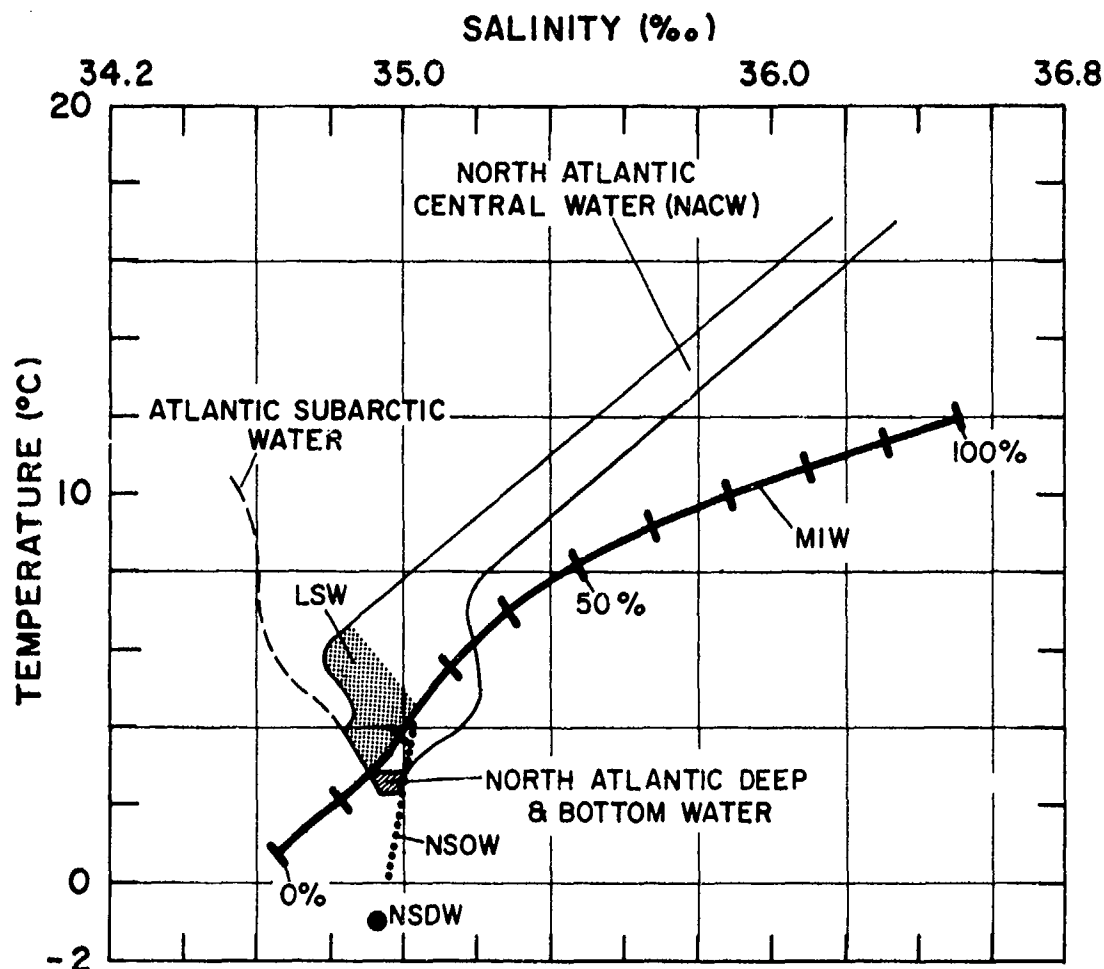


CONFIDENTIAL

(U) Figure 6. General Circulation Diagram and Location of Selected SQUARE DEAL Reference Points

CONFIDENTIAL

CONFIDENTIAL



AFTER RUBNOV (1968), DEFANT (1961),  
ELDER (1970), & SVERDRUP, et al. (1942)

ABBREVIATIONS:

LSW: LABRADOR SEA WATER  
MIW: MEDITERRANEAN INTERMEDIATE WATER  
NSDW: NORWEGIAN SEA DEEP WATER  
NSOW: NORWEGIAN SEA OVERFLOW WATER

UNCLASSIFIED

(U) Figure 7. Generalized Northeast Atlantic T-S Diagram

CONFIDENTIAL

# CONFIDENTIAL

(U) The fourth major water mass affecting the exercise area was Norwegian Sea Overflow Water (NSOW). This very cold, low salinity water mass enters the North Atlantic across the Faeroe-Iceland Ridge and through the Faeroe Channel (Herman, 1967), and has been found just above the bottom throughout the northern Maury Trough (Lee and Ellet, 1965). Lesser amounts of NSOW occur at intermediate depths along the western side of Rockall Trough, that apparently entering the area across the Wyville-Thomson Ridge (Ellet and Roberts, 1973).

(U) The effects of various water masses on northeast Atlantic sound velocity structures have been discussed in detail by Fenner and Bucca (1971). A brief discussion of these effects specific for the exercise area is given in the SQUARE DEAL Environmental Acoustic Summary (Maury Center for Ocean Sciences, 1975). A more detailed discussion of the effects of MIW, LSW, and NSOW on sound velocity at selected SQUARE DEAL reference points (including the Porcupine Bank time-series station) is given in Appendix A. Appendix A also contains temperature-salinity-sound velocity comparisons for the selected reference positions (Figs. 49-61).

## B. Temperature-Salinity (T-S) Relations Along the SQUARE DEAL Baselines (U)

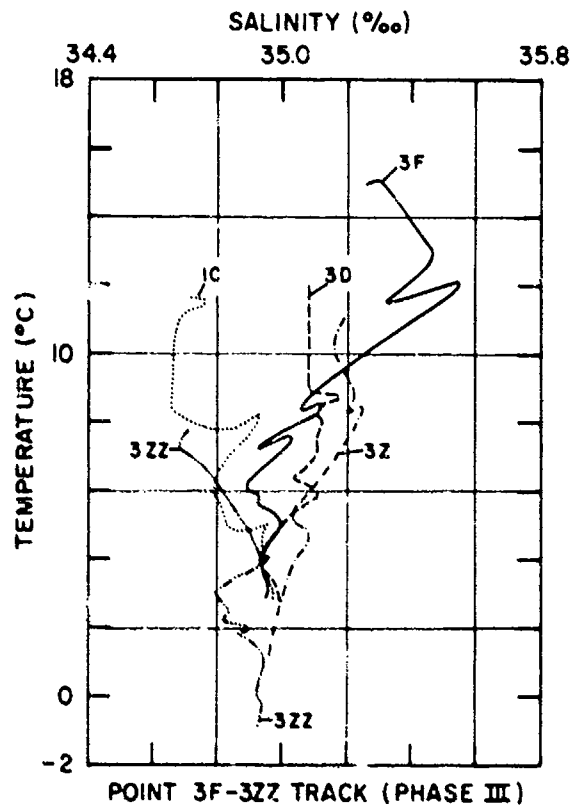
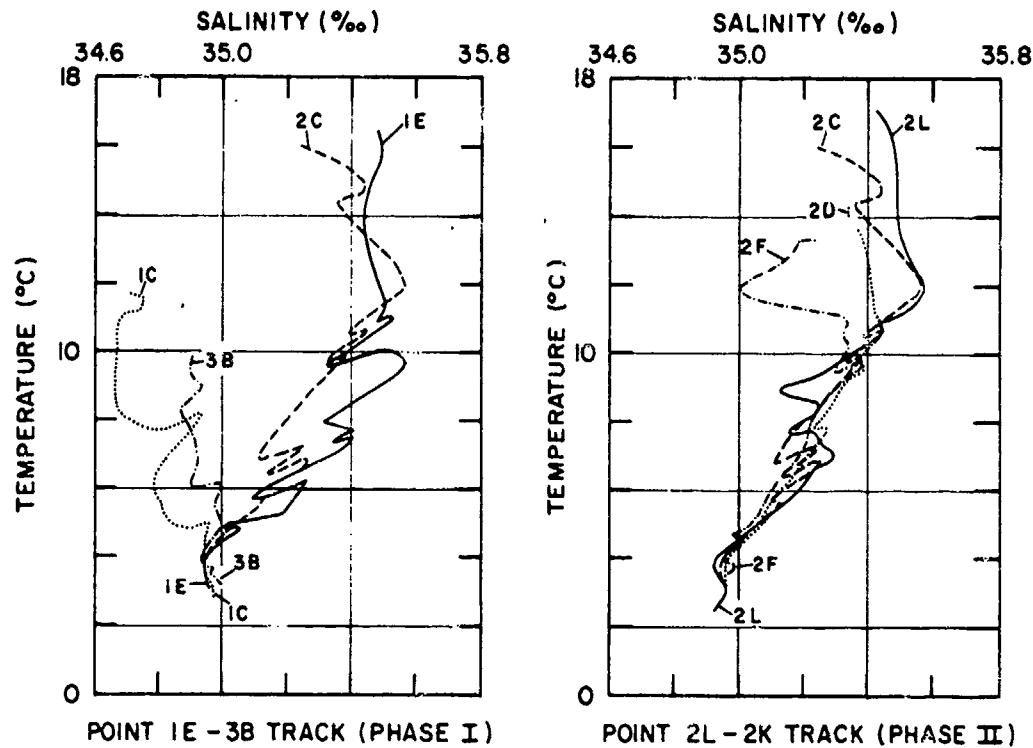
(U) Figure 8 shows composite plots of T-S diagrams along the three major SQUARE DEAL baselines. T-S diagrams used in this figure also are presented in Appendix A. Along the 1E-3B track (phase I), surface temperatures varied by more than  $8^{\circ}\text{C}$  and surface salinities by more than  $0.8^{\circ}/_{\text{oo}}$ . MIW was the predominant intermediate water mass at points 1E and 2C, while at 1C and 3B, LSW predominated. In addition, the track crossed the North Atlantic Current between points 2C and 1C (Fig. 6). Along the 2L-2K track (phase II), oceanographic conditions were less variable. Surface temperatures varied by less than  $4^{\circ}\text{C}$  and surface salinities by less than  $0.3^{\circ}/_{\text{oo}}$ . MIW was the predominant

intermediate water mass along the 2L-2K track, except between points 2L and 2C and west of Porcupine Bank, where the track crossed two separate LSW flows. This track started south of the North Atlantic Current, crossed the south wall north of point 2L, crossed the north wall north of point 2C, and lay within the main flow of the current north of about  $54^{\circ}\text{N}$ . Along the 3F-3ZZ track (phase III), surface temperatures varied by more than  $7^{\circ}\text{C}$  and surface salinities by about  $1.2^{\circ}/_{\text{oo}}$ . In addition, near-bottom temperatures varied by nearly  $4^{\circ}\text{C}$  along the length of the track and by more than  $2^{\circ}\text{C}$  between points 3Z and 3ZZ. LSW was the predominant intermediate water mass at point 1C. At point 3D, both MIW and NSOW were present. NSOW dominated much of the water column at point 3Z, while Norwegian Sea Deep Water (NSDW) was the predominant water mass at point 3ZZ. The 3F-3ZZ track began in the North Atlantic Current, crossed the main flow of Irminger Current near point 3D, and crossed the meandering Polar Front twice between points 3Z and 3ZZ. Generally, oceanographic conditions were more complex along the 3F-3ZZ track than along any other SQUARE DEAL baseline.

## C. Temperature at 10m Depth (U)

(U) Figure 9 shows contours of average temperature at 10 m based on all SQUARE DEAL oceanographic data. Temperature at 10 m varied from greater than  $18^{\circ}\text{C}$  along about  $47^{\circ}\text{N}$  to less than  $9.5^{\circ}\text{C}$  over the southern tip of the Reykjanes Ridge and to less than  $8^{\circ}\text{C}$  in the Norwegian Basin. Over the Faeroe-Iceland Ridge, the intense Polar Front caused a compression of the  $8^{\circ}\text{C}$  through  $12^{\circ}\text{C}$  isotherms. A lesser compression of the  $12^{\circ}\text{C}$  through  $14^{\circ}\text{C}$  isotherms occurred along about  $24^{\circ}\text{W}$  between about  $50^{\circ}\text{N}$  and  $55^{\circ}\text{N}$  and in the southwestern part of the exercise area. Near-surface fronts have been shown in both regions during August by Baranov (1972). These frontal zones apparently are caused by the north wall of the meandering North Atlantic Current. Throughout most of the exercise area,

CONFIDENTIAL

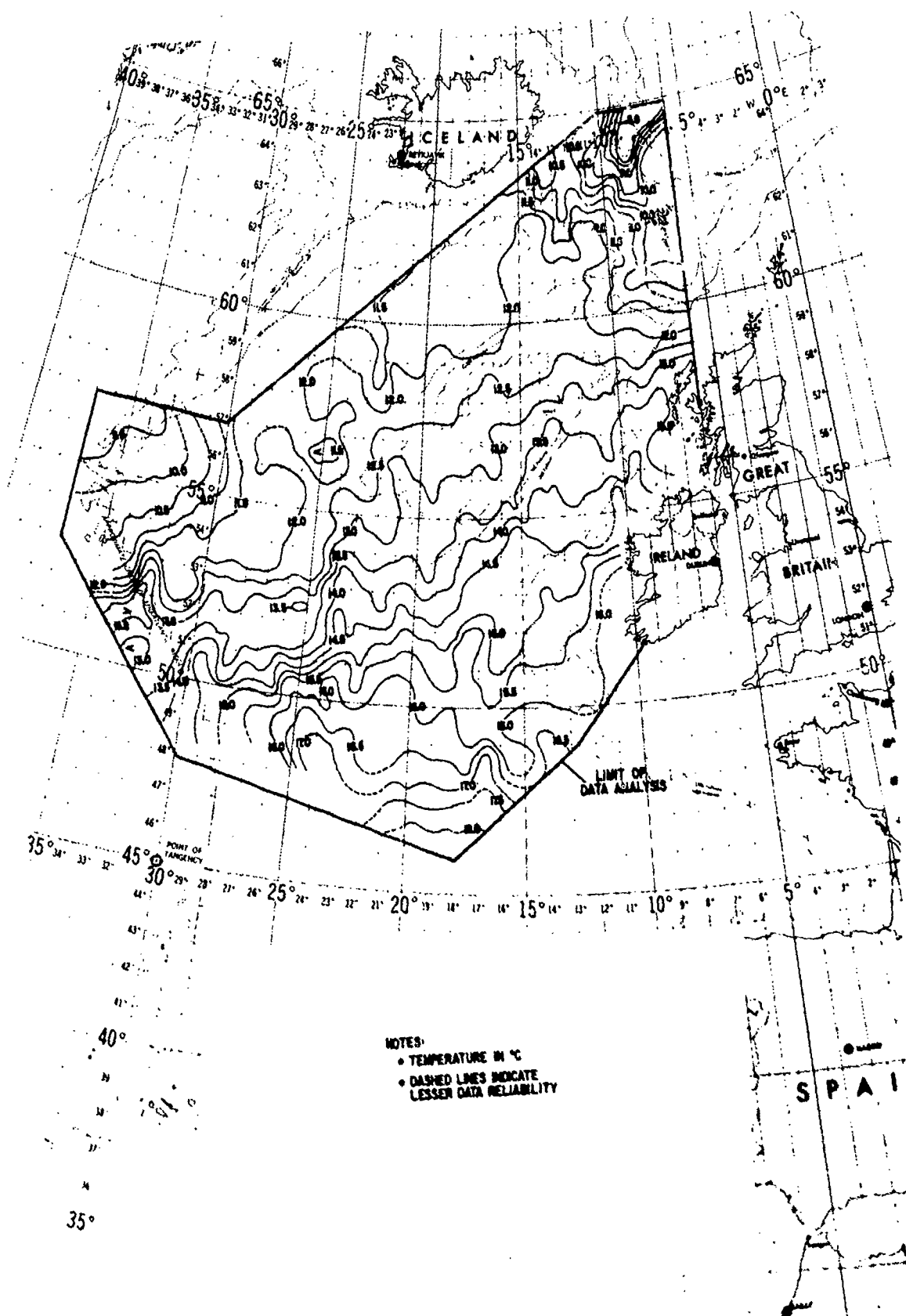


UNCLASSIFIED

(U) Figure 8. T-S Diagram Composites Along the Three Major SQUARE DEAL Baselines

CONFIDENTIAL

CONFIDENTIAL



UNCLASSIFIED

(U) Figure 9. Average Temperature at 10 m Depth

CONFIDENTIAL

# CONFIDENTIAL

the orientation of the isotherms at 10 m was similar to that of the North Atlantic Current (Fig. 6).

(U) Figure 10 shows contours of the standard deviation in average temperature at 10 m depth. Standard deviations ranged from less than 0.2 m/sec along the southern, western, and eastern boundaries of the exercise area to greater than 1.0 m/sec in regions over the Faeroe-Iceland Ridge, west of Porcupine Bank, and near the crest of the Mid-Atlantic Ridge. All three of these regions contain frontal zones. The extremely complex isopleth patterns also reflect temporal changes in the data base. These changes were caused by the diurnal heating/cooling cycle as well as the passage of several storms through the exercise area (see discussion of meteorology in section VII). Nevertheless, throughout most of the exercise area, standard deviations in temperature at 10 m depth were less than 0.4 m/sec.

## IV. Temporal Variability (U)

### A. Long-Term Variability Throughout the Exercise Area (U)

(U) Figure 11 shows examples of temporal variability in sound velocity at selected SQUARE DEAL reference points for time periods greater than five days. The data used in this figure are identified in Table 2 (Appendix B). Significant amounts of temporal variability occurred throughout the exercise area, much of which was caused by internal waves with a semidiurnal period similar to that of the tides in the northeast Atlantic (NAVOCEANO, 1965). Similar internal waves have been detected in sound velocity data from the CHURCH GABBRO Exercise (Fenner and Bucca, 1973) and the NORLANT-72 Exercise (Fenner and Bucca, 1974). Temporal variability in sound velocity structure also was caused by mixing of MIW, LSW, and NSOW. The significant temporal variability at points 1C, 2A/2AA, 2BA/2BB, 2C/2CA, 2FA/3QB, 3A/3AA, and 3F probably was the result of both internal waves and

mixing between NACW and various intrusive water masses. At the Porcupine Bank time-series station and at points 2C/2CA and 3ZZ, temporal variability resulted in a change from a bichannel to single channel sound velocity structure in a period of about 11 days. At points 2A/2AA, 2FA/3QB, and 3A/3AA, the sound velocity at the intermediate maximum changed significantly over a period of 9 to 10 days, resulting in changes in the "strength" of the USC. Such temporal changes in sound velocity structure probably had significant effects on sound propagation, particularly in shallow water where the upper channel was the only available sound transmission path.

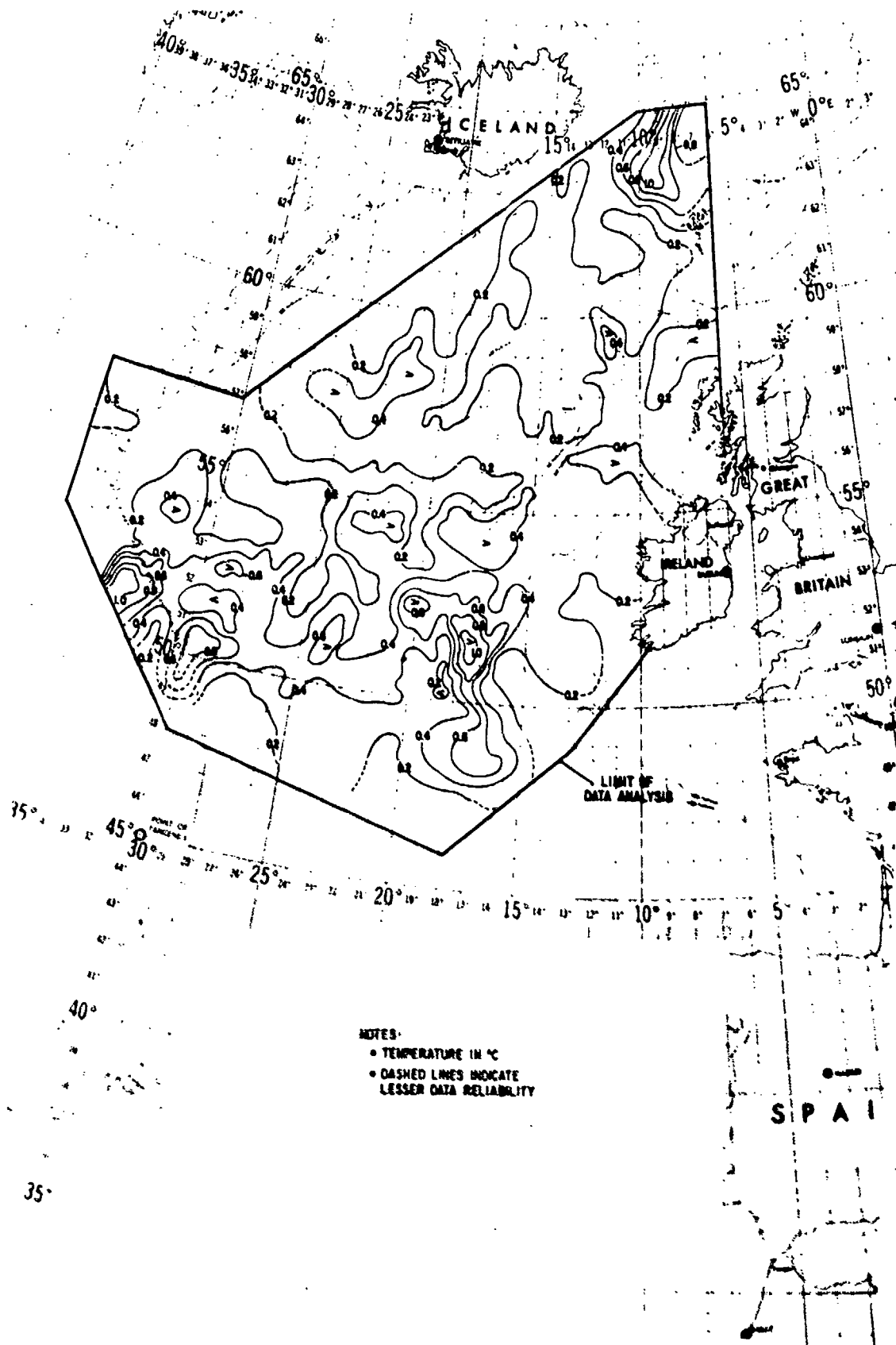
### B. Time-Series Studies (U)

(C) Figure 12 shows a time-series plot and a contoured presentation of sound velocity data at point 1C during phase I. The data used in this figure are identified in Table 3 (Appendix B). During phase I, a significant amount of temporal variability occurred at point 1C. Between 5 and 10 August, the depth of the DSC axis varied by 140 m and axial velocity varied by 3.9 m/sec. Critical depth varied between about 1900 and 2000 m and allowed ample depth excess for convergence zone propagation from a near-surface source. Although the data distribution was insufficient to determine exact internal wave periods, the convoluted form of the sound velocity isopleths below the DSC axis indicates that internal waves were responsible for some of the observed temporal variability. The remainder of this variability probably was caused by mixing between LSW and NACW. Internal waves with diurnal and semidiurnal periods also may have partially caused the similar periodicity in the spectral ambient noise intensity observed at Acoustic Data Capsule (ACODAC) 1C (Maury Center for Ocean Science, 1974).

(C) Figure 13 presents a time-series analysis at point 2C during phase II. The data used in this figure are identified in Table 4 (Appendix B). These data were too shallow to reliably



CONFIDENTIAL



UNCLASSIFIED

(U) Figure 10. Standard Deviation in Average Temperature at 10 m Depth

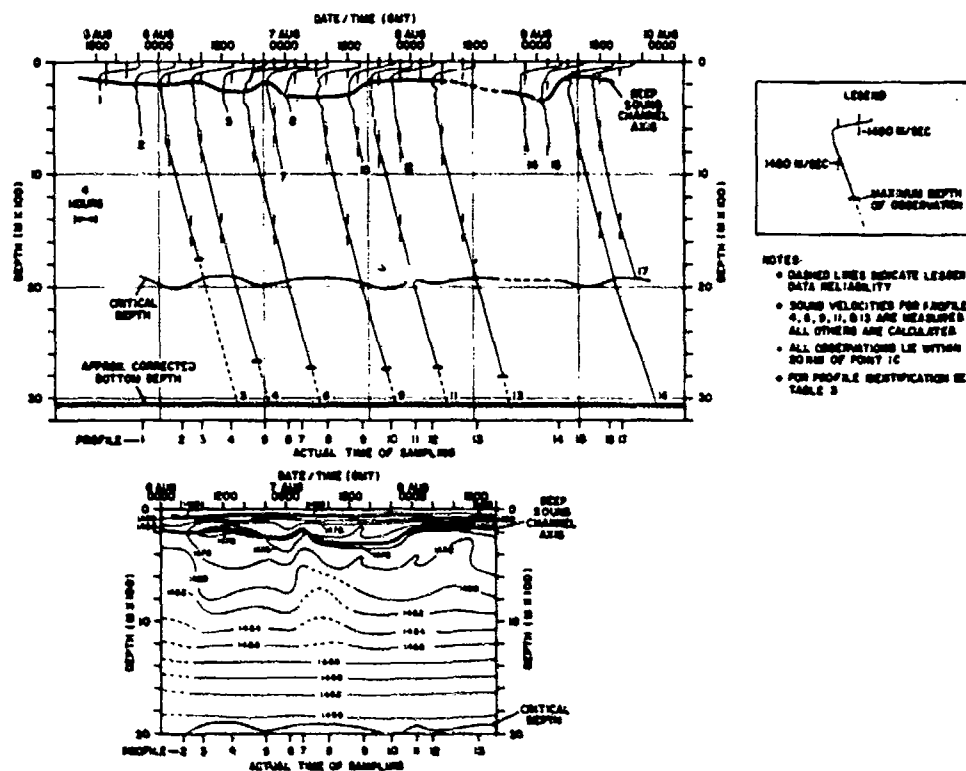
CONFIDENTIAL

CONFIDENTIAL

(U) Figure 11. Temporal Variability of Sea Surface Temperature (SST) and Sea Level Pressure (SLP) Anomalies in the North Atlantic Ocean, 1950-1970.

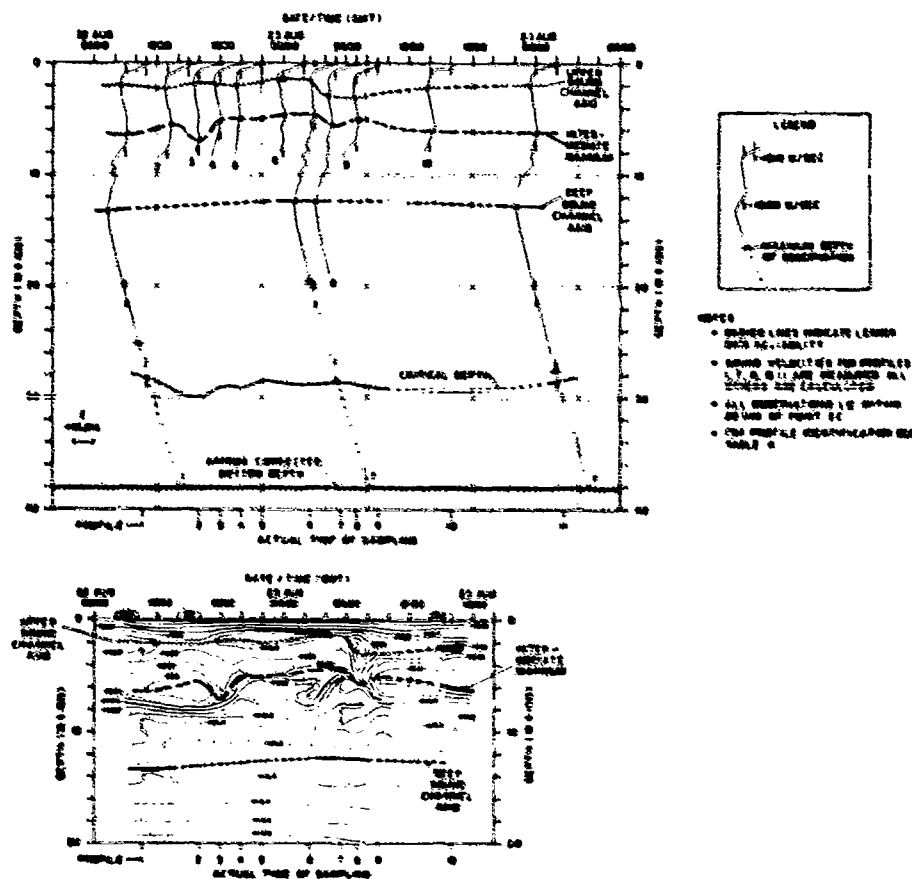
(U) Figure 11. Temporal Variability of Selected Reference Points

CONFIDENTIAL



UNCLASSIFIED

(U) Figure 12. Time-Series Plot of Sound Velocity at Point 1C During Phase I



UNCLASSIFIED

(U) Figure 13. Time-Series Plot of Sound Velocity at Point 2C During Phase II

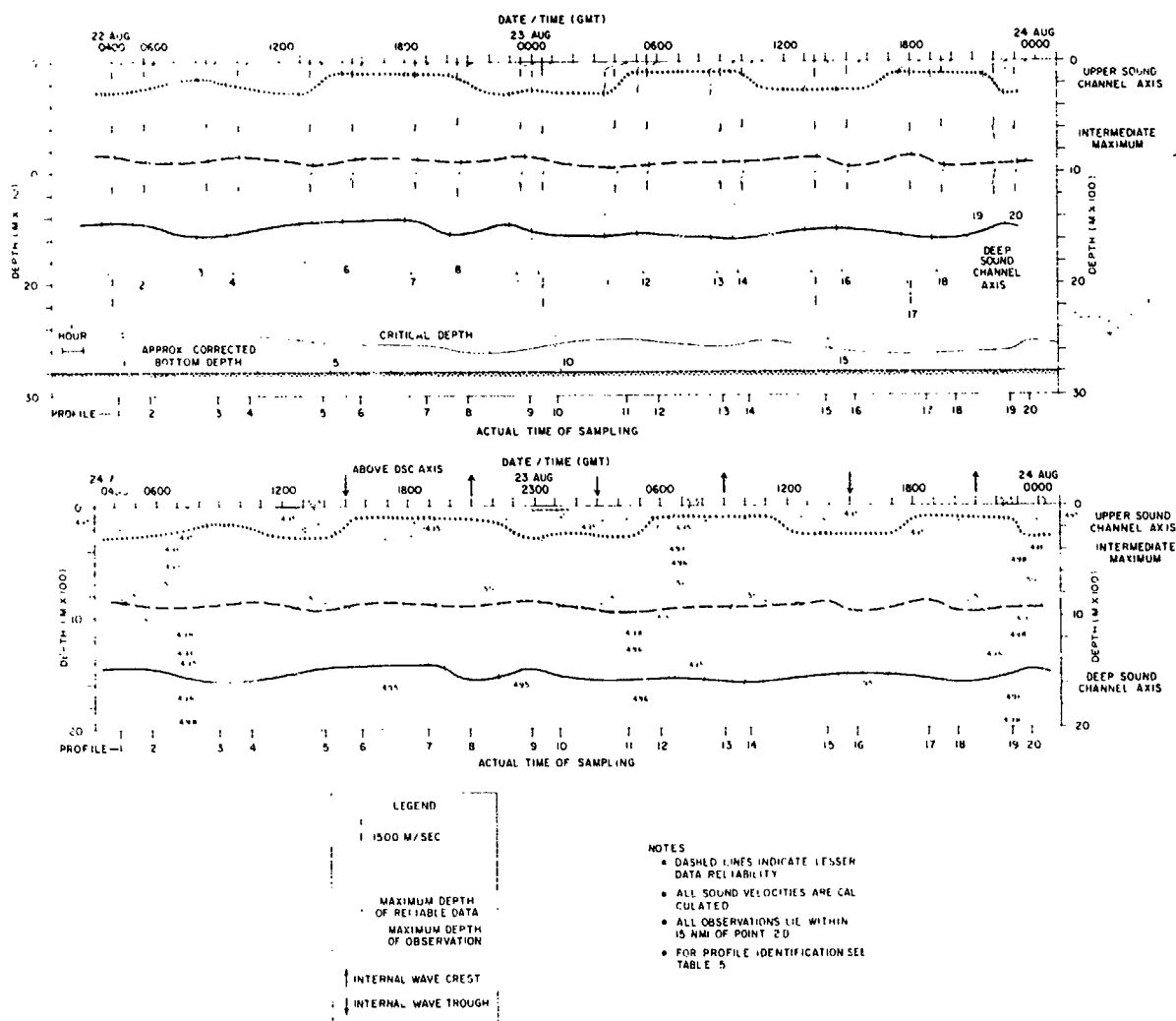
CONFIDENTIAL

CONFIDENTIAL

determine DSC variability, but were deep enough to define temporal variability in the bichannel sound velocity structure. During the period 22-24 August, the depth of the USC axis varied by 180 m and upper axial velocity varied by 2.7 m/sec. The depth and velocity of the intermediate maximum varied by 250 m and 3.1 m/sec, respectively. Although critical depth varied by about 200 m, depth excess was consistently greater than 800 m, more than enough for convergence zone formation considering a near-surface source. The relatively large variability in sound velocity at the USC axis and intermediate maximum probably was caused by both internal waves and mixing between NACW and MIW. However, since point 2C lay between two major MIW flows (Fig. 6), it may not have been equally

affected by MIW during various exercise phases. Temporal variability should have had pronounced effects on ambient noise levels measured at ACODAC 2C during phase II.

(C) Figure 14 presents a time-series analysis at point 2D during phase II, the data for which are identified in Table 5 (Appendix B). These data were well spaced temporally and consisted primarily of SANDS SV/STD stations taken on 22-23 August. Internal waves with a period of approximately 12 hours are discernable in Figure 14. The variations in the sound velocity at the USC axis and intermediate maximum (both 1.0 m/sec) were considerably less than that at point 2C during approximately the same time period (Fig. 13). This indicates that internal waves were



UNCLASSIFIED

(U) Figure 14. Time-Series Plot of Sound Velocity at Point 2D During Phase II

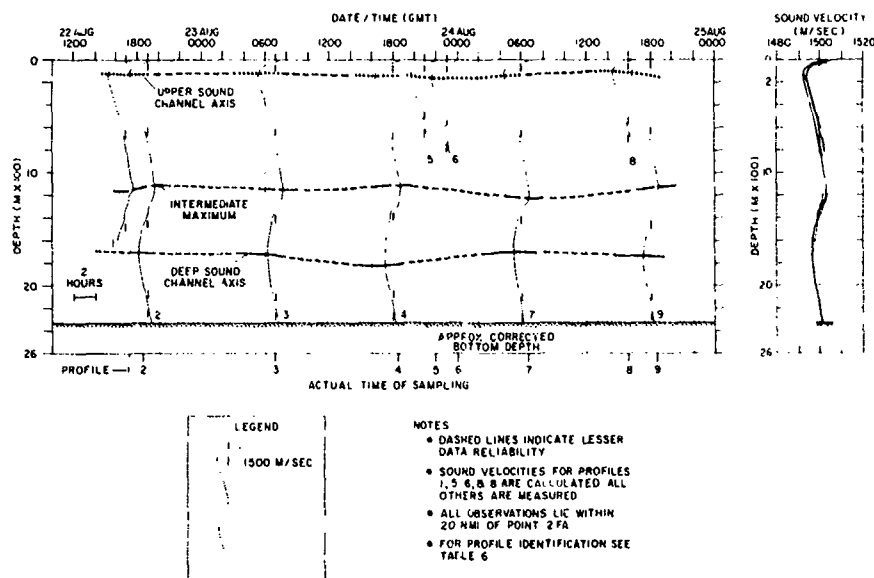
CONFIDENTIAL

CONFIDENTIAL

primarily responsible for the temporal variability at point 2D this is understandable since point 2D lay in the center of Rockall Trough (a region not strongly affected by either MIW or NSOW flows). Depth excess at point 2D varied between 400 and 600 m, the minimum necessary for reliable convergence zone formation from a near-surface source.

(C) Figure 15 shows a time-series plot of sound velocity profiles at point 2FA during phase II. The data are identified in Table 6 (Appendix B). Since these data were insufficient to prepare

a contoured presentation, a sound velocity composite is shown, and indicates that the maximum variability at point 2FA occurred at the surface (approximately 5 m/sec). However, the variability at depths between about 500 and 1600 m was more than half that at the surface, owing mainly to the presence of MIW at point 2FA. At point 2FA, the mean sound velocity at the USC axis (about 1493 m/sec) was approximately 3 m/sec less than that at the DSC axis (about 1496 m/sec). Although point 2FA was bottom-limited, the well-defined USC probably acted as a sound propagation path for sources within the upper channel throughout the exercise.



UNCLASSIFIED

(U) Figure 15. Time-Series Plot of Sound Velocity at Point 2FA During Phase II

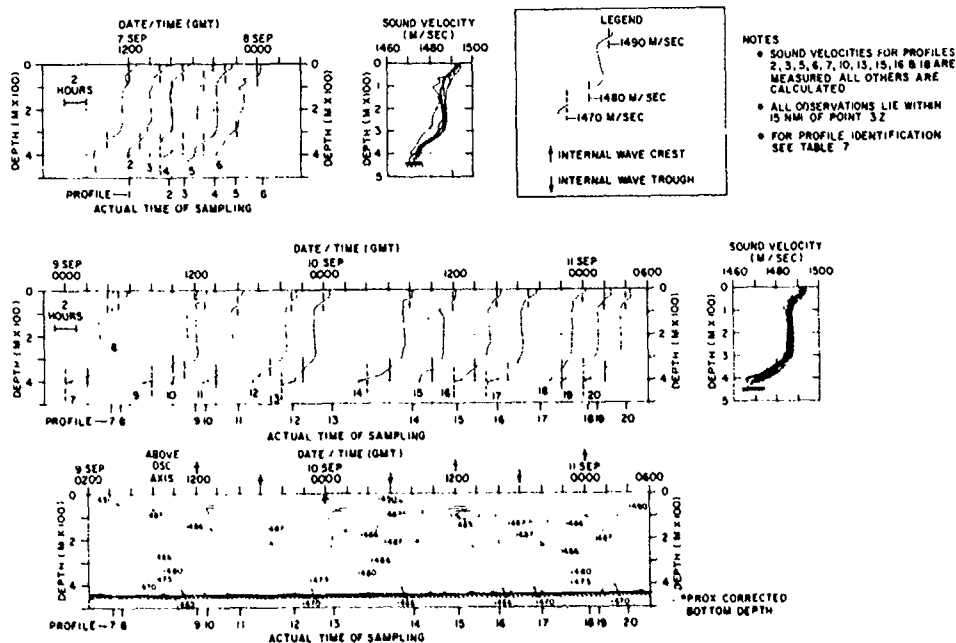
CONFIDENTIAL

CONFIDENTIAL

(U) Figure 16 shows time-series plots, a contoured presentation, and composites of sound velocity data at point 3Z during phase III. The data used in this figure are identified in Table 7 (Appendix B). Since the minimum sound velocity at point 3Z lay at or just above the bottom, no DSC has been indicated in Figure 16. However, the observed near bottom minimum coincided with the very cold, low salinity NSOW core. The various sound velocity isopleths just above the bottom on the contoured section indicate that the NSOW flow over the Faeroe-Iceland Ridge was sporadic during phase III of SQUARE DEAL. This flow was partially controlled by the internal waves with a 12 hour period. Similar internal waves were observed during the International "Overflow" Expedition in 1960 (Magaard and Krauss, 1967). However, as noted by Dietrich (1967), NSOW pulsations also are controlled by the tides in the

shallow region over the crest of the Faeroe-Iceland Ridge.

(C) At point 3Z, minimum sound velocities varied by 10.8 m/sec (between 1463.8 and 1474.6 m/sec) during the period 7-11 September. This extreme variation was caused by pulsations of NSOW, was greater than that observed along the Subarctic Convergence during NORLANT-74 (9.5 m/sec, Fenner and Bucca, 1974), and should have pronounced effects on sound propagation at point 3Z. Here, propagation was limited to bottom bounce paths, since the shallow topography of the Faeroe-Iceland Ridge extended to the depth of the DSC axis and a well defined USC was absent. Turbidity and strong bottom currents are thought to be associated with NSOW pulsations (Cherkis et al., 1973), and these pulsations may have led to anomalously high ambient noise levels in the data recorded by Western Electric Company (WECO) Survey Array 3Z.



UNCLASSIFIED

(U) Figure 16. Time-Series Plot of Sound Velocity at Point 3Z During Phase III

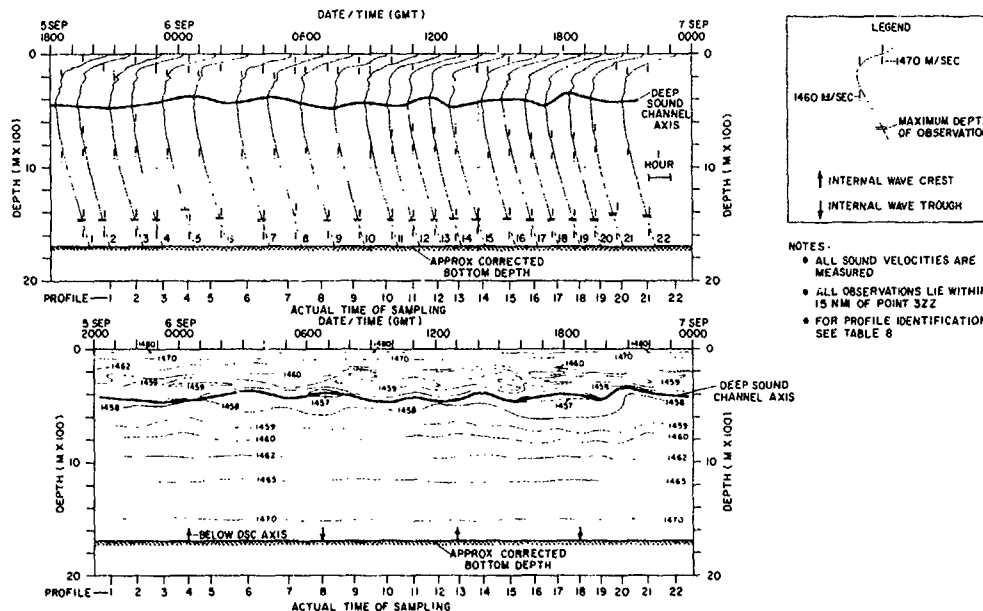
CONFIDENTIAL

CONFIDENTIAL

(C) Figure 17 presents a time-series sound velocity analysis at point 3ZZ (Norwegian Basin) during phase III. The data used in this figure are identified in Table 8 (Appendix B). These data were particularly well spaced temporally and consisted entirely of SANDS SV/STD stations taken on 5-6 September. Internal waves with a 12 hour period are evident in the contoured section, causing a 120 m variation in the depth of the DSC axis

The single channel structure during phase II was extremely complex, and the DSC axis coincided with one of several T-S perturbations at the approximate level of the MIW core.

(U) During phase I, the bichannel structure was transitory in nature and had a roughly diurnal periodicity, probably caused by internal waves. However, the data distribution at the phase I station was inadequate to



UNCLASSIFIED

(U) Figure 17. Time-Series Plot of Sound Velocity at Point 3ZZ During Phase III

and a 1.5 m/sec variation in deep axial velocity. These variations were similar to those caused by internal waves at point 2D (Fig. 14). Although point 3ZZ was bottom-limited by the relatively shallow topography of the northern flanks of the Faeroe-Iceland Ridge, DSC propagation was possible at this location.

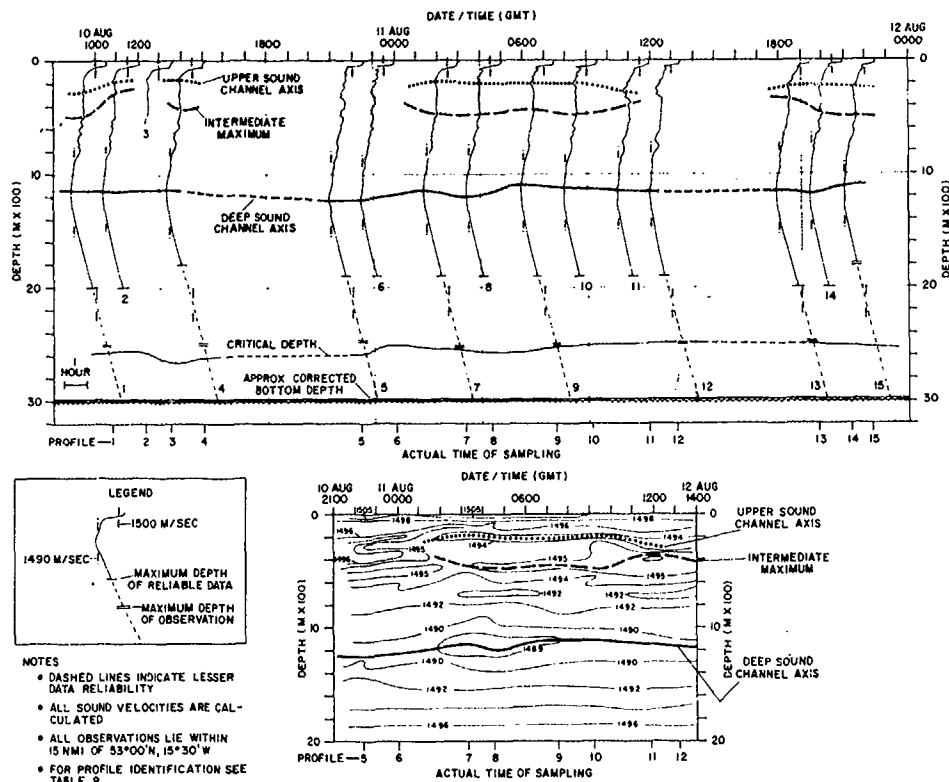
(U) Figures 18 and 19 show time-series sound velocity analyses at the western edge of Porcupine Bank during phases I and II, respectively. The data used in these figures are identified in Tables 9 and 10 (Appendix B). The two occupations of the time-series station were separated by approximately 10 days. During these 10 days, the bichannel sound velocity structure shown on Figure 18 (phase I) was replaced by a single channel structure (Fig. 19).

define these internal waves. During phase II, internal waves with a 12 hour period are evident in the contoured section. During both phases, these internal waves caused variations in DSC velocity similar to those found at point 2D during phase II (Fig. 13). However, internal waves were not solely responsible for the major change in the sound velocity structure that occurred between the two occupations of the Porcupine Bank time-series station. Rather, this basic change was caused by a combination of internal waves and mixing between intrusive water masses.

(U) In the opinion of the author, the temporal variability observed at the Porcupine Bank time-series station during phase I was caused by internal waves and mixing between high salinity MIW and the upper lobe of low salinity

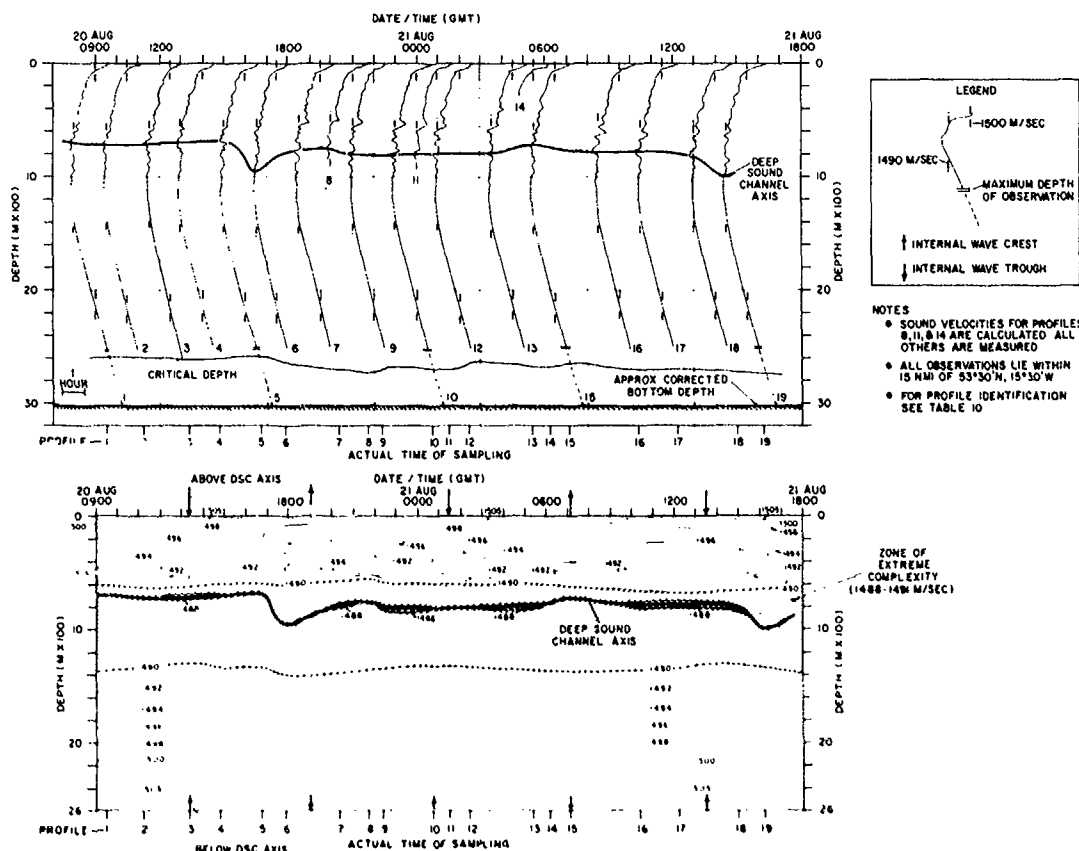
CONFIDENTIAL

CONFIDENTIAL



UNCLASSIFIED

(U) Figure 18. Time-Series Plot of Sound Velocity West of Porcupine Bank During Phase I



UNCLASSIFIED

(U) Figure 19. Time-Series Plot of Sound Velocity West of Porcupine Bank During Phase II

CONFIDENTIAL



# CONFIDENTIAL

LSW. In this case, the T-S minimum generally characterizing LSW was indistinguishable from that marking the bottom of the NACW layer. Apparently, a large cell of upper-lobe LSW migrated from the west into the vicinity of Porcupine Bank near the end of the phase I and caused a change from a bichannel to a single channel sound velocity profile sometime between 12 and 20 August. A similar cold water cell was observed about 150 nm west of the time-series site in July 1975 (Howe and Tait, 1967). The presence of upper-lobe LSW west of Porcupine Bank during phase II had significant effects on sound velocity structures above about 1500 m. The effects of this low salinity water mass also are discernable in the average areal contours of various sound velocity parameters.

## C. Summary of SQUARE DEAL Temporal Variability (U)

(C) Temporal variations in sound velocity occurred throughout the exercise area, and was responsible for basic alterations in sound velocity structures in several regions. These included changes from a bichannel to a single channel structure, changes in the "strength" of the USC, and changes in the width of the DSC. Changes of this type probably had significant effects on sound propagation and may have caused short-term propagation anomalies. Such anomalies might be expected at the ACODAC 1C, 2C, and 3D sites, in the regions west of Porcupine Bank and surrounding Rockall Plateau, and over the crest of the Faeroe-Iceland Ridge. Generally, variations at the USC and intermediate maximum greater than about 1.0 m/sec were caused by the combined effects of internal waves and mixing between NACW and various intrusive water masses. DSC sound velocity variations greater than about 2.0 m/sec were caused by similar combined effects. The 10.8 m/sec variation in deep axial velocity at point 3Z was caused by boluses of NSOW pulsating over the Faeroe-Iceland Ridge, and is the

greatest such variation yet found in a LRAPP exercise area.

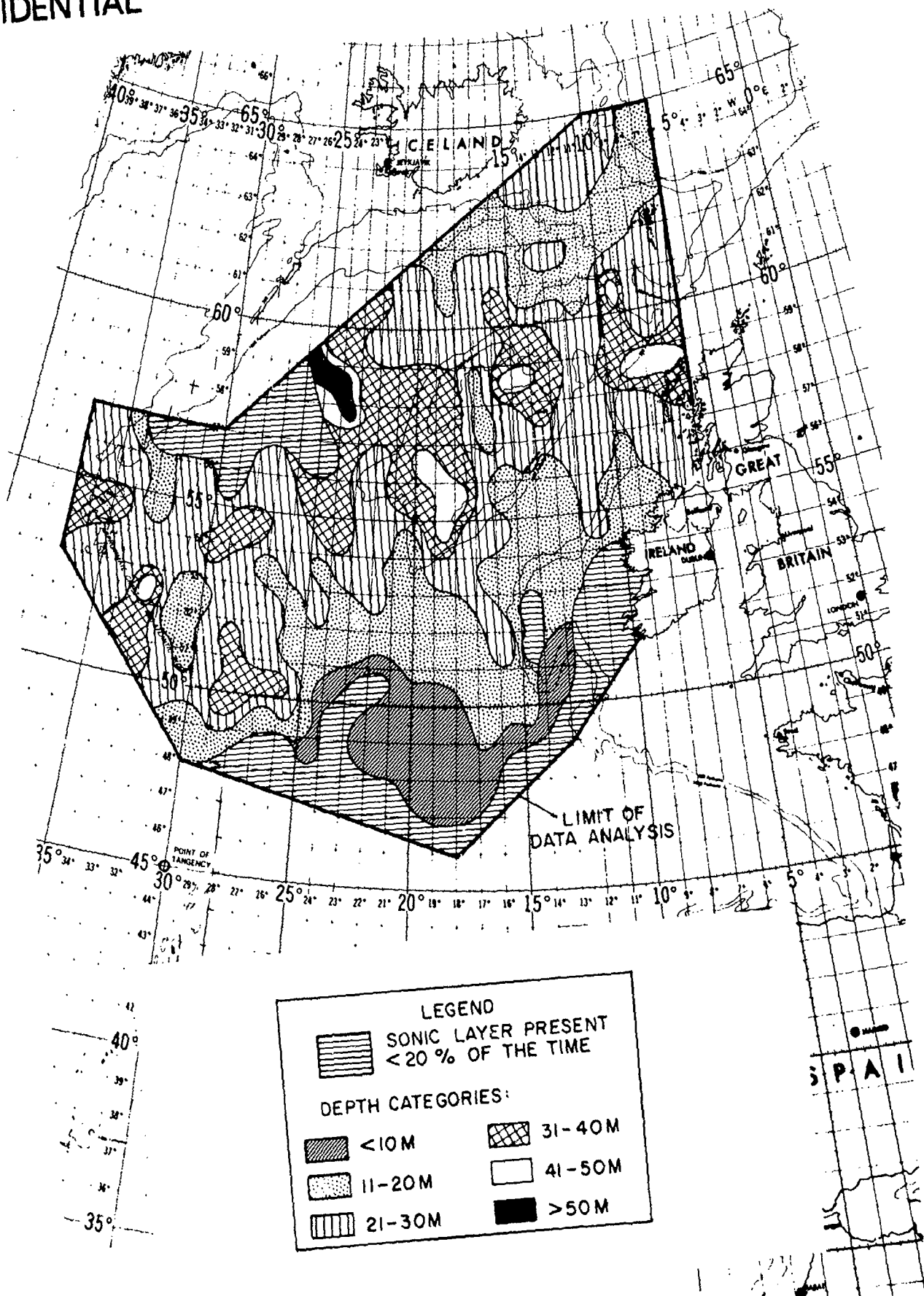
## V. Spatial Variability of Selected Sound Velocity Parameters (U)

(C) In the following sections, the average sound velocity structure of the SQUARE DEAL exercise area is defined in terms of several sound velocity parameters. These include the four most significant inflection points on the sound velocity profiles in this area: sonic layer depth, the USC axis, the intermediate sound velocity maximum, and the DSC axis. Regions where any of these features did not occur because of shallow topography are indicated in the appropriate figures. The USC and intermediate maximum were not uniformly present throughout the exercise area because of variability in oceanographic conditions. Therefore, regions where the USC and intermediate maximum were present less than 20% of the time (effectively absent), 20-80% of the time (transitory), and greater than 80% of the time (permanent) also are indicated on the appropriate figures. A bichannel profile occurs when a USC axis, an intermediate maximum, and a DSC axis are all present. According to Hanna (1969), significant transmission from a source to a receiver in the USC occurs when the upper channel is well developed. Furthermore, receivers located at the bottom of the upper channel (i.e., just above the depth of the intermediate maximum) can perform better than those located at the USC axis due to their position in the convergence zones at the bottom of the upper channel.

### A. Sonic Layer Depth (U).

(U) Figure 20 shows regions with similar average sonic layer depth, and Figure 21 shows regions where a sonic layer was present less than 20% of the time (absent), 20-80% of the time (transitory), and greater than 80% of the time (permanent). Both figures are based on all SQUARE DEAL environmental data. The sonic layer was quite sporadic during SQUARE DEAL, owing to

CONFIDENTIAL

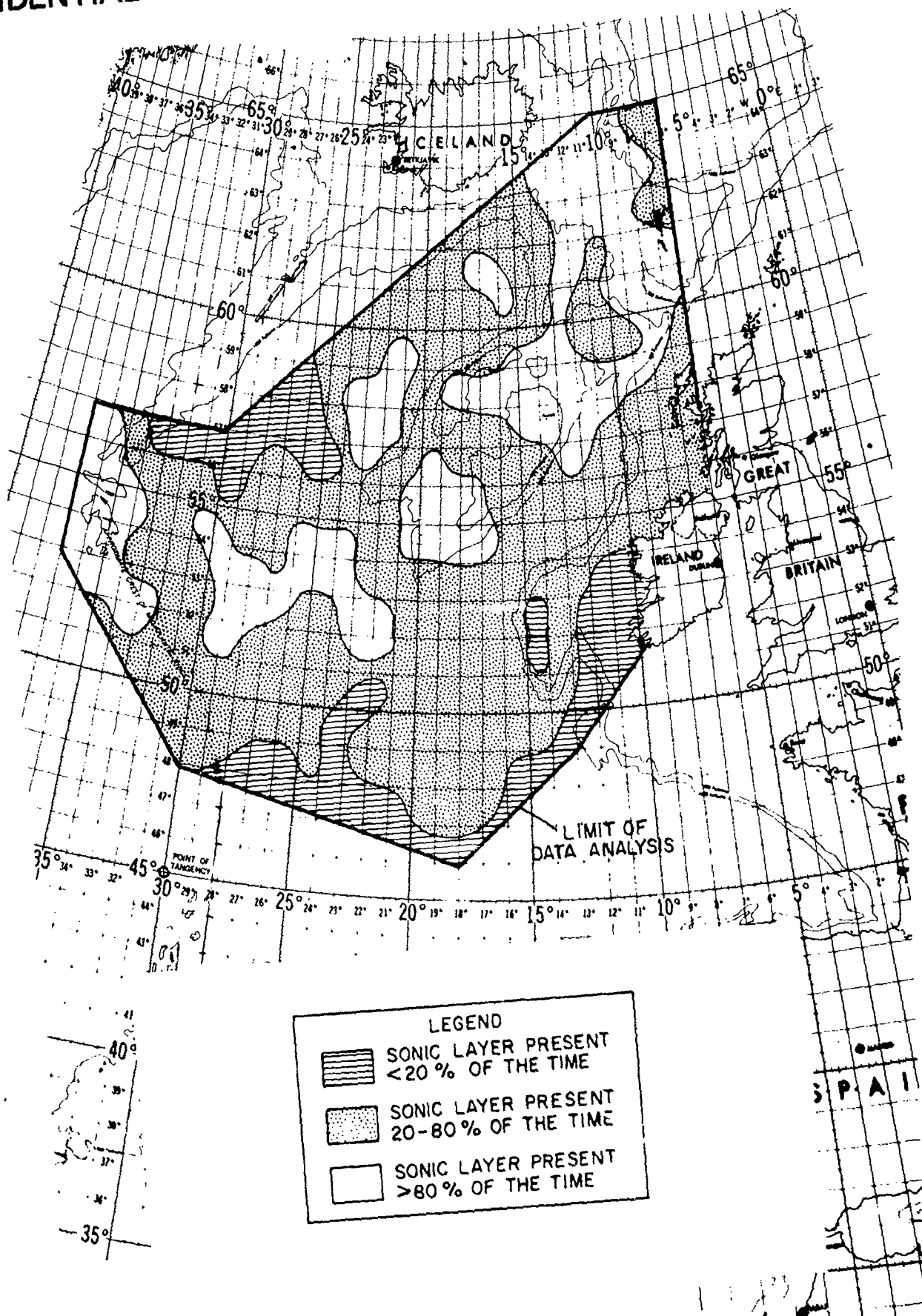


UNCLASSIFIED

(U) Figure 20. Regions With Similar Average Sonic Layer Depth

CONFIDENTIAL

CONFIDENTIAL



UNCLASSIFIED

(U) Figure 21. Persistence of Sonic Layer

CONFIDENTIAL

# CONFIDENTIAL

both diurnal effects and the passage of several storms through the exercise area (see discussion of meteorology in section VII). Generally, a shallower sonic layer (less than 20 m deep) occurred in the southern Maury Trough. Throughout most of the exercise area, sonic layers were transitory in nature. However, permanent sonic layers occurred in a broken band oriented southwest to northeast up the center of the exercise area. This band had the same general orientation as the North Atlantic Current (Fig. 6) and a near-surface front shown for August by Baranov (1972). Within this band, average sonic layer depths were generally deeper than 30 m.

(C) The sonic layer is an efficient sound propagation path only when the wave length of the transmitted signal is short enough to fit into the layer. For this reason, low frequency underwater sound does not propagate well within the surface duct unless the layer is unusually deep. All of the frequencies used during SQUARE DEAL were significantly lower than the theoretical minimum that could propagate in a 50 m deep sonic layer. Consequently, surface duct paths probably were not a significant factor in SQUARE DEAL acoustic propagation.

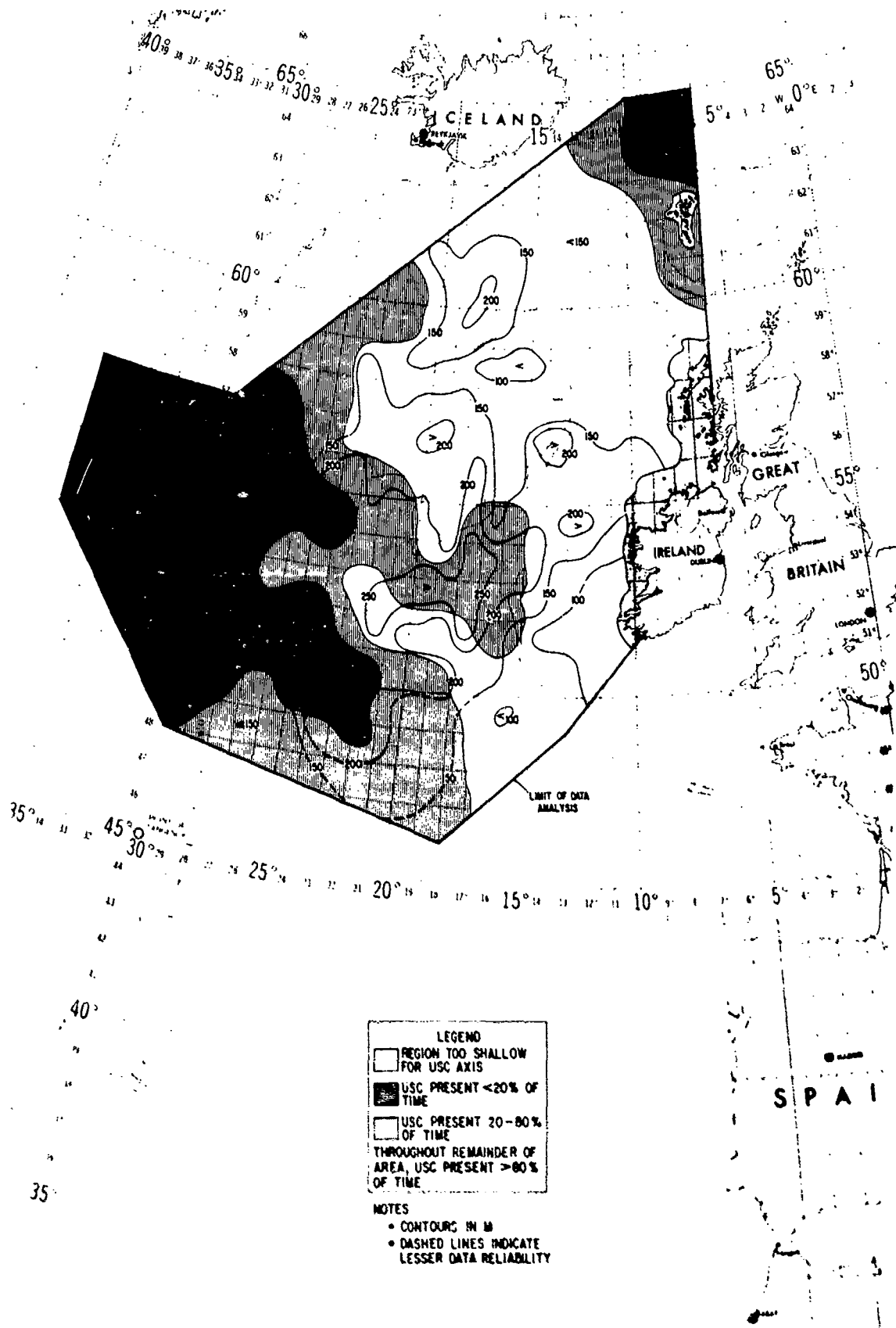
## B. Upper Sound Channel (USC) Axis (U)

(C) Figure 22 shows the average depth of the USC axis based on one-degree square averages of all oceanographic observations collected during the exercise. In general, a permanent USC was present in the eastern half of the exercise area, and USC structures were absent west of  $20^{\circ}\text{W}$  to  $25^{\circ}\text{W}$ . In between these two regions, a transitory USC occurred. The eastern boundary of the region where a USC was absent generally coincided with the subsurface position of the Subarctic Convergence during summer 1968 (Rossov and Kislyakov, 1972). By definition, this front separates colder, lower salinity subarctic waters (such as LSW) from warmer, higher salinity subtropical waters (such as MIW and NACW). When

present, the USC axis varied between 100 and 250 m, and was generally shallowest over Porcupine Bank and the Faeroe Plateau. Of particular interest is the region due west of Porcupine Bank where a permanent USC was absent. This tongue-shaped region roughly corresponded to the flow of LSW from the west that was detected at the Porcupine Bank time-series station (Figs. 18 and 19), even though this flow lay several hundred meters below the depth of the USC axis. The transitory nature of the USC west of Porcupine Bank may be the result of intensive mixing of LSW with NACW and MIW. Further north, a transitory USC occurred over the Faeroe-Iceland Ridge, but disappeared almost entirely in the northeast corner of the exercise area. The USC should have been an effective sound propagation path for sources in the channel in the shallow water regions over Porcupine Bank and the Rockall Plateau, but was too sporadic for effective propagation over the Faeroe-Iceland Ridge. Figure 23 shows standard deviations in the average depth of the USC axis that were approximately 50 m throughout the eastern half of the exercise area. This indicates that the USC was an extremely stable feature when present.

(U) Figure 24 shows average isopleths of sound velocity at the USC axis. When a USC was present, its velocity varied from greater than 1501 m/sec in the south to less than 1486 m/sec in regions along  $25^{\circ}\text{W}$ , in the northern Maury Trough, and over the Faeroe-Iceland Ridge. The upper axial velocity isopleths were far more convoluted than those for upper axial depth (Fig. 22). This indicates that the USC was more stable in terms of depth than in terms of sound velocity. In the region between about  $20^{\circ}\text{W}$  and  $25^{\circ}\text{W}$ , the sound velocity at the USC axis changed rapidly over relatively short distances, as would be expected in the presence of a subsurface front. In the anomalous region west of Porcupine Bank, the isopleths indicate a flow emanating from the west and northwest. The standard deviations in

CONFIDENTIAL

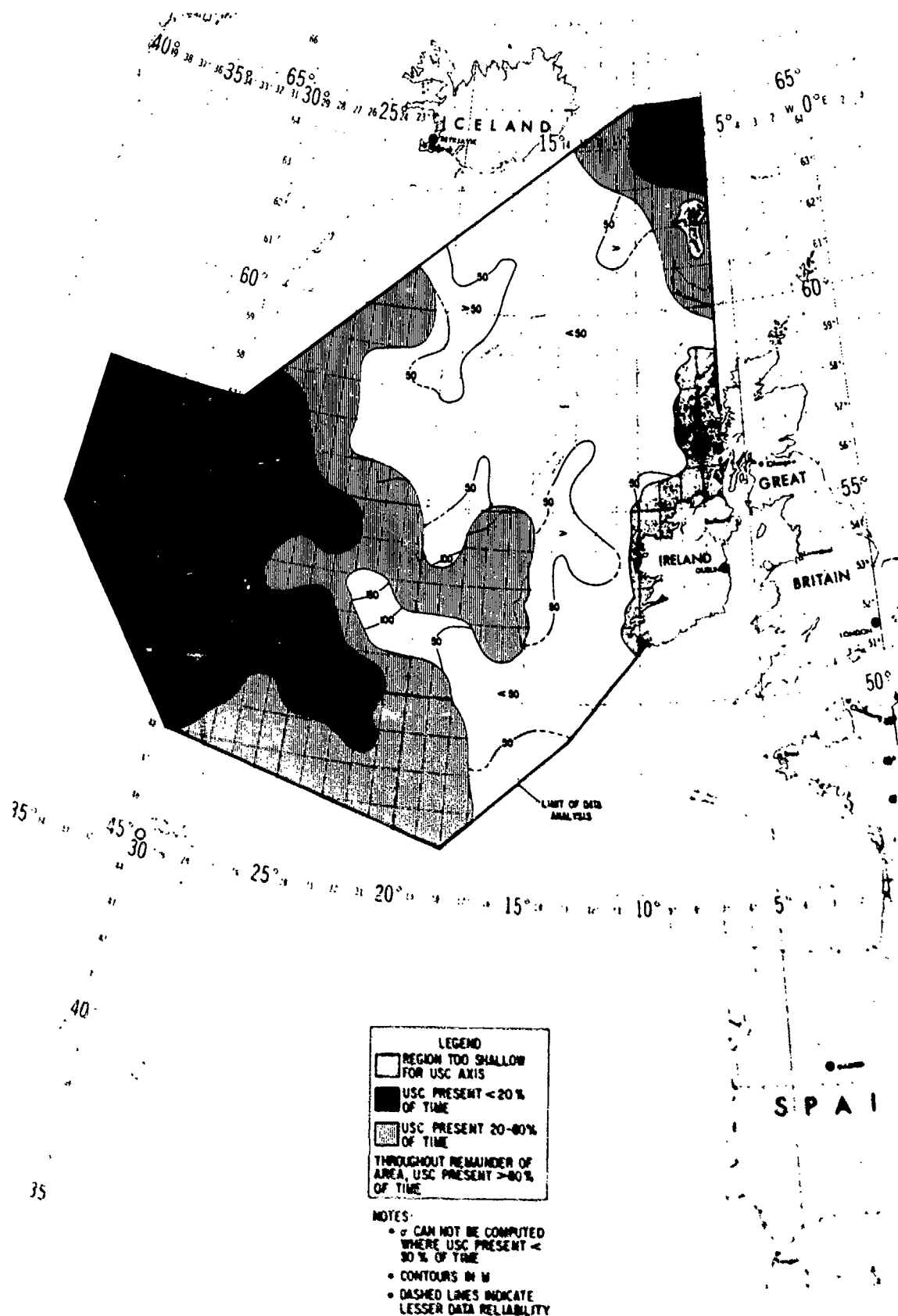


UNCLASSIFIED

(U) Figure 22. Average Depth of Upper Sound Channel Axis

CONFIDENTIAL

CONFIDENTIAL

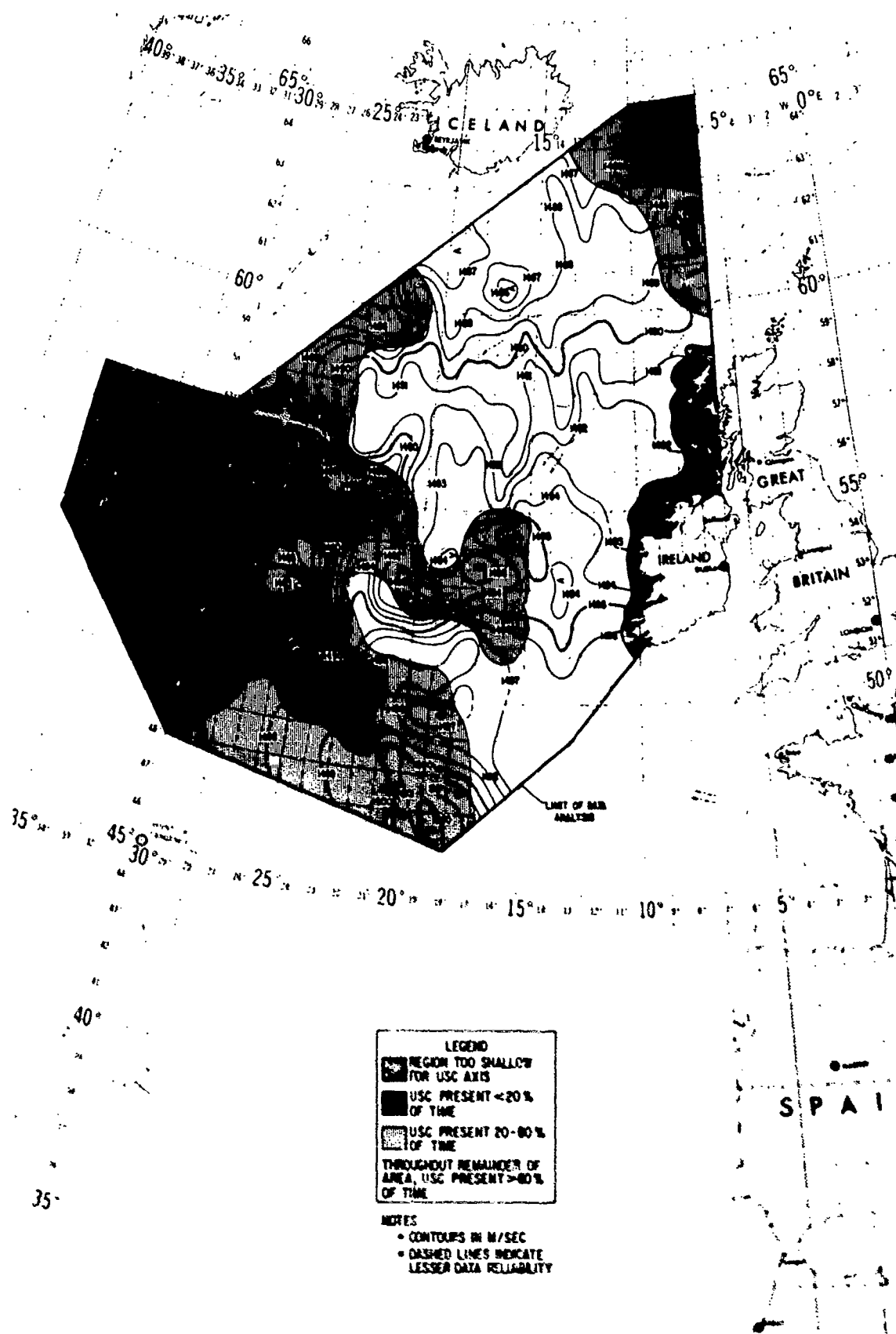


UNCLASSIFIED

(U) Figure 23. Standard Deviation in Average Depth of Upper Sound Channel Axis

CONFIDENTIAL

CONFIDENTIAL



UNCLASSIFIED

(U) Fig. 24. Average Sound Velocity at Upper Sound Channel Axis

CONFIDENTIAL

# CONFIDENTIAL

the sound velocity at the USC axis shown in Figure 25 varied from less than 0.5 m/sec to greater than 2.5 m/sec, but were generally less than 1.0 m/sec throughout the eastern half of the exercise area.

## C. Intermediate Sound Velocity Maximum (U)

(U) Figure 26 shows the intermediate sound velocity maximum based on all SQUARE DEAL environmental data. Again, a permanent maximum was present in the eastern half of the exercise area, but disappeared west of 20°W to 25°W. When present, the maximum varied in depth from about 300 m to greater than 1100 m. In the anomalous tongue-shaped region due west of Porcupine Bank, the intermediate maximum lay at depths less than 500 m and coincided with the approximate depth of maximum winter cooling. However, in Rockall Trough and south of Porcupine Bank, intermediate sound velocity maxima occurred at depths greater than 1000 m that either coincided with or lay below the MIW salinity maximum. A maximum occurred sporadically over the Faeroe-Iceland Ridge, but was absent in the southern Norwegian Sea. Figure 27 presents standard deviations in the average depth of the intermediate sound velocity maximum. These varied from less than 50 m to greater than 200 m, but were generally less than 100 m throughout most of the eastern half of the exercise area, indicating that the intermediate maximum was somewhat less stable than the USC (Fig. 23) in terms of depth. This is understandable since the intermediate maximum was more strongly affected by intrusive water masses.

(U) Figure 28 shows isopleths of average sound velocity at the intermediate maximum. This parameter varied from greater than 1505 m/sec south of Porcupine Bank to less than 1487 m/sec in the regions along about 25°W and over the Faeroe-Iceland Ridge. South of Porcupine Bank and in Rockall Trough where the intermediate maximum coincided with the high salinity MIW core, the sound velocity at the maximum was

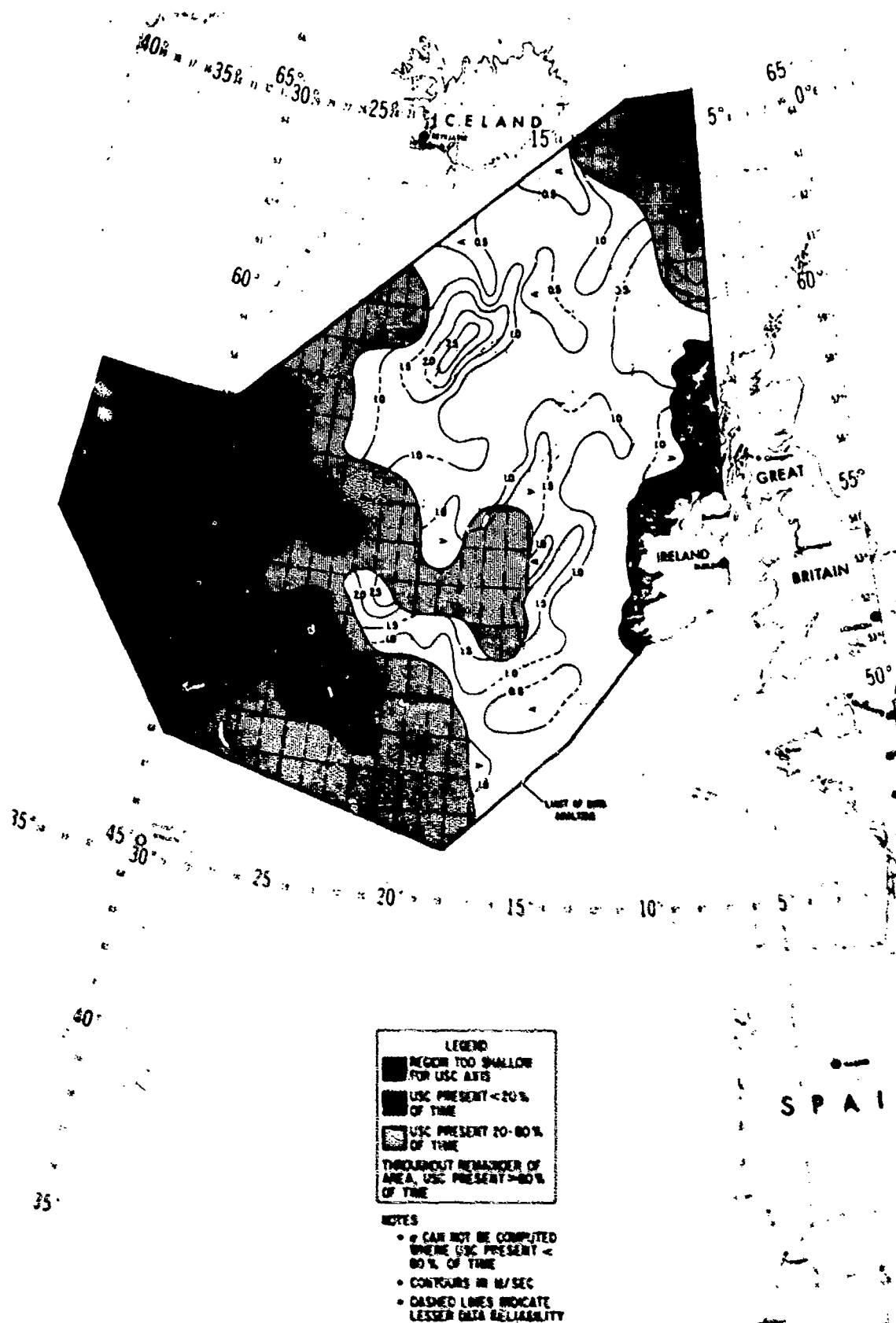
greater than 1500 m/sec. However, in the anomalous tongue west of Porcupine Bank, sound velocities at the maximum were generally less than 1496 m/sec. Lower sound velocities would be expected in the presence of a low salinity flow from the west and northwest (upper-lobe LSW). In three regions approximately along 25°W, along about 52°N, and over the Faeroe-Iceland Ridge, sound velocity at the intermediate maximum changed rapidly over relatively short distances. Frontal zones at intermediate depths have been observed in all three regions. These frontal zones are the subsurface position of the Subarctic Convergence, the intensive mixing zone west of Porcupine Bank, and the Polar Front. The standard deviations in the average sound velocity at the intermediate maximum (Fig. 29) varied from less than 0.5 m/sec to greater than 3.0 m/sec. As expected, these standard deviations showed more variation than those for upper axial velocity (Fig. 25).

## D. Strength of Upper Sound Channel (U)

(C) Figure 30 shows contours of the "strength" of the USC based on one-degree square averages of all SQUARE DEAL environmental data. "Strength" is defined as the difference between the average sound velocity at the intermediate sound velocity maximum or at the bottom and the average sound velocity at the USC axis. As previously mentioned, a well-developed USC can act as a sound propagation path for sources in the upper channel (Hanna, 1969). Hanna did not define the term "well developed", but does show instances of USC propagation for profiles with "strengths" of about 3 and 11 m/sec. During SQUARE DEAL, sound propagation via the USC was observed along a KINGSFORT SUS run between points 2BB and 3AB (Maury Center for Ocean Science, 1974). Based on the isopleths in Figure 43, the "strength" of the USC along the 2BB-3AB track was approximately 4 m/sec except near point 3AB, where it was less than 3 m/sec. Considering these data and Hanna's findings, it is safe to assume that



**CONFIDENTIAL**

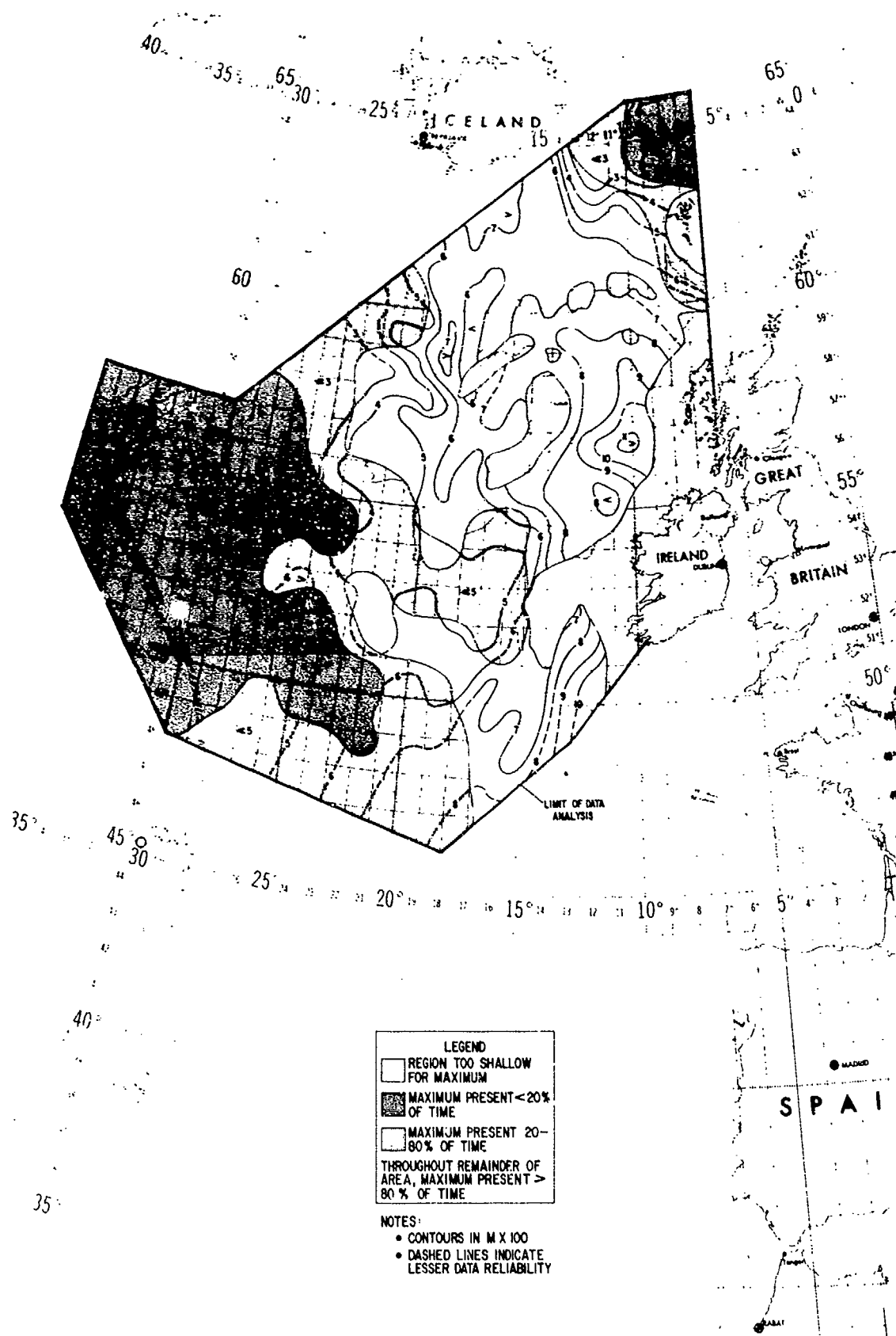


UNCLASSIFIED

(U) Figure 25. Standard Deviation in Average Sound Velocity at Upper Sound Channel Axis

**CONFIDENTIAL**

CONFIDENTIAL

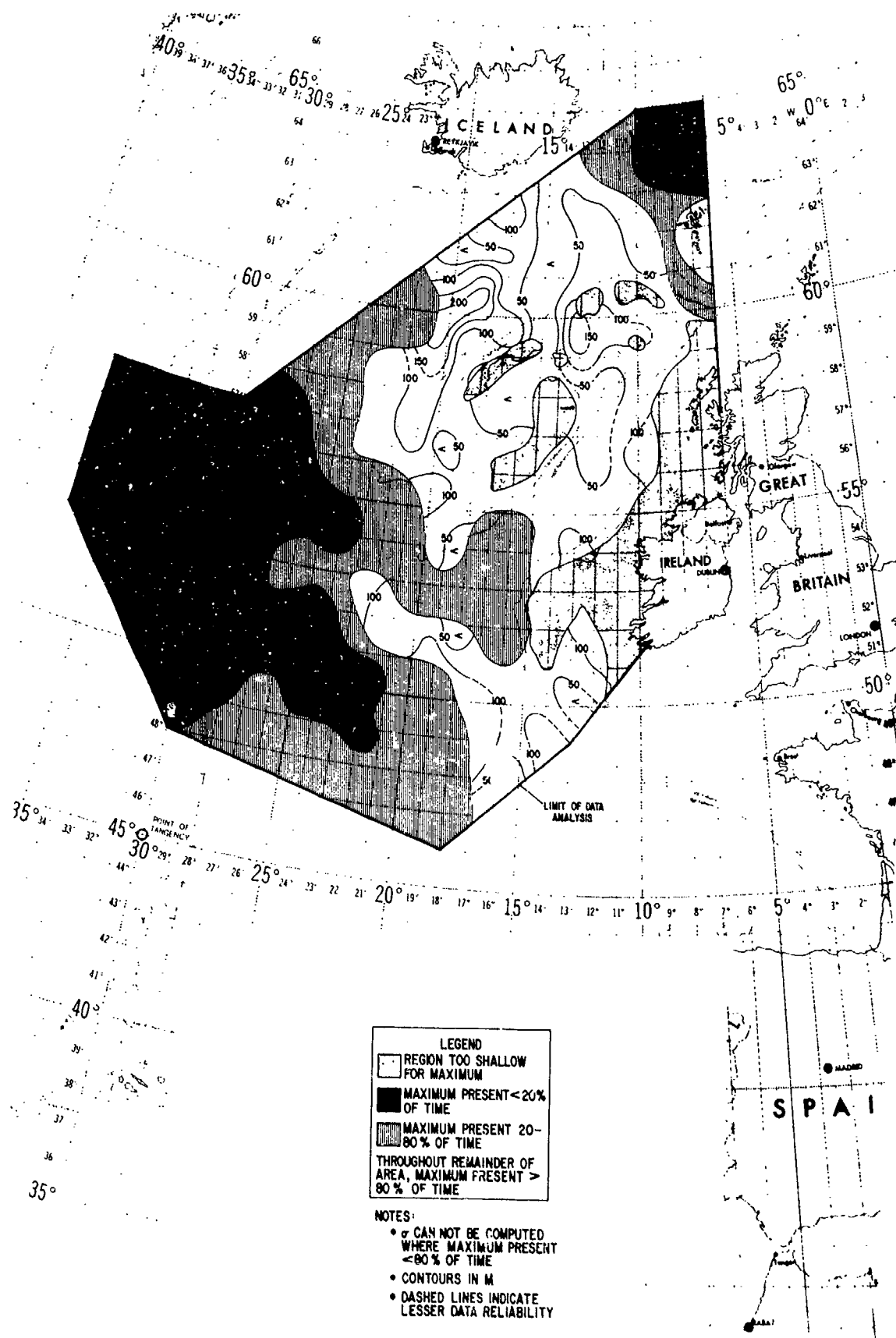


UNCLASSIFIED

(U) Figure 26. Average Depth of Intermediate Maximum

CONFIDENTIAL

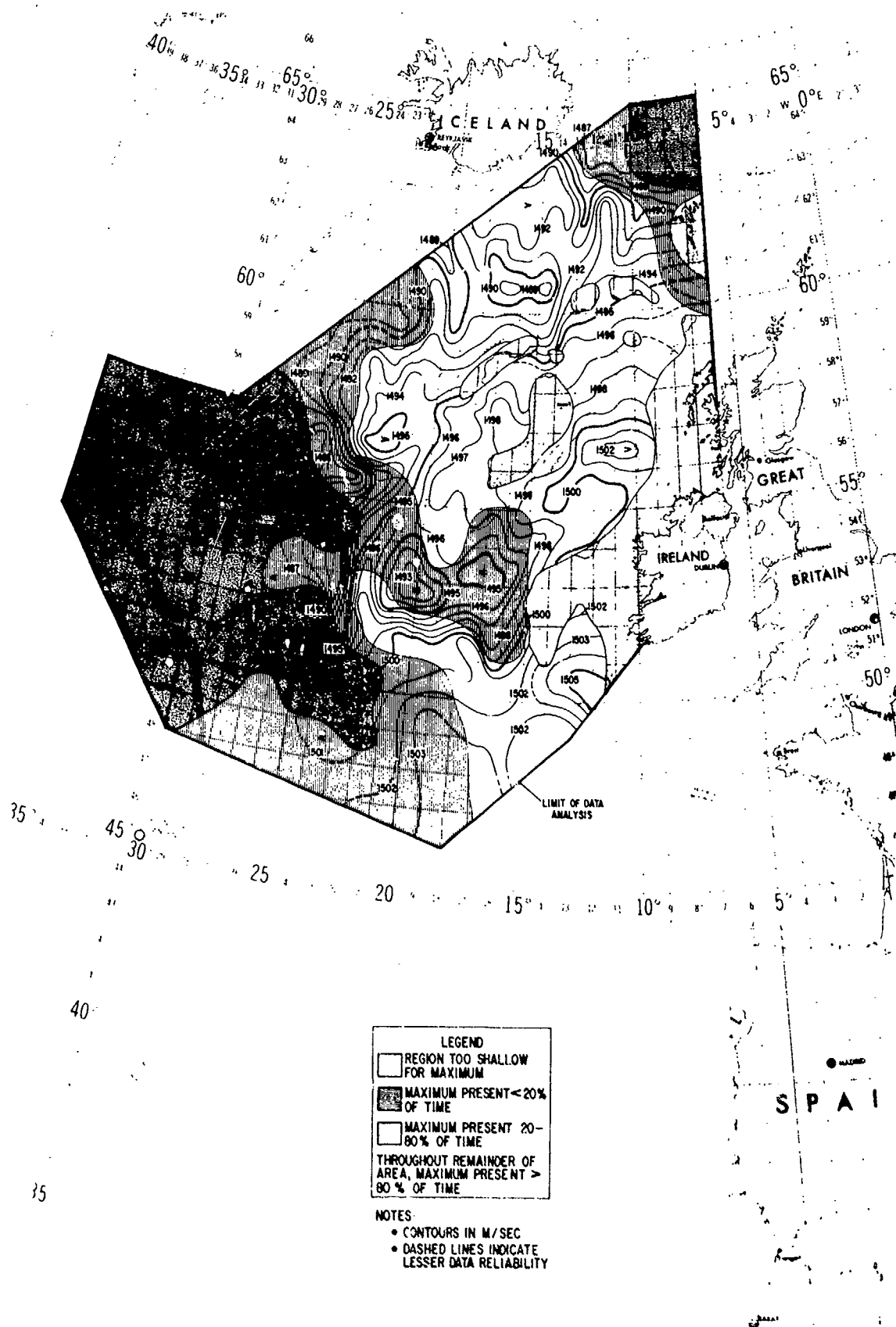
CONFIDENTIAL



UNCLASSIFIED

(U) Figure 27. Standard Deviation in Average Depth of Intermediate Maximum

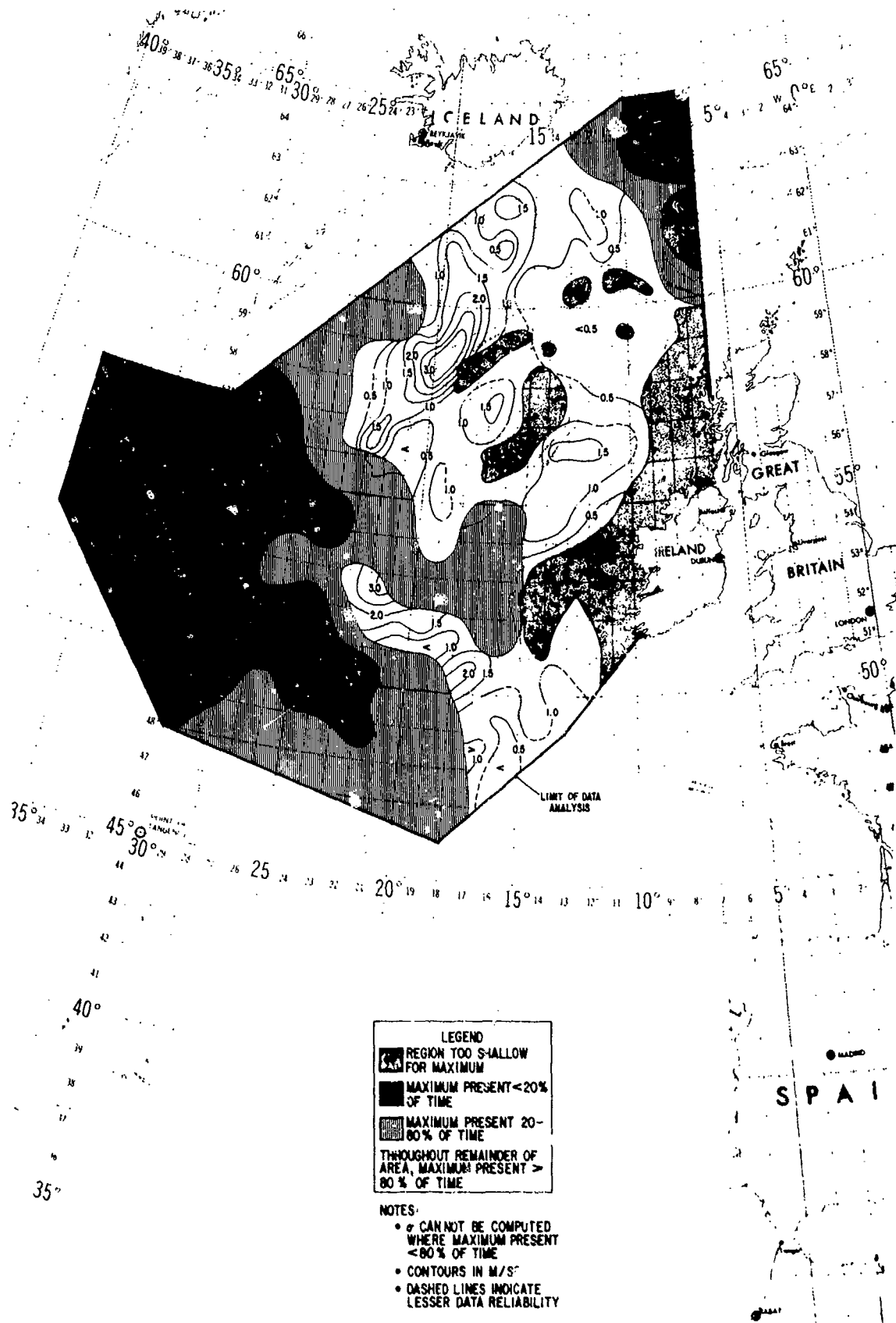
CONFIDENTIAL



UNCLASSIFIED

(U) Figure 28. Average Sound Velocity at Intermediate Maximum

CONFIDENTIAL

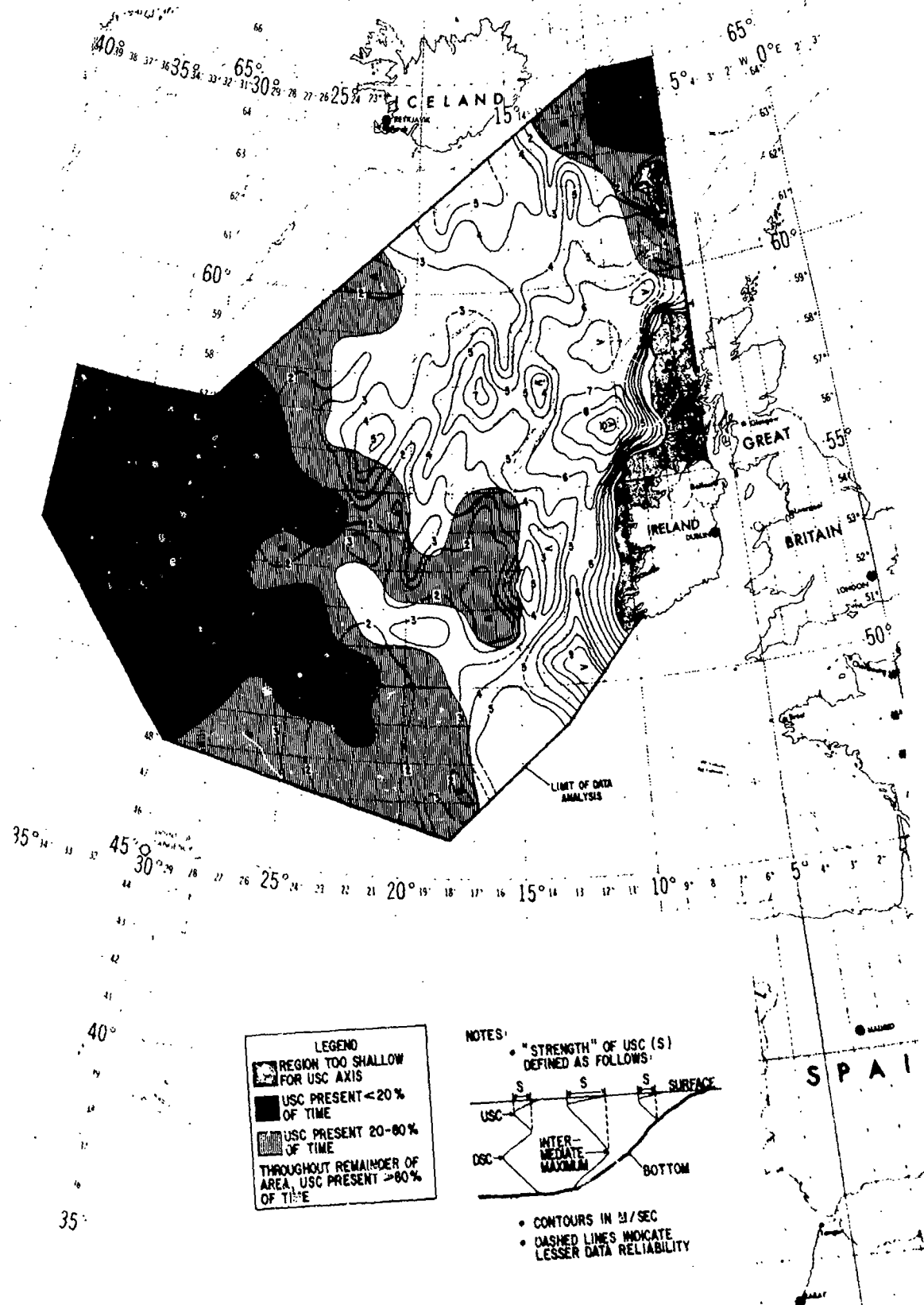


UNCLASSIFIED

(U) Figure 29. Standard Deviation in Average Sound Velocity at Intermediate Maximum

CONFIDENTIAL

CONFIDENTIAL



UNCLASSIFIED

(U) Figure 30. "Strength" of Upper Sound Channel

CONFIDENTIAL

some USC propagation was possible during SQUARE DEAL in regions where the "strength" of the USC exceeded 3 m/sec. Such regions occurred throughout most of the eastern half of the exercise area except over the shallowest portions of Porcupine Bank, in the anomalous tongue due west of Porcupine Bank, and over the Faeroe-Iceland Ridge.

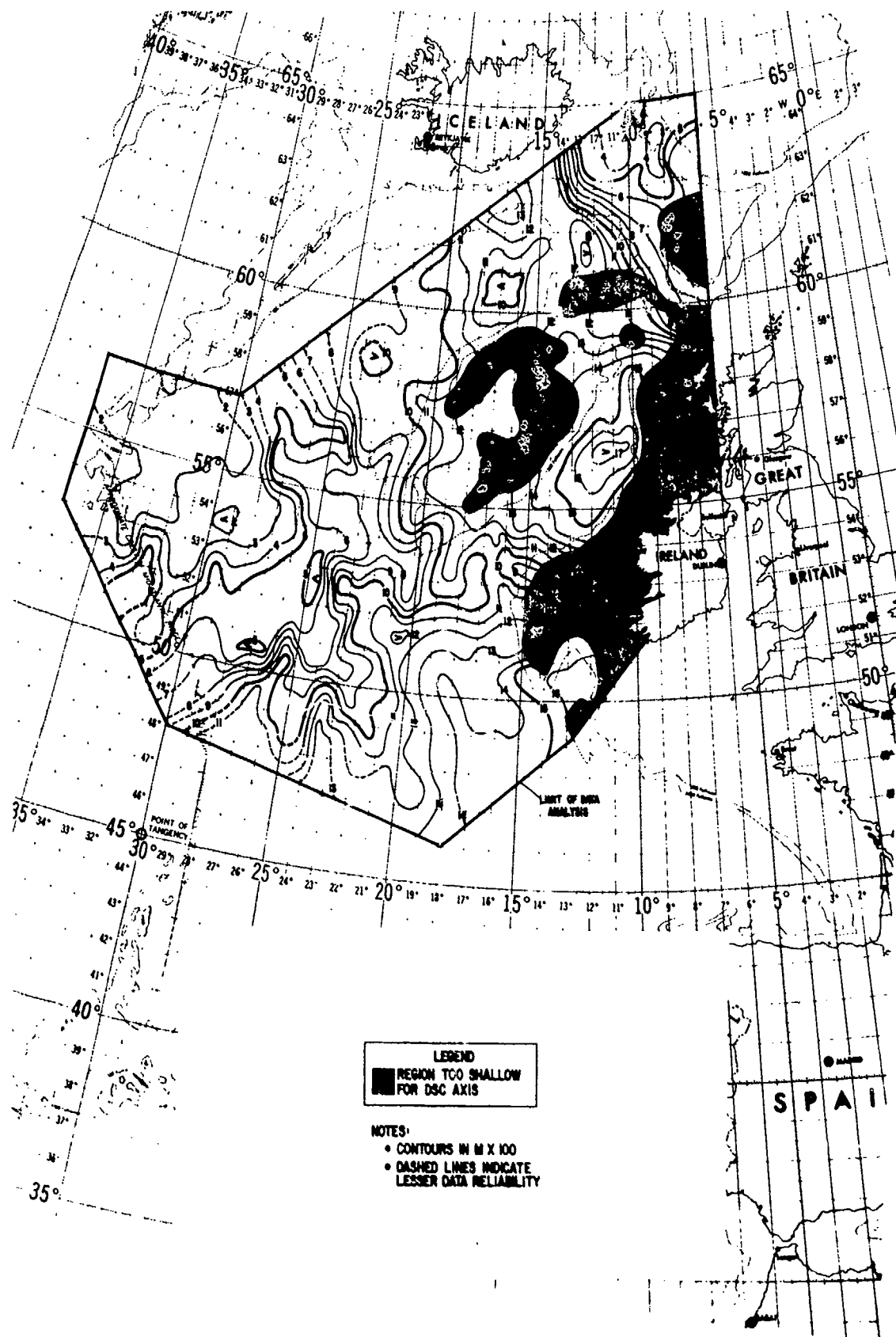
## E. Deep Sound Channel (DSC) Axis (U)

(C) Figure 31 shows the average depth of the DSC axis based on one-degree square averages of all exercise environmental data. A DSC axis was present throughout the exercise area at depths that varied from less than 100 m over the southern end of the Reykjanes Ridge to more than 1600 m in Rockall Trough and the region south of Porcupine Bank. The isopleths shown in Figure 31 indicate two frontal zones at intermediate depths, one over the Faeroe-Iceland Ridge and one between 20°W and 25°W. The first zone corresponds to the Polar Front, the second to the subsurface position of the Subarctic Convergence (Rossov and Kislyakov, 1972). Generally the DSC was controlled by LSW in regions where the axis was less than 900 m deep, except over the Faeroe-Iceland Ridge. Here, NSOW caused a sound velocity minimum just above the bottom. In regions where the DSC was deeper than 1200 m, it was controlled by either MIW (southeast part of exercise area and Rockall Trough) or by NSOW (foot of Faeroe-Iceland Ridge). Axial depths of less than 900 m at about 53°N, 15°W indicate an intrusion of upper-lobe LSW that extended east as far as Porcupine Bank. No DSC was present over Porcupine Bank, much of the Rockall Plateau, or the Wyville-Thomson Ridge, precluding this sound propagation path. Over the Faeroe-Iceland Ridge, the DSC was too close to the bottom for effective propagation. However, throughout the remainder of the exercise area, the DSC probably was the most efficient path for underwater sound propagation.

(U) Figure 32 presents contours of standard deviation in average deep axial depth, which varied between less than 50 m and greater than 300 m. This figure indicates substantial variability in the depth of the DSC axis throughout the exercise area. Generally, standard deviations were less than 50 m south of Porcupine Bank, over the Rockall Trough, in the region west of 30°W, and over the Faeroe-Iceland Ridge. In these regions, deep axial depth was strongly controlled by MIW, LSW, and NSOW. Standard deviations were generally greater than 150 m along the southern boundary of the exercise area, in the region southwest of the Rockall Plateau, and in the northern Maury Trough; mixing of various intrusive water masses was detected in these areas during the exercise. Due to the greater effects of intermediate water masses, standard deviations in deep axial depth were greater than those for upper axial depth (Fig. 23) or the depth of the intermediate sound velocity maximum (Fig. 27).

(U) Figure 33 shows contours of average sound velocity at the DSC axis. Deep axial velocity varied from greater than 1496 m/sec south of Porcupine Bank and in the Rockall Trough to less than 1455 m/sec over the Faeroe-Iceland Ridge. The isopleths shown in this figure are extremely convoluted throughout the exercise area owing to mixing between various intermediate water masses. MIW flows from the south and southeast and LSW flows from the north and northwest are easily discernable in the various isopleth patterns. Generally, DSC axial velocities less than 1488 m/sec were controlled by low salinity LSW, except over the Faeroe-Iceland Ridge where NSOW was the predominant influence. Deep axial velocities greater than 1490 m/sec were primarily controlled by high salinity MIW. Axial velocities of less than 1488 m/sec west of Porcupine Bank offer additional evidence of a low salinity flow from the west and northwest. Along about 25°W, the subsurface Subarctic Convergence caused a compression of the deep axial velocity

CONFIDENTIAL



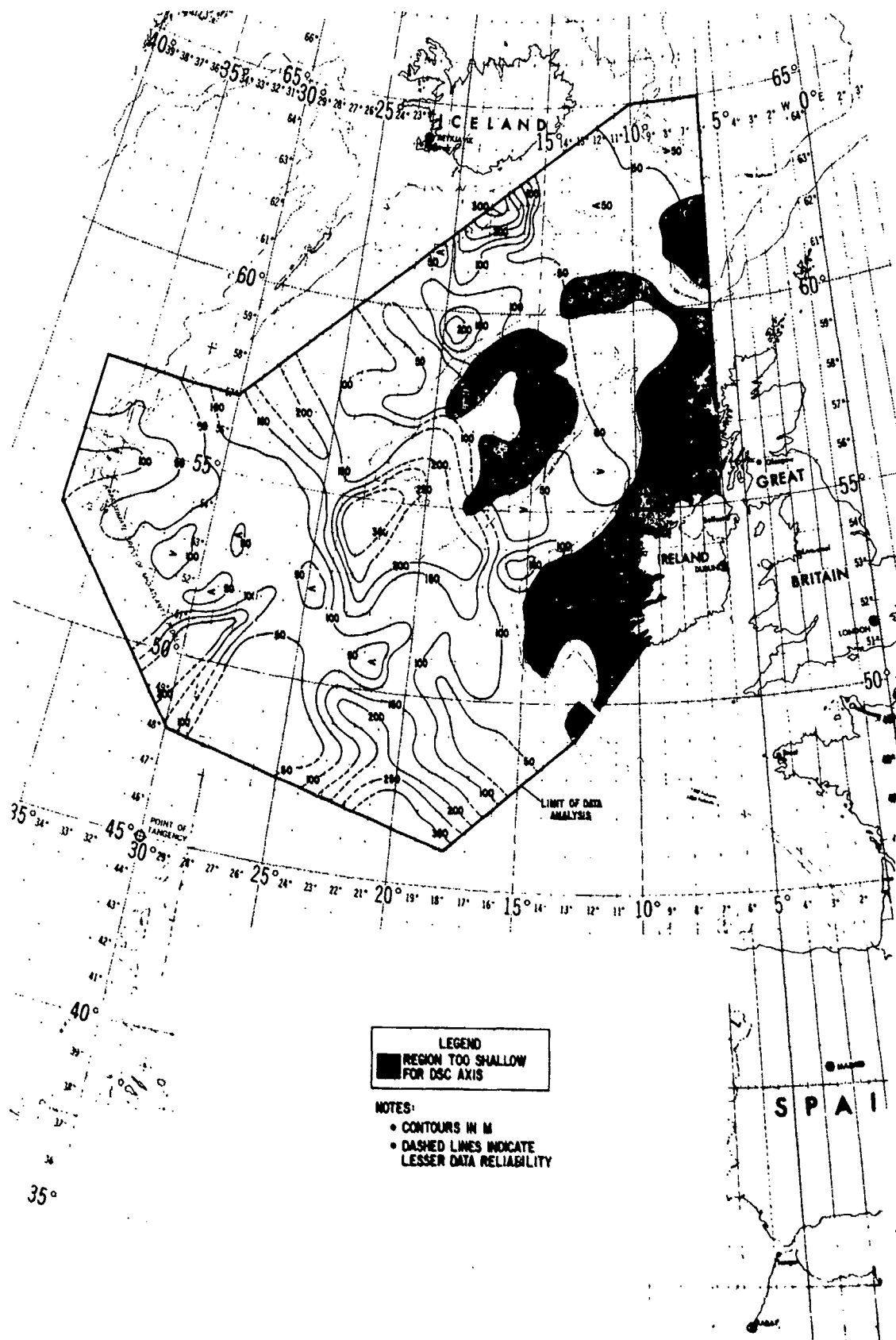
UNCLASSIFIED

(U) Figure 31. Average Depth of Deep Sound Channel Axis

CONFIDENTIAL



CONFIDENTIAL

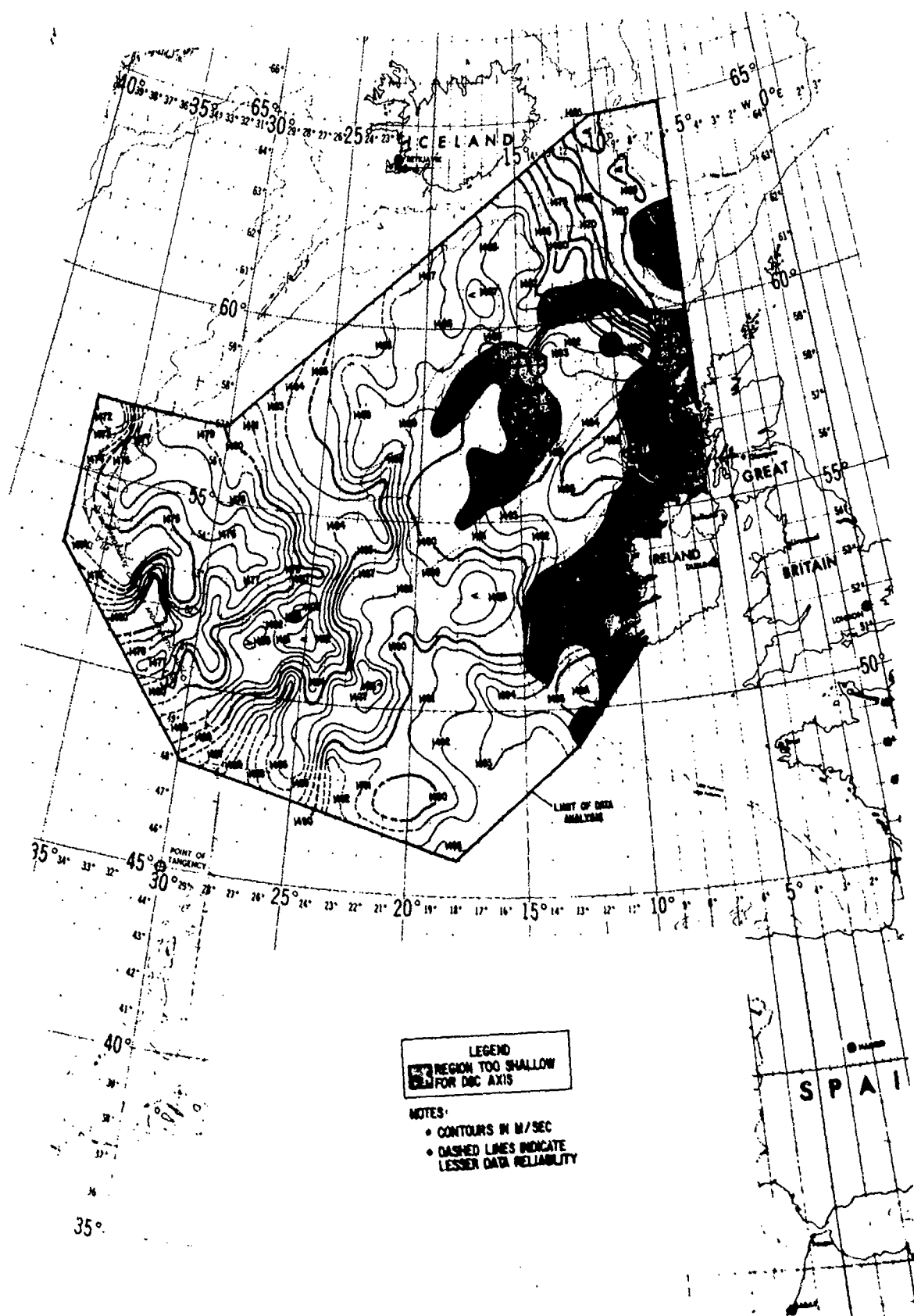


UNCLASSIFIED

(U) Figure 32. Standard Deviation in Average Depth to Deep Sound Channel Axis

CONFIDENTIAL

CONFIDENTIAL



UNCLASSIFIED

(U) Figure 33. Average Sound Velocity at Deep Sound Channel Axis

CONFIDENTIAL

# CONFIDENTIAL

isopleths and resulted in horizontal gradients as great as 0.2 m/sec/nm. In the northern Rockall Trough, mixing between NACW, MIW, and NSOW produced a horizontal gradient of nearly 0.5 m/sec. This gradient was even stronger than that found over the Faeroe-Iceland Ridge.

(U) Figure 34 presents standard deviations in the average sound velocity at the DSC axis. These standard deviations varied between less than 0.5 m/sec and greater than 2.5 m/sec, and were generally greater than 1.5 m/sec along frontal zones and in regions of intensive mixing. Over the exercise area as a whole, standard deviations in deep axial velocity were of the same general magnitude as those for upper axial velocity (Fig. 25) and sound velocity at the intermediate maximum (Fig. 29). The same was not true for standard deviations in the depth of the DSC axis (Fig. 33), indicating that the depth of the DSC axis was more sensitive to temporal and spatial fluctuations in the environment than was sound velocity at the DSC axis.

## F. Critical Depth (U)

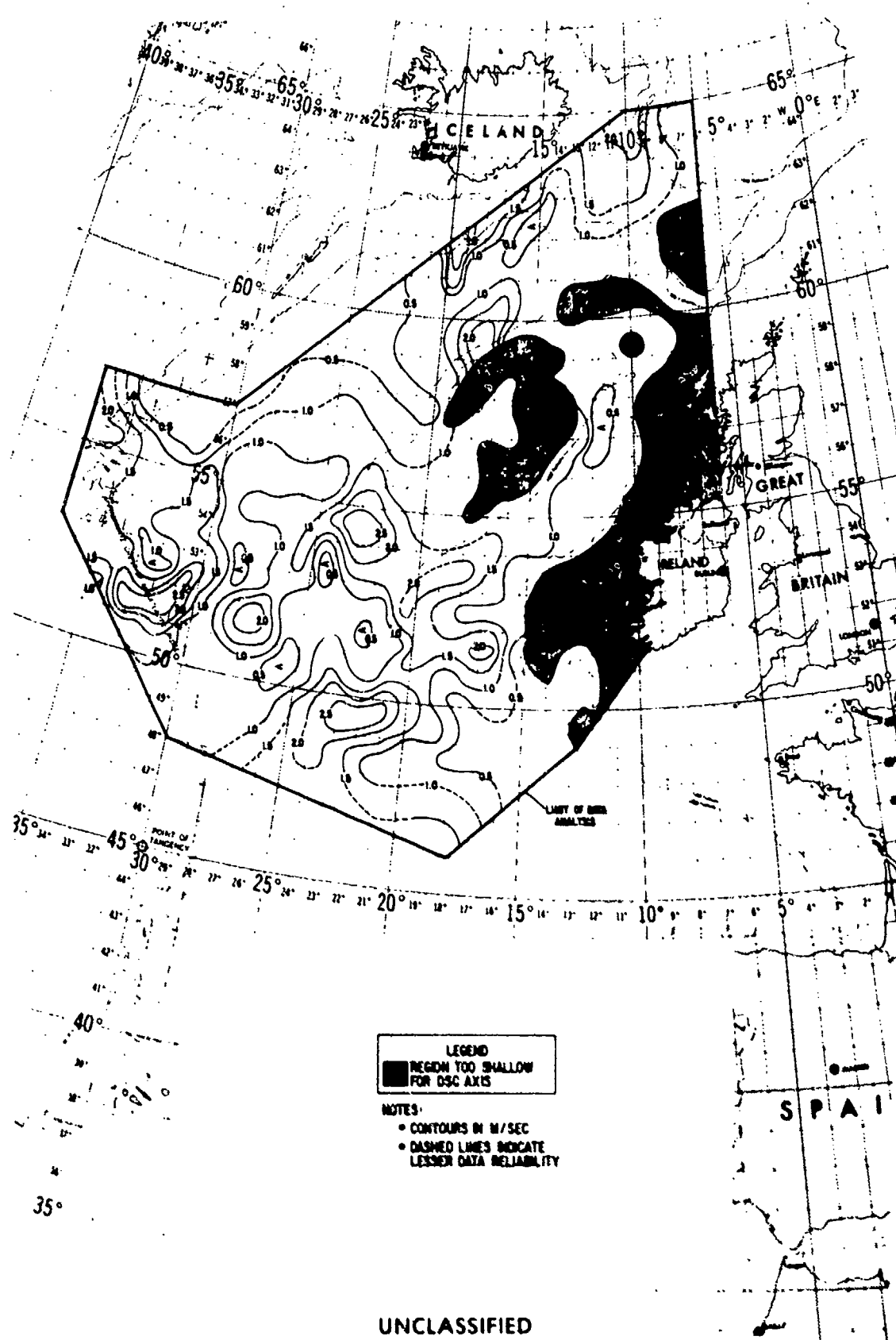
(U) Figure 35 shows average contours of critical depth based on all environmental data collected during the SQUARE DEAL Exercise. Since critical depth is strongly dependent on near-surface oceanographic conditions and circulation patterns, the various isopleths in Figure 35 are shown not only for regions deeper than critical depth (i.e., regions of depth excess), but also for regions where the bottom is shallower than critical depth (i.e., regions of depth difference). Critical depths varied from greater than 3400 m along about 47°N to less than 1500 m over the southern end of the Reykjanes Ridge and in the region surrounding the Faeroe Islands. Over the Faeroe-Iceland Ridge, extremely cold NSOW just above the bottom caused anomalously deep critical depths (greater than 2800 m at about 64°N, 12°W) and the intense Polar Front caused a marked compression of the critical depth

isopleths. South of the Faeroe-Iceland Ridge, the 2000 m isopleth delineates a flow of NSOW into the northern Maury Trough. However, throughout most of the exercise area, the orientation of the critical depth isopleths was determined by the circulation of the North Atlantic Current (Fig. 6), and was quite similar to the orientation of isotherms at 10 m depth (Fig. 9). Figure 36 presents standard deviations in average critical depth, which varied from less than 50 m to greater than 250 m. These standard deviations were generally higher in the vicinity of near-surface frontal zones, and resembled those for temperature at 10 m (Fig. 10).

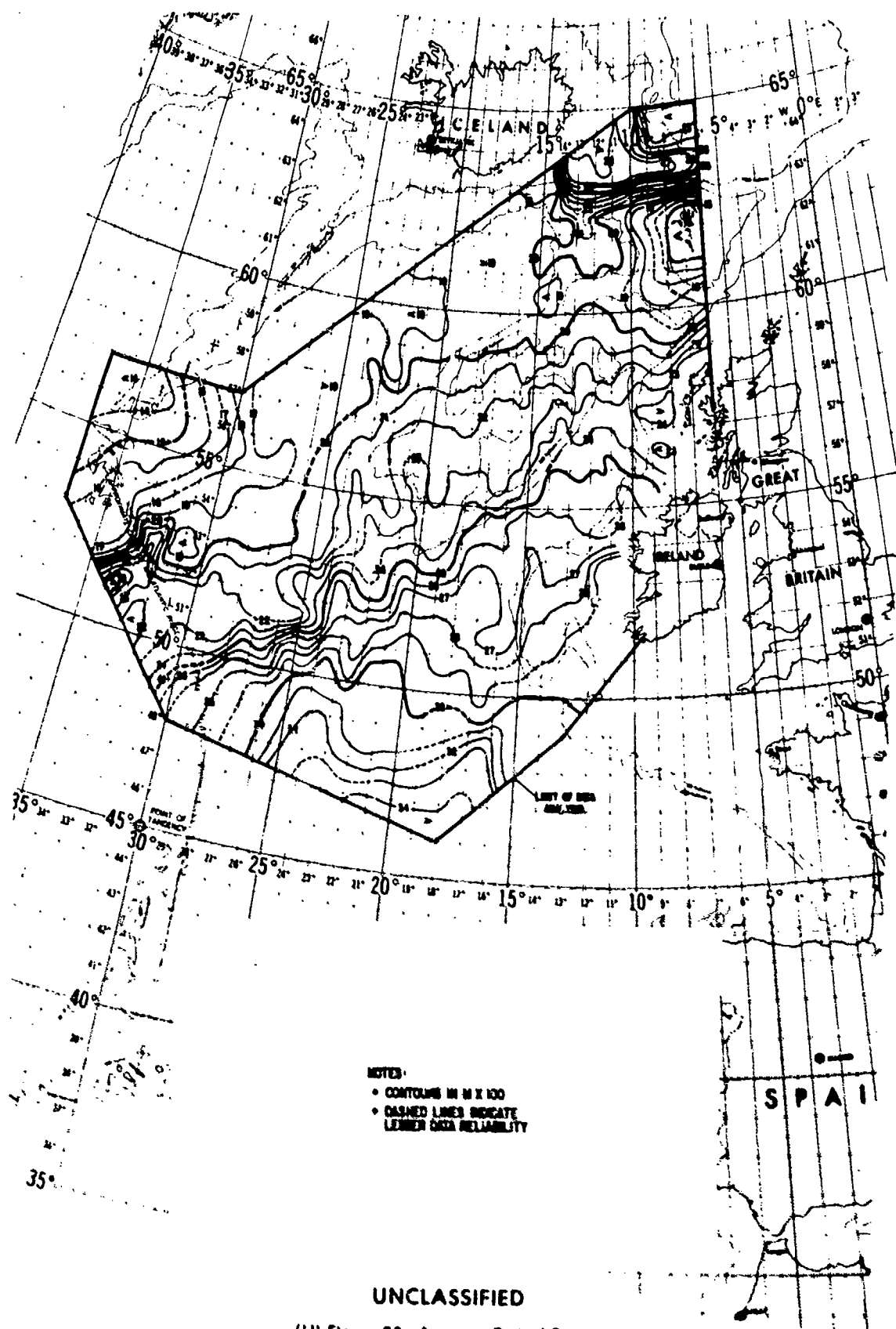
## G. Depth Difference/Depth Excess (U)

(C) Figure 37 depicts regions shallower and deeper than average critical depth. The former are regions of depth difference (bottom-limited); the latter are regions of depth excess. The bathymetric chart used to prepare Figure 37 is the same as given in the SQUARE DEAL Exercise Plan (Maury Center for Ocean Science, 1973). As a general rule, more than 400 m of depth excess are required for reliable convergence zone propagation from a near-surface source. The shallow bathymetry of Porcupine Bank, the Scotland continental shelf, Rockall Plateau, northern Rockall Trough, and the Faeroe-Iceland Ridge caused bottom-limited regions during SQUARE DEAL. However, in all these regions except the Faeroe-Iceland Ridge, a well developed USC occurred more than 80% of the time (Fig. 22). Consequently, long-range propagation for sources within the USC was possible in these shallow water regions.

(C) Other bottom-limited regions occurred over the crests of the Reykjanes and Mid-Atlantic Ridges (along the western boundary of the exercise area). However, between about 52°N and 53°N, the Gibbs Fracture Zone caused a region where depth excess was greater than 2000 m. The offset of this fracture zone apparently provided a transmission "window" through the



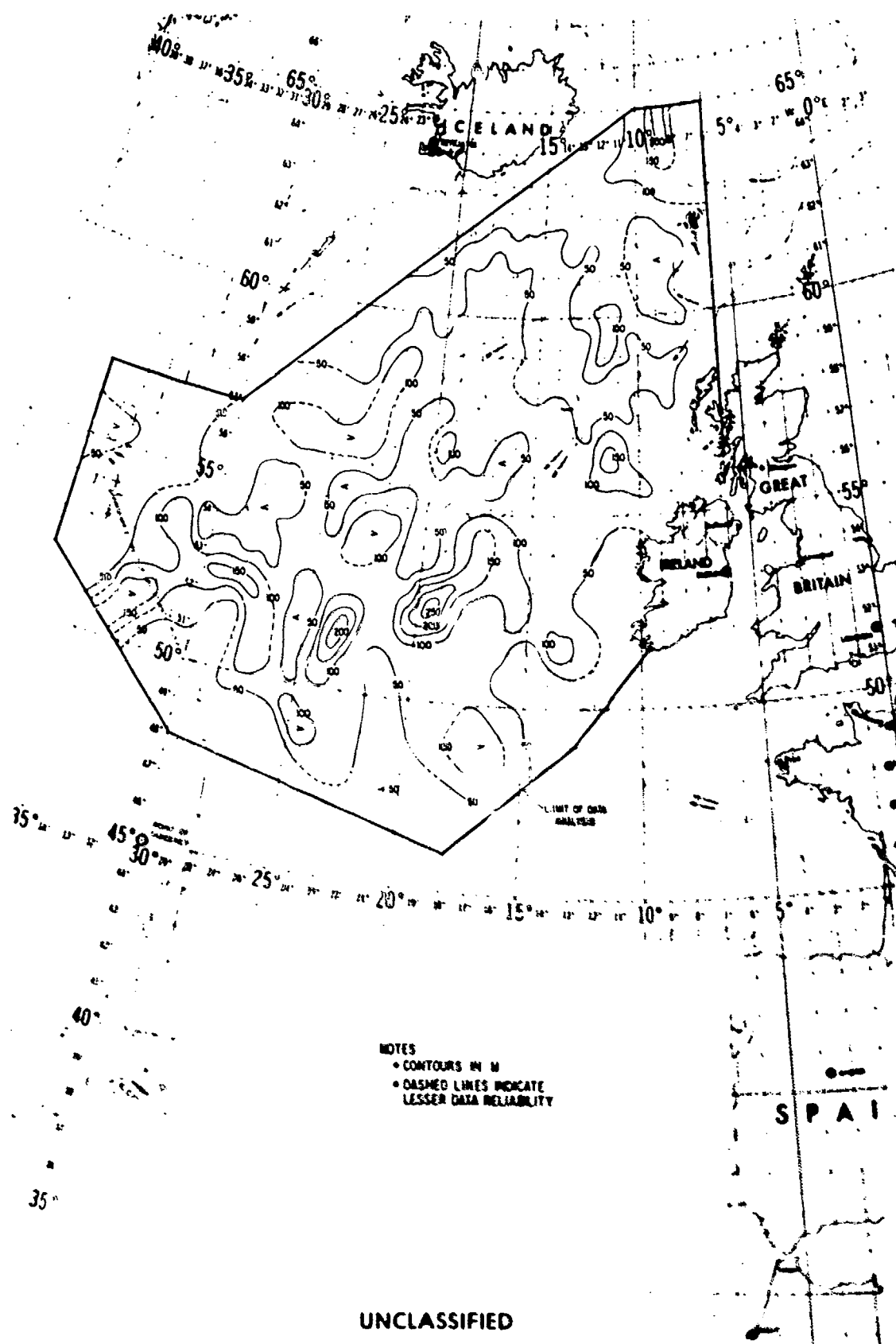
(U) Figure 34. Standard Deviation in Average Sound Velocity at Deep Sound Channel Axis



UNCLASSIFIED

(U) Figure 35. Average Critical Depth

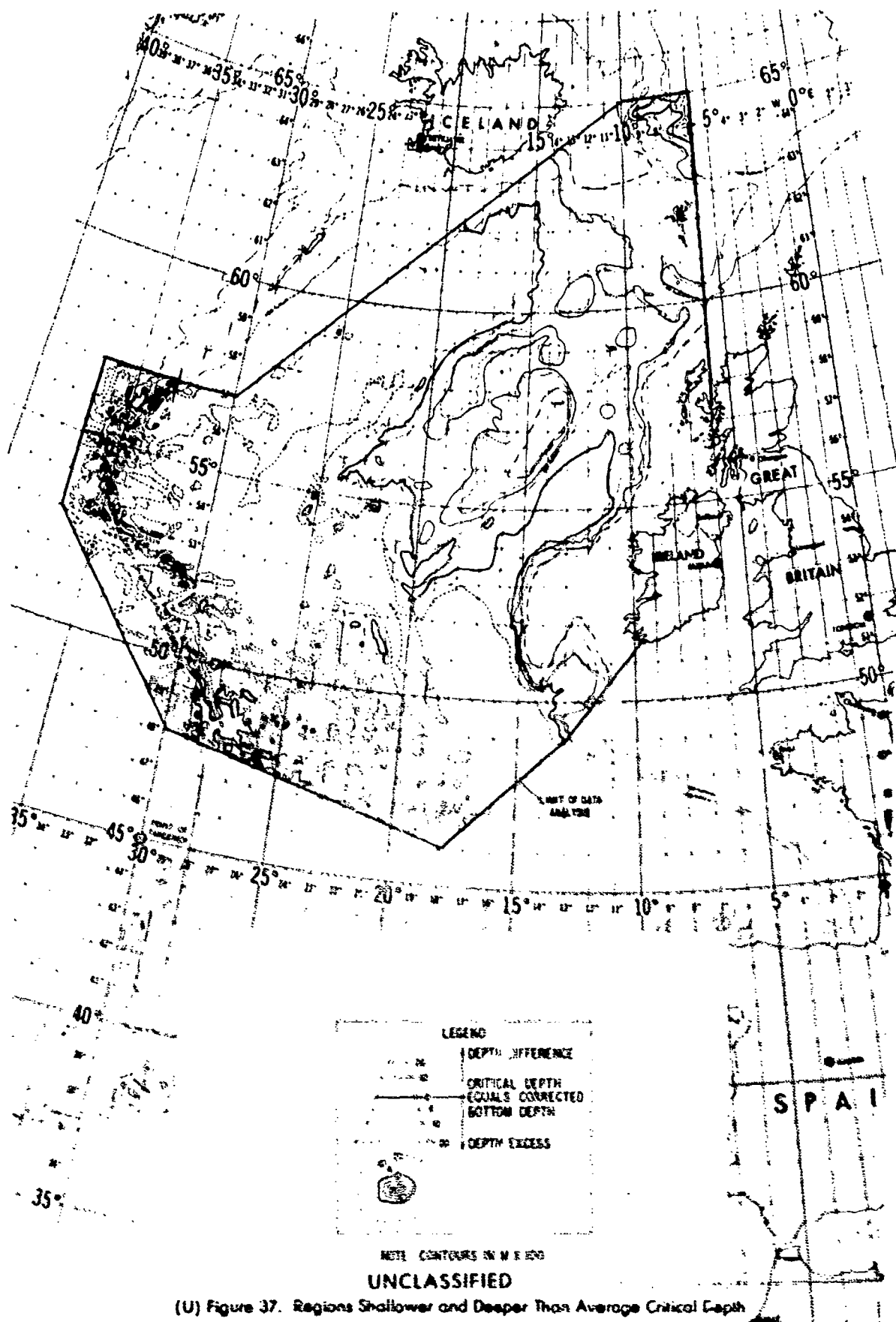
CONFIDENTIAL



(U) Figure 36. Standard Deviation in Average Critical Depth

CONFIDENTIAL

CONFIDENTIAL



(U) Figure 37. Regions Shallower and Deeper Than Average Critical Depth

CONFIDENTIAL

Mid-Atlantic Ridge during the exercise. Convergence zone propagation from a near-surface source should have been possible throughout most of the West European Basin and Maury Trough. However, acoustic propagation over the Faeroe-Iceland Ridge was blocked except for less reliable bottom bounce paths.

## VI. Spatial Variability in Sound Velocity Along SQUARE DEAL Baselines (U)

(C) Figures 38-41 show sound velocity profiles plotted at their position of observation, bathymetric profiles, and contoured sound velocity cross sections along four SQUARE DEAL baselines. These baselines and their corresponding acoustic events are as follows:

- Figure 38, point 1E to point 3B, WILKES phase Signal Underwater Sound I (SUS) run, 020600Z Aug - 042232Z Aug (event 2a).
- Figure 39, point 2L to point 2K, OLMEDA phase II SUS run, 220000Z Aug - 240313Z Aug (event 14b).
- Figure 40, point 2BB to point 3AB, KINGSPORT phase II CW tow, 182228Z Aug - 200073Z Aug (event 13a).
- Figure 41, point 3F to point 3ZZ, OLMEDA phase III SUS run, 071500Z Sep 101928Z Sep (event 22a).

Figures 38-40 are plotted so that the acoustic event begins on the left and proceeds to maximum range on the right. Figure 41 is plotted from south to north (although the SUS run was made from north to south) for continuity with Figure 39.

### A. Point 1E to Point 3B Track (Phase I) (U)

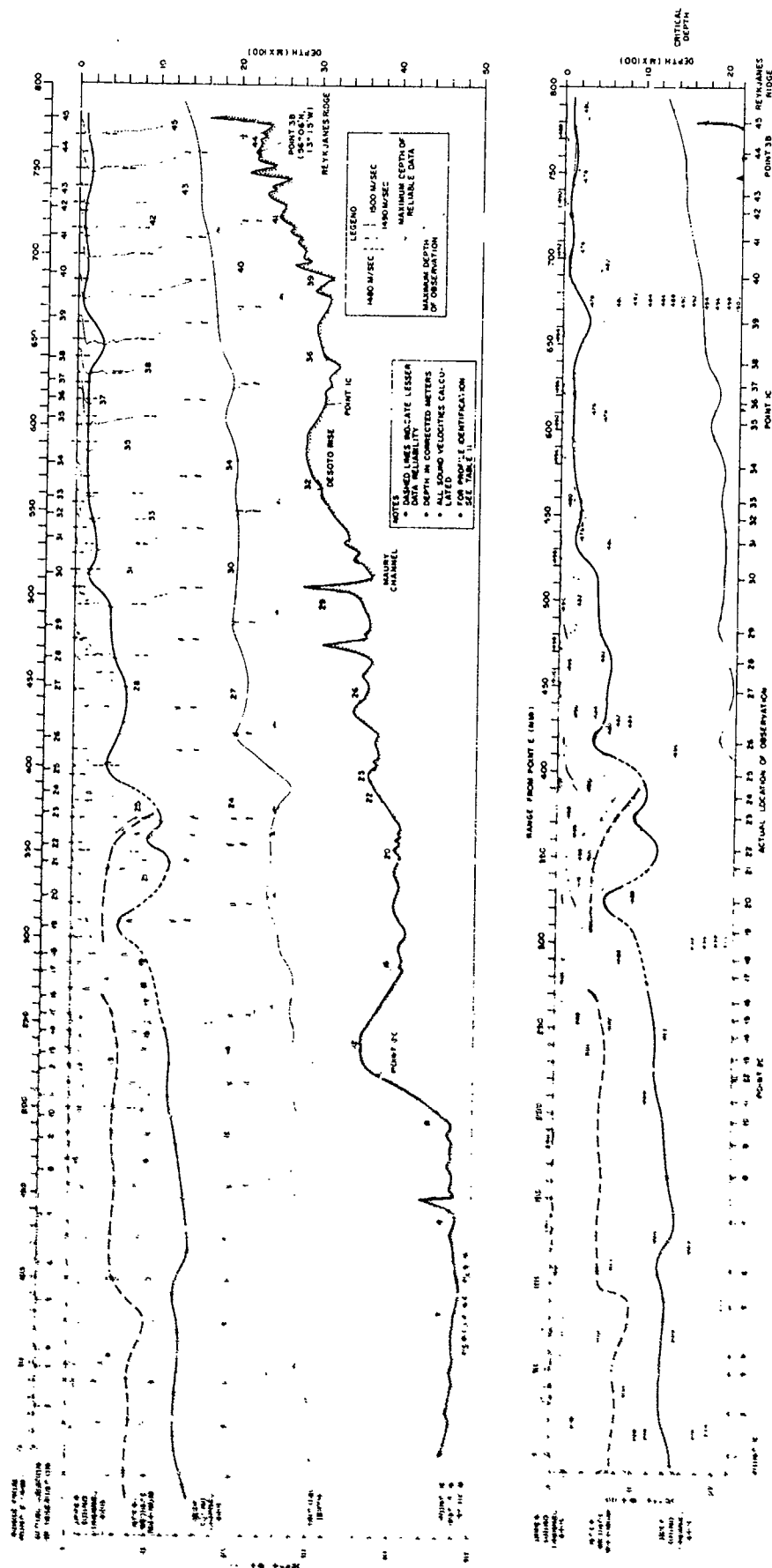
(C) The oceanographic data shown in Figure 38 were collected between 1 and 6 August and are identified in Table 11 (Appendix B). The bathymetric profile was recorded by WILKES. The overall sound velocity structure along the 1E-3B track was quite variable, since the first half of the track lay within the North Atlantic Current under the influence of L'W (Fig. 6). Surface sound velocities varied from about 1513 m/sec at point 1E to about

1489 m/sec at point 3B. A sporadic sonic layer to about 20 m occurred along most of the track. However, this surface duct was not deep enough to permit low frequency acoustic propagation. A continuous USC and intermediate sound velocity maximum occurred along the first 270 nm, but abruptly terminated when the track crossed the south wall of the North Atlantic Current. These features recurred within the core of the North Atlantic Current (310-390 nm from point 1E), but disappeared again when the track crossed the north wall of the current. The depth of the DSC axis increased to the northwest from about 1500 m at point 1E to less than 100 m in the region between points 1C and 3B. The sound velocity at the DSC axis varied from about 1493 m/sec near point 1E to about 1476 m/sec near point 1C. In the region where the track crossed the North Atlantic Current, deep axial depth and sound velocity changed rapidly and the USC and intermediate sound velocity maximum disappeared. Critical depth decreased to the northwest from greater than 3000 m at point 1E to about 1300 m near point 3B, showing its most abrupt change where the track crossed the North Atlantic Current. Since the DSC was uninterrupted along the track, DSC propagation probably was the most effective path for sound transmission between points 1E and 3B. Depth excess was greater than 400 m along the entire track, and allowed for unimpeded convergence zone propagation from a near-surface source. However, the region of intense mixing between ranges of 250 and 450 nm probably had an adverse effect on all types of acoustic propagation along the track, particularly in the region between ACODAC 1C and ACODAC 2C.

### B. Point 2L to Point 2K Track (Phase II) (U)

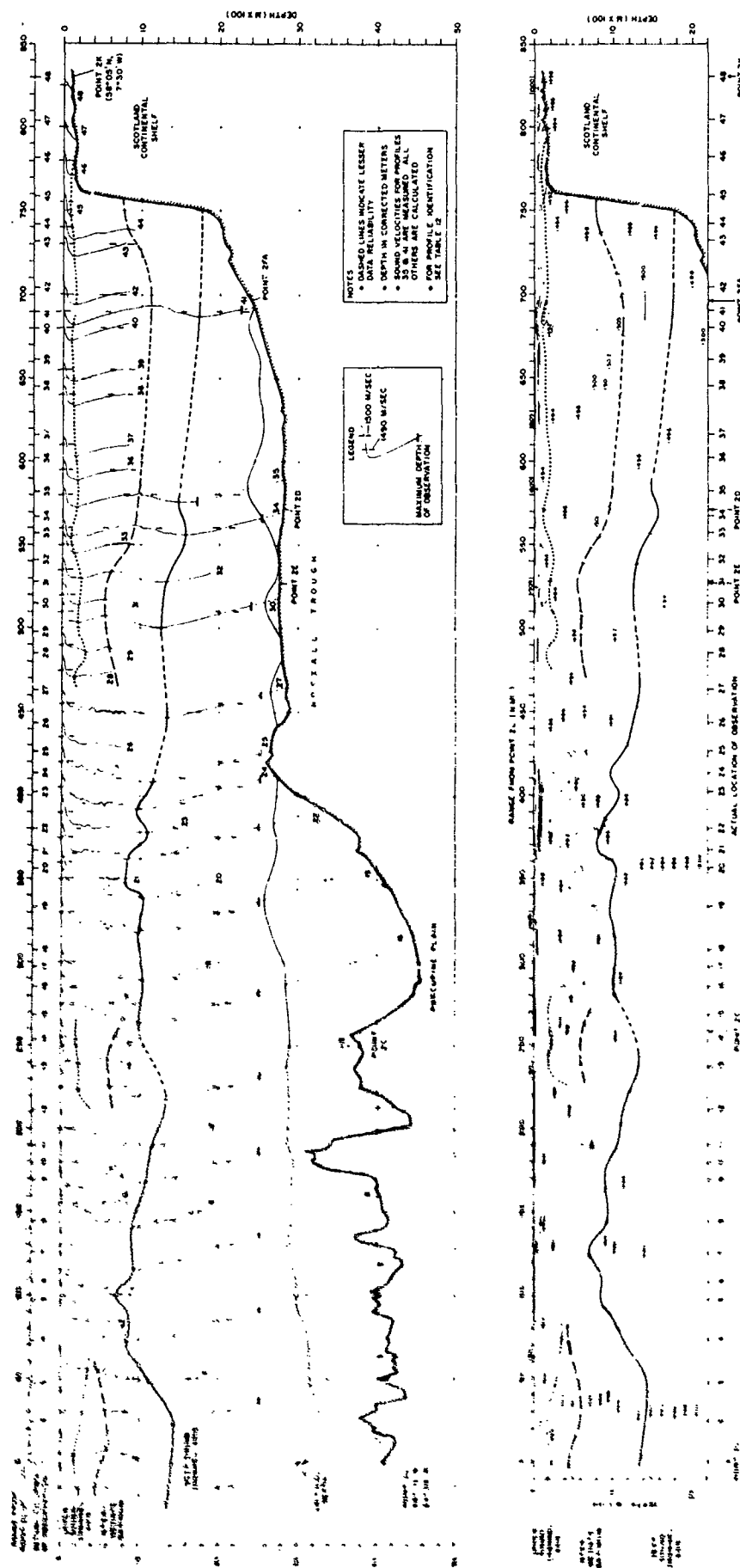
(C) The oceanographic data used in Figure 39 were collected between 20 and 25 August and are identified in Table 12 (Appendix B). The bathymetric profile is from WILKES (0-420 nm) and KINGSPORT (422-834 nm). Sound velocity





CONFIDENTIAL

(U) Figure 38. Sound Velocity Cross Section from Point 1E to Point 38 During Phase I



CONFIDENTIAL

(U) Figure 39. Sound Velocity Cross Section from Point 2L to Point 2K During Phase II

structures were quite complex and erratic along the 2L-2K track, since it cut in and out of the North Atlantic Current several times and also crossed the region of intense mixing due west of Porcupine Bank (Fig. 6). Surface sound velocities varied from about 1516 m/sec near point 2L to about 1502 m/sec near point 2FA. Near point 2K, surface sound velocities approached 1505 m/sec due to warming in the shallow waters over the Scotland continental shelf. No sonic layer was apparent along most of the 2L-2K track, precluding this sound transmission path. A USC and intermediate sound velocity maximum occurred near point 2L, around point 2C, and over Rockall Trough, but were absent along the rest of the track. Generally, bichannel sound velocity profiles occurred when the track was crossing or running parallel to the axis of the North Atlantic Current. Over Rockall Trough, the USC was very well defined and probably acted as a supplementary underwater sound transmission path for sources in the upper channel. Over the first 450 nm, however, the sound velocity structure above the DSC axis was dominated by rapidly changing microstructure that could have interfered with acoustic propagation.

(C) The depth of the DSC axis was quite erratic along the 2L-2K track, and varied from about 700 m at a range of 125 nm to greater than 1700 m at the foot of the Scotland continental shelf. The sound velocity at the DSC axis was equally erratic, and varied from about 1485 to about 1496 m/sec between these same two points. Between point 2L and a range of 125 nm, the depth of the DSC axis decreased by about 700 m and the axial sound velocity decreased by about 9 m/sec. These variations were reversed between 125 nm and point 2C. The DSC was particularly erratic over the Porcupine Plain due to mixing of LSW, MIW, and NACW. Critical depth decreased from about 3300 m near point 2L to less than 2400 m near point 2FA. Over Rockall Trough, critical depth lay less than 400 m above the bottom, thus limiting convergence zone formation for

a near-surface source. Northeast of point 2FA, the track was interrupted by the shallow bathymetry of the Scotland continental shelf. Over most of the 2L-2K track, the DSC was uninterrupted and DSC propagation was the most effective propagation path. Limited convergence zone propagation from a near-surface source should have been possible along the first 350-400 nm of track. Over Rockall Trough, sound transmission from a near-surface source was confined to the USC and less reliable bottom bounce paths. All modes of acoustic propagation probably were degraded by the intense mixing west of Porcupine Bank (i.e., between the ACODAC 2C and ACODAC 2D sites).

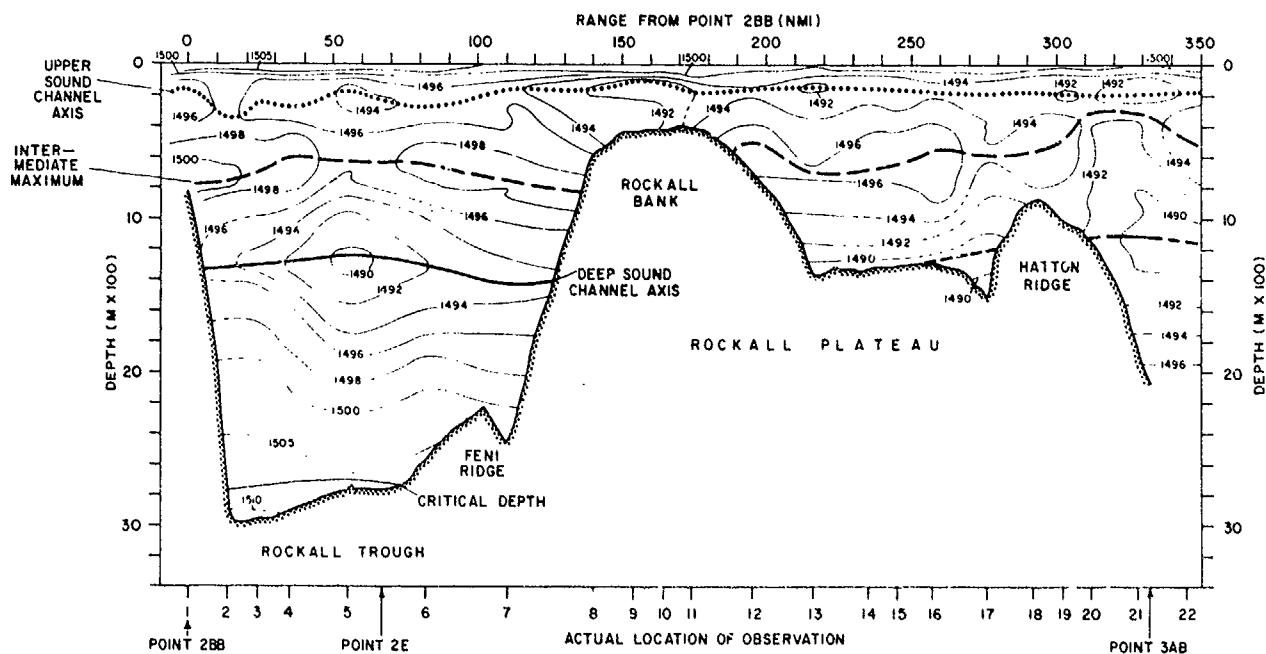
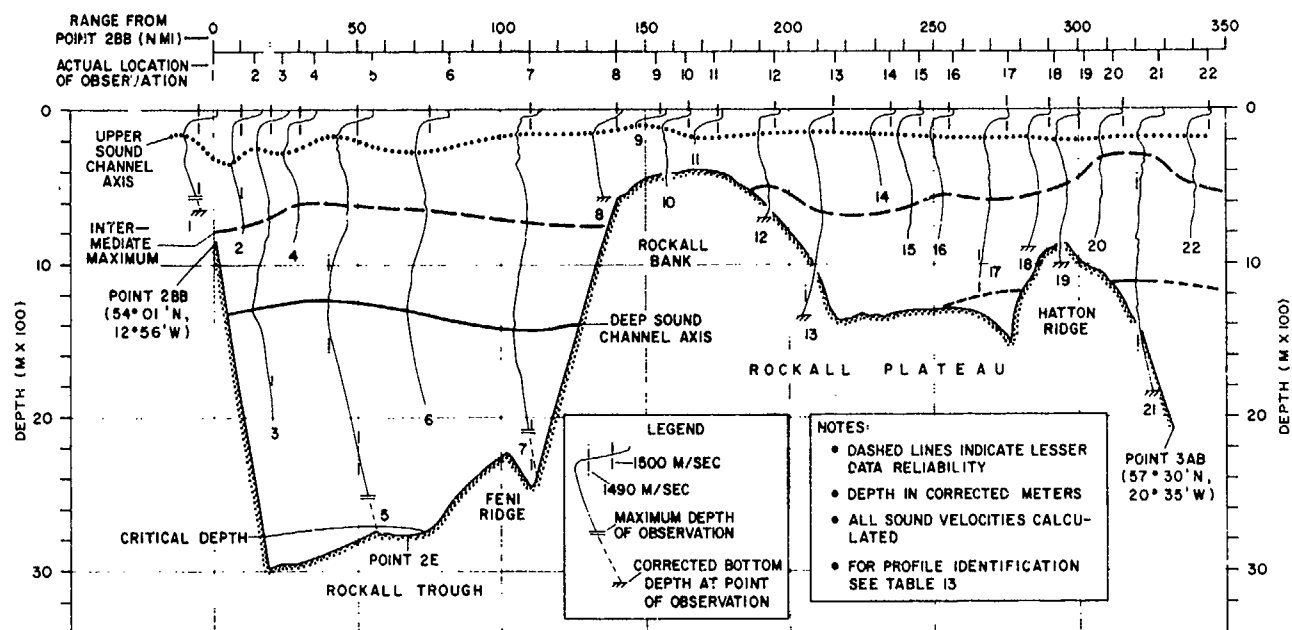
#### C. Point 2BB to Point 3AB Track (Phase II) (U)

(C) The oceanographic data used in Figure 40 were collected between 17 and 21 August and are identified in Table 13 (Appendix B). The bathymetric profile was recorded by KINGSPORT. The shallow bathymetry of the Rockall Plateau extended into the DSC and even above the depth of the intermediate sound velocity maximum along the 2BB-2AB track. However, a well-developed USC occurred along the entire track. This USC evidently acted as a reliable acoustic path along this track as indicated by the relatively low propagation losses observed in Ambient Noise Buoy (ANB) 2BB data for event 13a (Maury Center for Ocean Science, 1974). This is significant, since Rockall Bank was only 400 m below the surface at a range of 170 nm. DSC propagation was possible only in the deeper parts of Rockall Trough.

#### D. Point 3F to Point 3ZZ Track (Phase III) (U)

(C) The oceanographic data shown in Figure 41 were collected between 4 and 11 September and are identified in Table 14 (Appendix B). The bathymetric profile was collected by KANE (points 3F-3D) and KINGSPORT (points 3D-3ZZ). The sound velocity structure along the 3F-3ZZ track was more complex and

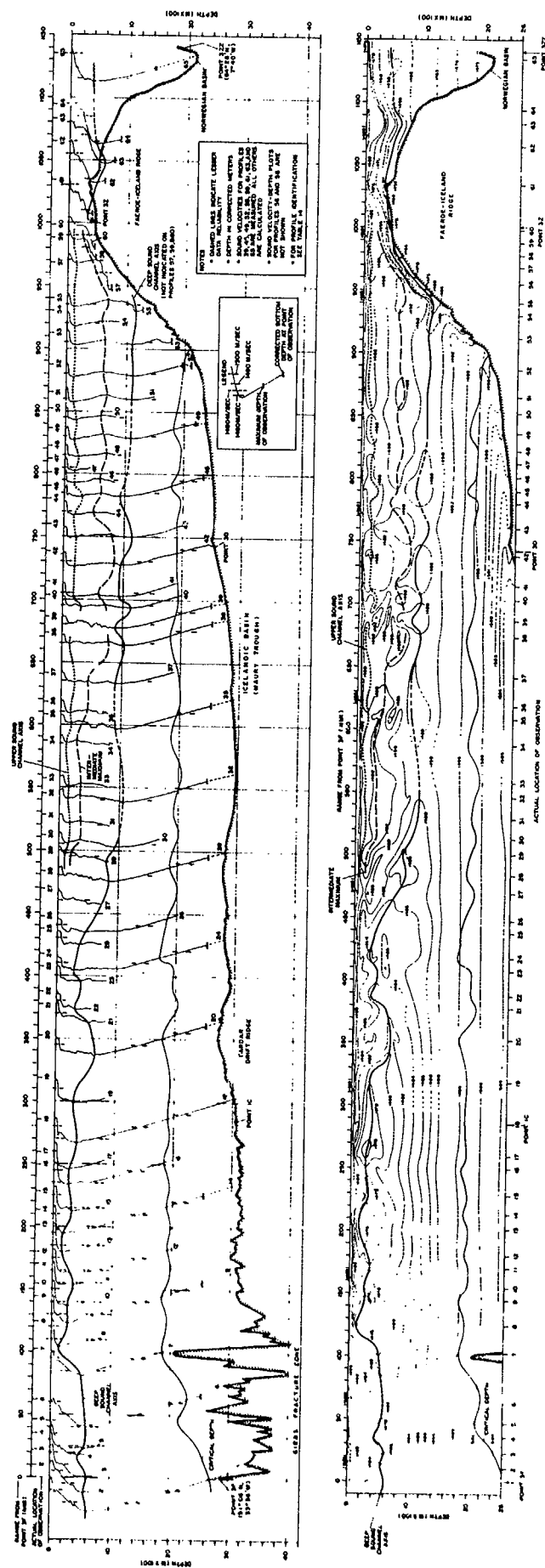
CONFIDENTIAL



CONFIDENTIAL

(U) Figure 40. Sound Velocity Cross Section from Point 2BB to Point 3AB During Phase II

CONFIDENTIAL



CONFIDENTIAL

(U) Figure 41. Sound Velocity Cross Section from Point 3F to Point 3ZZ During Phase III

variable than along any other SQUARE DEAL baseline owing to the wide variety of intermediate water masses. LSW, MIW, and NSOW were all encountered between points 3F and 3ZZ. In addition, the track crossed the North Atlantic Current, the Irminger Current, and the Polar Front (Fig. 6). Surface sound velocities varied from about 1508 m/sec at point 3F to about 1482 m/sec at point 3ZZ. However, along most of the track, the surface sound velocity was between 1495 and 1498 m/sec. A sporadic sonic layer at depths of 20–80 m occurred along much of the 3F–3ZZ track, and was sometimes complicated by in-layer negative gradients. Even when well established, the surface duct was not deep enough to support low frequency acoustic propagation. A USC and intermediate sound velocity maximum occurred between a range of about 500 nm and point 3Z. These structures briefly disappeared when the track crossed the Irminger Current at a range of 670–700 nm. Between points 3D and 3Z, the USC was well-developed and probably acted as a supplementary sound transmission path for sources located in the upper channel.

(C) Both the depth and sound velocity at the DSC axis were extremely variable and erratic along the 3F–3ZZ track. The depth of the DSC axis varied from about 130 m at 120 nm to 1150 m at ranges of 760 and 940 nm. The sound velocity at the axis varied from about 1474 m/sec to about 1489 m/sec between ranges of 120 and 760 nm, and was approximately 1457 m/sec at the crest of the Faeroe–Iceland Ridge. At point 3F, the DSC axis was controlled by the North Atlantic Current. At ranges between 100 nm and about 300 nm, the DSC axis roughly coincided with the low salinity LSW core (less than 400 m deep with sound velocities less than 1478 m/sec). Between about 300 and 500 nm, deep axial depth and sound velocity increased to the northeast in a region of transition that marked the southern edge of the Irminger Current. Between about 500 nm and the foot of the Faeroe–Iceland Ridge, the DSC axis

lay just below the depth of the MIW salinity maximum (900–1200 m deep with sound velocities greater than 1486 m/sec). North of about 910 nm, the DSC axis coincided with the NSOW T–S minimum. Along the southern flank of the Faeroe–Iceland Ridge, the DSC axis lay just above the bottom and apparently ceased to exist in the region around point 3Z. However, over the first 940 nm of track, the DSC was uninterrupted, and probably was the most reliable path for acoustic transmission.

(C) Between a range of 940 nm and the crest of the Faeroe–Iceland Ridge (over a distance of 94 nm), the depth of the DSC axis decreased from 1150 to 320 m (gradient of about 8.8 m/nm). In this same region, the sound velocity at the DSC axis decreased from 1484.6 to 1456.8 m/sec (gradient of about 0.3 m/sec/nm). These extremely large horizontal gradients were caused by mixing of NSOW and NACW across the Polar Front. The Polar Front itself lay between point 3Z and the crest of the Ridge (i.e., between profiles 60 and 61 of Fig. 41). Here, the sound velocity at the DSC axis changed from 1470.0 m/sec to 1456.8 m/sec over a distance of 36 nm (gradient of nearly 0.4 m/sec/nm) and surface sound velocities changed from 1494.5 to 1485.0 m/sec (gradient of about 0.3 m/sec/nm). These gradients were nearly as intense as those encountered at intermediate depths at the northern end of the Rockall Trough (Fig. 33).

(C) Critical depth decreased from about 2700 m at point 3F to less than 1900 m at a range of about 100 nm as the track crossed the north wall of the North Atlantic Current. Critical depth then gradually decreased to a minimum value of 1740 m at a range of about 420 nm. Over the Maury Trough, critical depth varied between about 1800 and 2100 m, and generally increased to the northeast, reaching a value of 2100 m at the foot of the Faeroe–Iceland Ridge. Between ranges of about 100 and 850 nm, depth excess was greater than 400 m and

should have been adequate for convergence zone propagation from a near-surface source. Beyond about 900 m, the Faeroe-Iceland Ridge and the intense Polar Front apparently impeded underwater propagation between the Maury Trough and the Norwegian Basin. All modes of propagation probably were degraded by the intense mixing between ranges of about 500 and 700 m where the track crossed the Irminger Current. This region lay between the ACODAC 1C and ACODAC 3D sites.

(C) Near point 3D, the sound velocity structure was extremely complex throughout the water column owing to mixing within the Irminger Current, transient MIW cells at intermediate depths, and descending boluses of NSOW near the bottom (Fig. 6). As noted by Dietrich (1967), the concentration of NSOW along the southern flanks of the Faeroe-Iceland Ridge is subject to temporal variability due to pulsations caused by tidal effects and internal waves. Such temporal variability also occurred at point 3D in the bottom 500 m of the water column. Temporal variability throughout the water column probably was responsible for the extreme fluctuations in ambient noise intensity recorded by ACODAC 3D (Maury Center for Ocean Science, 1974). The unusually high median noise levels at the bottom hydrophone of ACODAC 3D might be partially caused by turbidity and strong bottom currents associated with NSOW boluses in the Maury Trough (originally noted by Cherkis et al., 1973).

## E. Summary of Spatial Sound Velocity Variability Along the Three Major SQUARE DEAL Baselines (U)

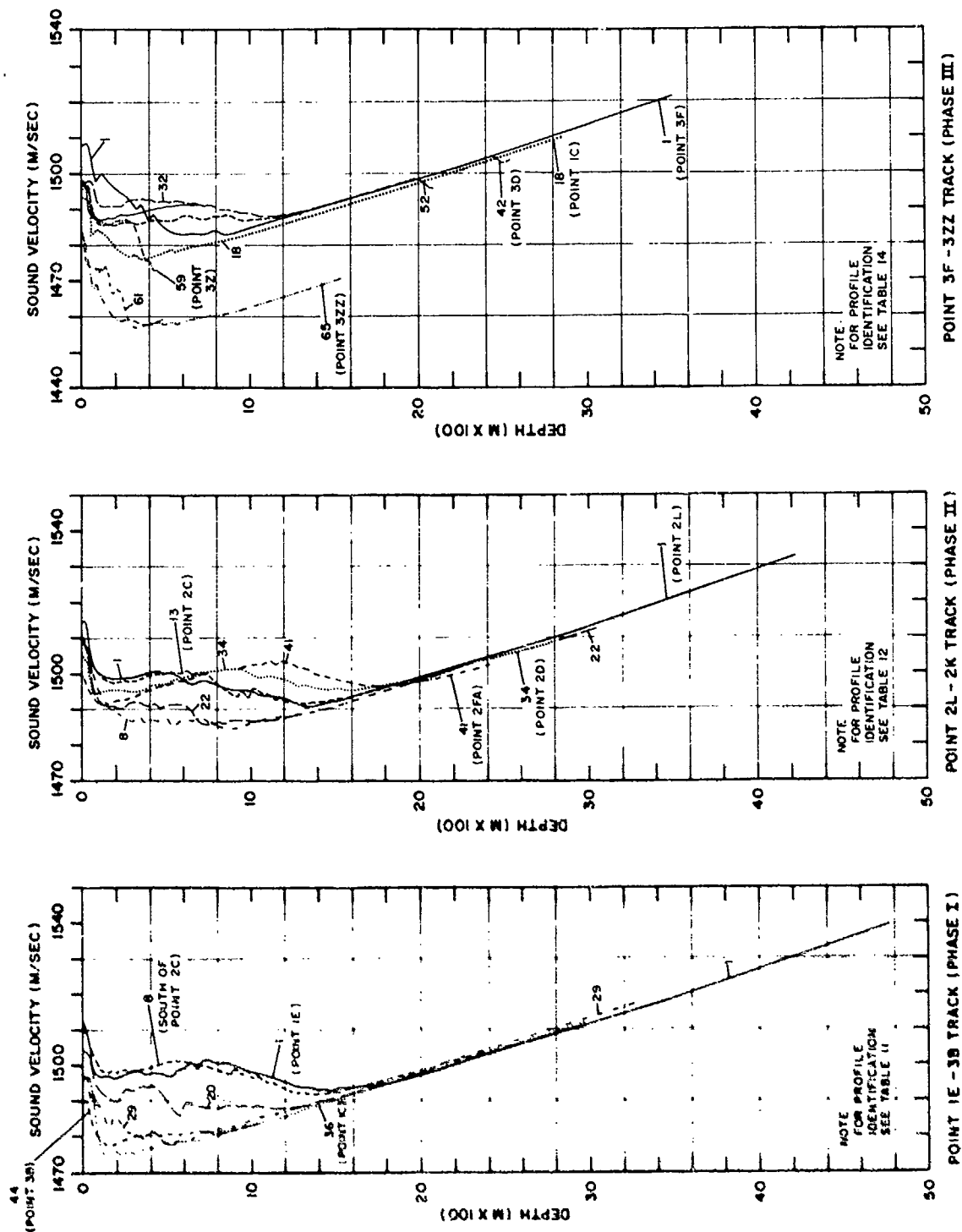
(U) Figure 42 shows composite plots of sound velocity profiles at selected intervals along the 1E-3B track (phase I), 2L-2K track (phase II), and 3F-3ZZ track (phase III). All sound velocity profiles shown in this figure have been extended to the approximate corrected bottom at the point of observation. Each profile is identified by the same number it bears in either Figure 38,

39, or 41. The data used to construct the sound velocity composites generally are the same used in Figure 8 (T-S composites).

(U) Along the 1E-3B track, sound velocities varied by about 24 m/sec at the surface, about 24 m/sec at 200 and 500 m, and about 16 m/sec at 1000 m. Below 1600 m, the various sound velocity profiles merge, with the exception of profile 29. The six profiles show a steady progression toward lower sound velocities to the northwest along the track. The large sound velocity variations (more than 20 m/sec) in the upper 800 m of the water column were caused by variations in surface conditions and differing intermediate water masses (MIW for profiles 7 and 9, LSW for profiles 29, 36, and 44).

(U) Along the 2L-2K track, sound velocities varied by about 14 m/sec at the surface, about 10 m/sec at 200 m, about 13 m/sec at 500 m, and about 17 m/sec at 1000 m. At about 1800 m, the various profiles merge, but diverge again below about 2000 m. At a depth of 2400 m, the sound velocity at point 2FA was nearly 4 m/sec less than at point 2L due to the presence of NSOW. The seven profiles do not show a logical progression up the 2L-2K track because of repeated crossings of the North Atlantic Current, LSW flows, and the intensive mixing zone west of Porcupine Bank. The large sound velocity variation at 1000 m was caused by differing intermediate water masses (LSW for profile 8, MIW for profile 41).

(U) Sound velocities throughout the water column varied more along the 3F-3ZZ track than along any other SQUARE DEAL baseline. This was due to the wide variety of intermediate water masses along the track. Sound velocities varied by about 26 m/sec at the surface, about 36 m/sec at 200 m, about 34 m/sec at 500 m, about 26 m/sec at 1000 m, and about 21 m/sec at 1500 m. The eight sound velocity profiles never merge, but split into two sets, each set typical of conditions on one side of the Polar Front. The first set



UNCLASSIFIED

(U) Figure 42. Sound Velocity Variability Along the Three Major SQUARE DEAL Baselines



(profiles 1, 18, 32, 42, 52, and 59) fall on the warm side of the Polar Front, the second set (profiles 61 and 65) on the cold side. The first set of profiles does not show a logical progression up the 3F-3ZZ track, but does show an overall sound velocity variation that is less than that observed along the phase I and II baselines. The second set of profiles displays a progression toward lower sound velocities northeast of the Polar Front. The bottom sound velocities for all profiles in the first set (except profile 1) were affected by NSOW (lower sound velocities at the bottom).

(U) The wide variety of sound velocity profiles shown in Figure 55 is a good indicator of the complexity of sound velocity structures throughout the northeast Atlantic during summer. Because of this complexity, propagation patterns inferred along the four SQUARE DEAL baselines should be considered representative only for these tracks and not for other regions of the exercise area. However, erratic spatial variations in sound velocity and temporal variability induced by internal waves probably caused short-term propagation anomalies throughout the SQUARE DEAL Exercise area.

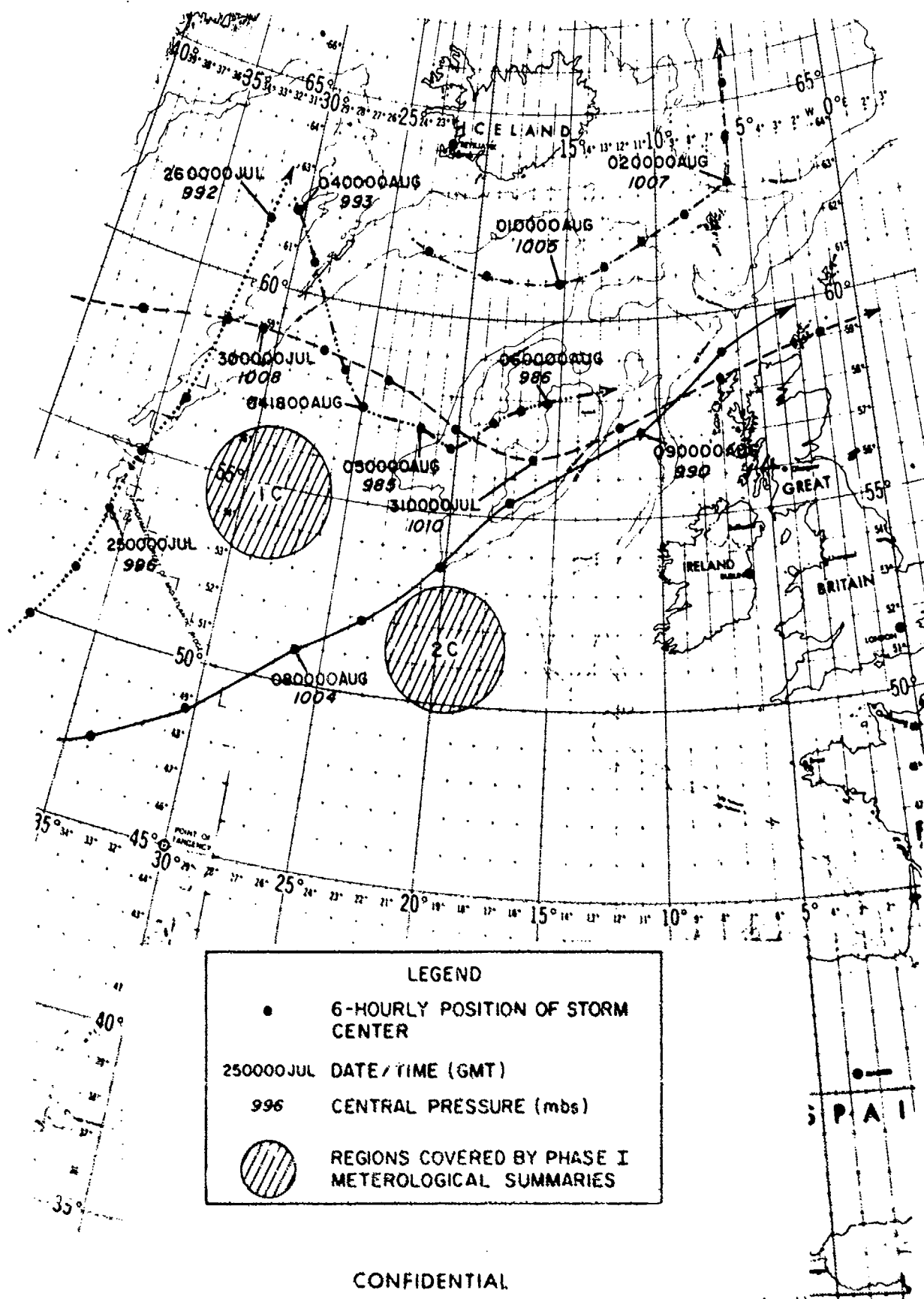
## VII. Meteorology (U)

(U) Surface meteorological data were collected by most participating ships during SQUARE DEAL. Meteorological observations collected during the exercise were analyzed to produce 6 hour averages of wind speed, predominant wind direction, wave height, and swell height within a 100 nm radius of the two ACODAC sites during each exercise phase. Surface weather charts from the National Weather Service were used to hindcast meteorological conditions for those periods when observations were not available and to produce storm track charts for each exercise phase.

### A. Phase I (25 Jul-10 Aug) (U)

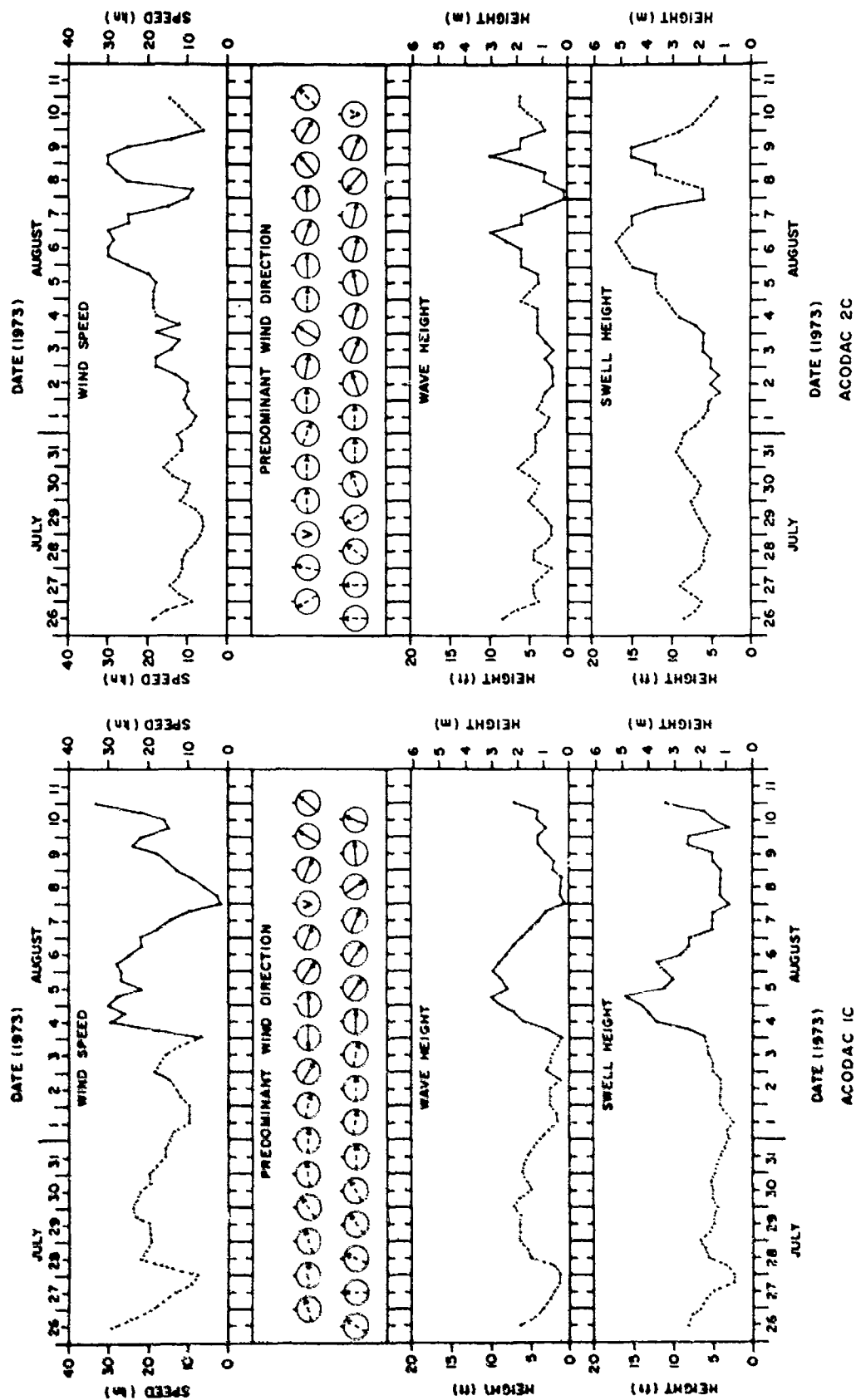
(C) Figure 43 shows major storm tracks during phase I. Surface meteorological conditions within 100 nm of the phase I ACODAC sites are shown in Figure 44. The first half of the meteorological records at both ACODAC 1C and 2C is based on hindcasted values. The frequency of lowpressure systems during phase I was slightly greater than normal. A moderate storm, with a central pressure of approximately 995 millibars (mb), passed about 250 nm west of ACODAC 1C at the beginning of phase I. Southwesterly winds of 30 kn and waves and swells to 8 ft briefly occurred as this storm moved rapidly north-northeast. The strong pressure gradient occurring after the storm passed maintained generally westerly winds of about 20 kn with waves and swells from 4-6 ft for the next three days. On 30-31 July, a weak storm moving easterly at 25 kn passed about 200 nm north of ACODAC 1C and resulted in moderate winds and seas. On 1 August, a weak storm on an easterly track passed over the northern Maury Trough along about 61°N. This storm, however, did not have significant effects at ACODAC 1C. During the first week of operations, the ACODAC 2C site was not appreciably affected by major storms, and experienced light westerly winds (averaging 12 kn) with waves of 3-4 ft and swells of 5-6 ft.

(C) During the second week of phase I, a deepening storm moved southeast from Greenland and reached a position about 200 nm northeast of ACODAC 1C by 041800Z August. The storm then moved due east at about 15 kn. High seas and swells from this storm caused the premature termination of the WILKES SUS run on 042223Z August. This severed storm attained a central pressure of 985 mb at 050000Z August, and markedly affected both ACODAC sites. Westerly winds reached 30 kn with 7-10 ft waves and 10-15 ft swells at ACODAC 1C on 4-6 August, and at ACODAC 2C on 5-7 August. After about two days respite, a moderate storm with a central pressure near 1000 mb moved from southwest to



CONFIDENTIAL

(U) Figure 43. Major Storm Tracks During Phase I (25 Jul-10 Aug)



NOTES  
 • ARROWS INDICATE DIRECTION WIND IS BLOWING  
 • 'v' INDICATES VARIABLE WIND DIRECTION  
 • DASHED LINES AND ARROWS INDICATE WINDCASTS

UNCLASSIFIED

(U) Figure 44. Meteorological Conditions Near Phase I ACODAC Sites

northeast directly between the ACODAC 1C and 2C sites. On 8 August, ACODAC 2C had northwest winds of 30 kn with 8-10 ft waves and 12-15 ft swells. On 9 August, winds at ACODAC 1C reached 25 kn from the southwest with 5-7 ft waves and 8 ft swells. After a dramatic reduction in winds and seas following the passage of this storm, it deepened and expanded rapidly northwest of Ireland, and caused increasing southwesterly winds and rising seas until the completion of phase I.

(C) The 30 kn winds (Beaufort force 6-7) experienced at ACODAC 1C between 4 and 5 August probably caused higher ambient noise intensities in the 250 Hz band, at least for the shallower hydrophones. This storm also should have had pronounced effects on ambient noise intensities measured by WECO Survey Array 1A, which was closer to the major development of the storm (050000Z August) than was ACODAC 1C (Fig. 43). ACODAC 2C was not operational during the passage of the major phase I storm. The southeast to northwest storm that passed between the two ACODAC sites on 8 August probably had pronounced effects on ambient noise intensities measured by WECO Survey Array 1B and MABS I at point 1BA. Both sites should have experienced wind speeds and surface conditions similar to those at ACODAC 2C on 8 August (Fig. 44). During the passage of the final phase I storm, ACODAC 2C again was not operational.

## B. Phase II (15-27 Aug) (U)

(C) Figure 45 shows major phase II storm tracks, and Figure 46 shows a summary of meteorological conditions within 100 nm of the phase II ACODAC sites. The first and last parts of the ACODAC 2C record are based on hindcasts. However, the majority of the ACODAC 2D record is based on measurements made during the exercise. Most of phase II was seasonally normal, and no major storms passed close enough to affect markedly either ACODAC or any other phase II acoustic receiver. Surface meteorological conditions for WECO Survey Arrays 2A and 2B, Moored

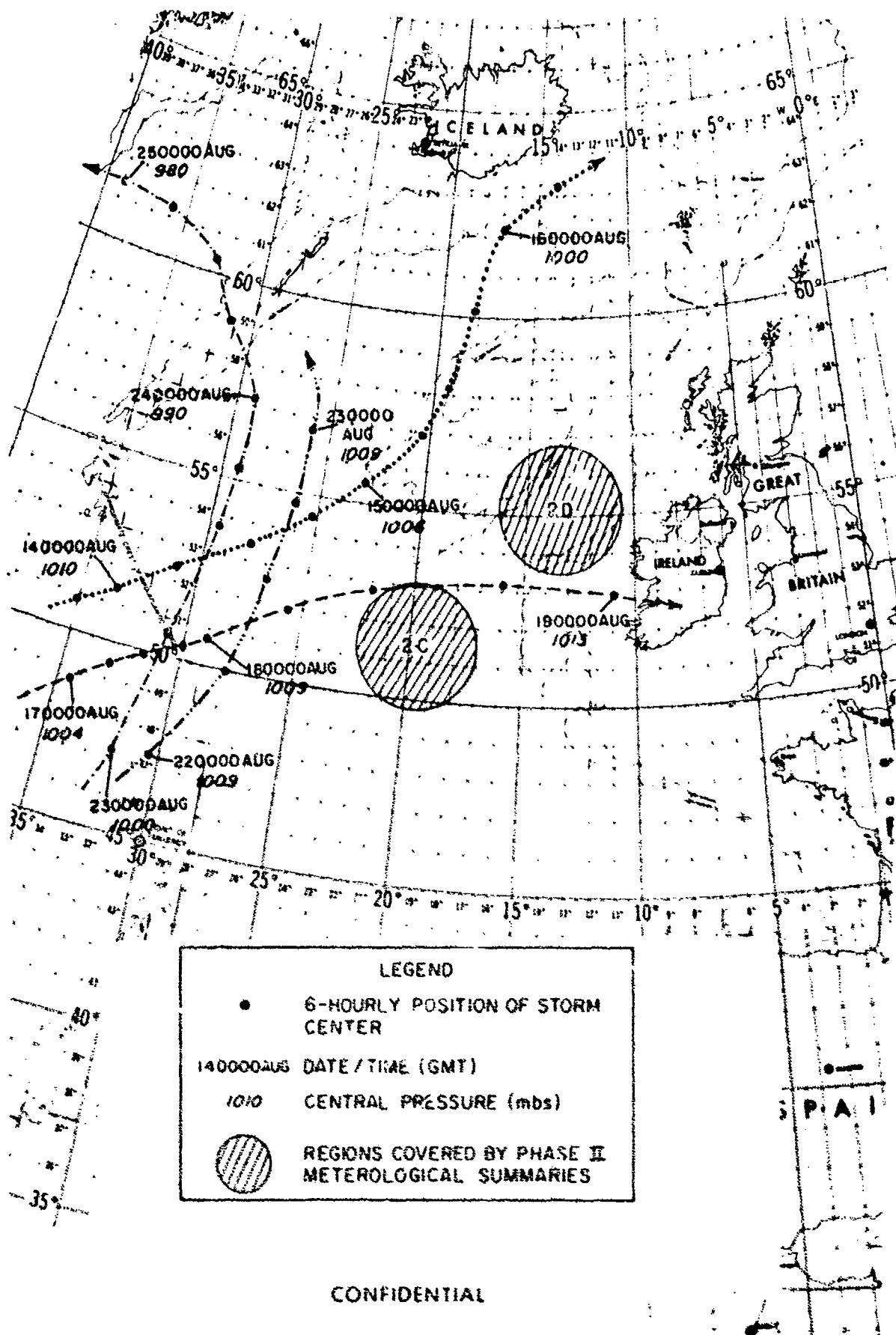
Acoustic Buoy (MABS) I at point 2AA, and ANB 2BB probably were quite similar to those at ACODAC 2D (Fig. 46).

(C) Between 14 and 16 August, a moderate storm passed about 300 nm northwest of the ACODACs, moving generally northeast. Between 18 and 20 August, a weak storm moved east to west between the two ACODAC sites. The central pressures of these two storms did not drop below 1000 mb. In both cases, west to northwest winds increased to 15-20 kn and caused approximately 5 ft waves and swells of 5-8 ft. Between 22 and 24 August, two separate moderate storms on south-to-north parallel tracks passed about 325 nm west of ACODAC 2C and about 450 nm west of ACODAC 2D. Winds briefly increased to 20 kn from the south and caused 5 ft waves. Swells of about 5 ft persisted during the passage of these storms at both sites. These two storms combined and deepened between Iceland and Greenland, and caused southerly winds of 15-20 kn, approximately 5 ft waves, and slowly increasing swells (5-7 ft) during the remainder of phase II at both ACODAC sites.

## C. Phase III (2-16 Sep) (U)

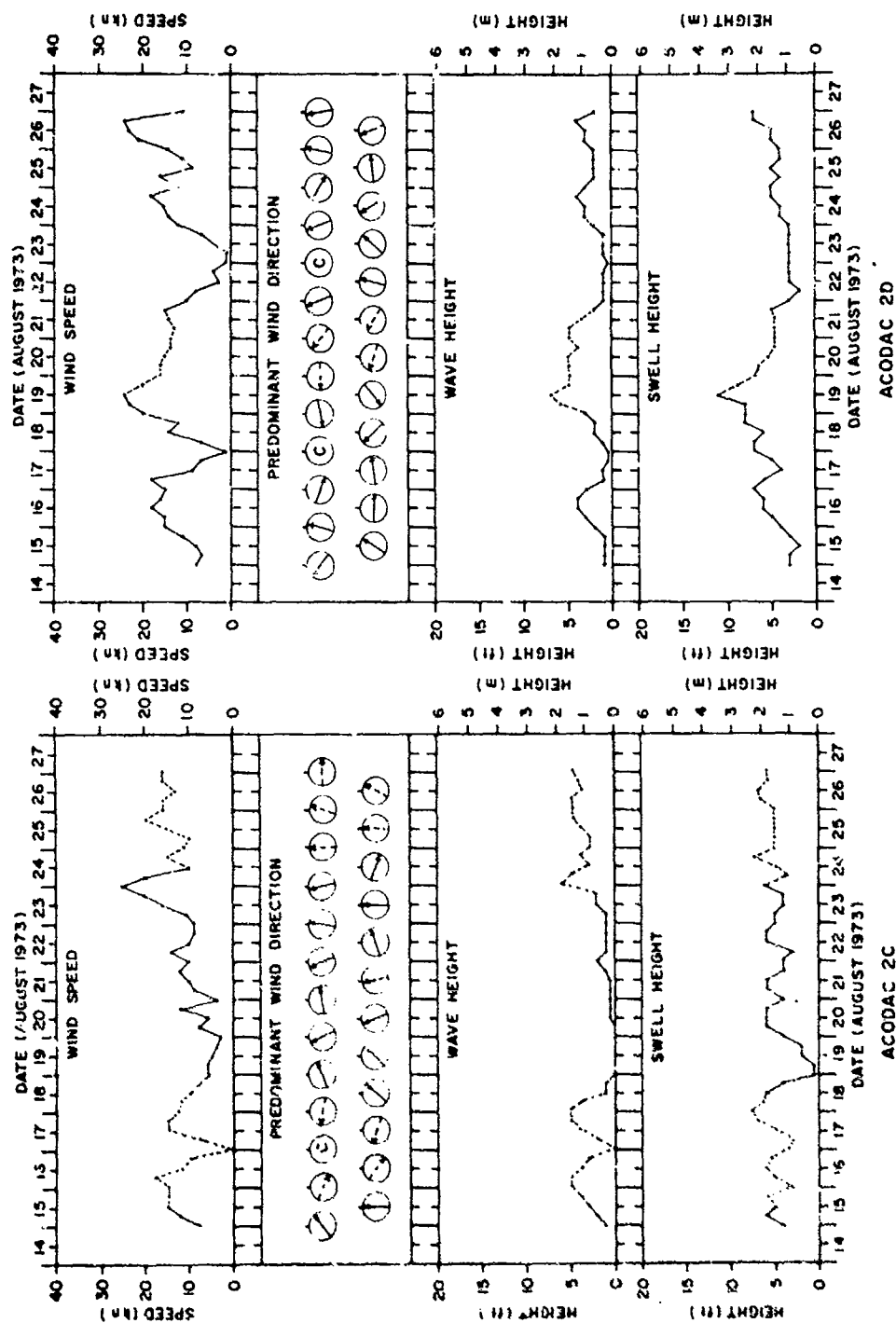
(C) Figure 47 shows major storm tracks during phase III. Surface meteorological summaries within 100 nm of ACODACs 1C and 3D are shown in Figure 48. The last parts of both records are based on hindcasts. During phase III, the advent of winter storm patterns caused an increasing frequency and intensity of storms. Both ACODAC sites were affected by a 50% greater frequency of storms than normally expected. The phase commenced with a moderate storm (central pressure of 993 mb) that passed northwest of both ACODACs on a southwest to northeast course. Southwesterly winds of 18-23 kn, 6-7 ft waves, and 10-12 ft swells affected ACODAC 1C on 4-5 September and ACODAC 3D on 5-6 September. After about two days of relative calm another moderate, but weakening, storm approached ACODAC 1C from the southeast on 7 September.

CONFIDENTIAL



(U) Figure 45. Major Storm Tracks During Phase II (15-27 Aug)

CONFIDENTIAL

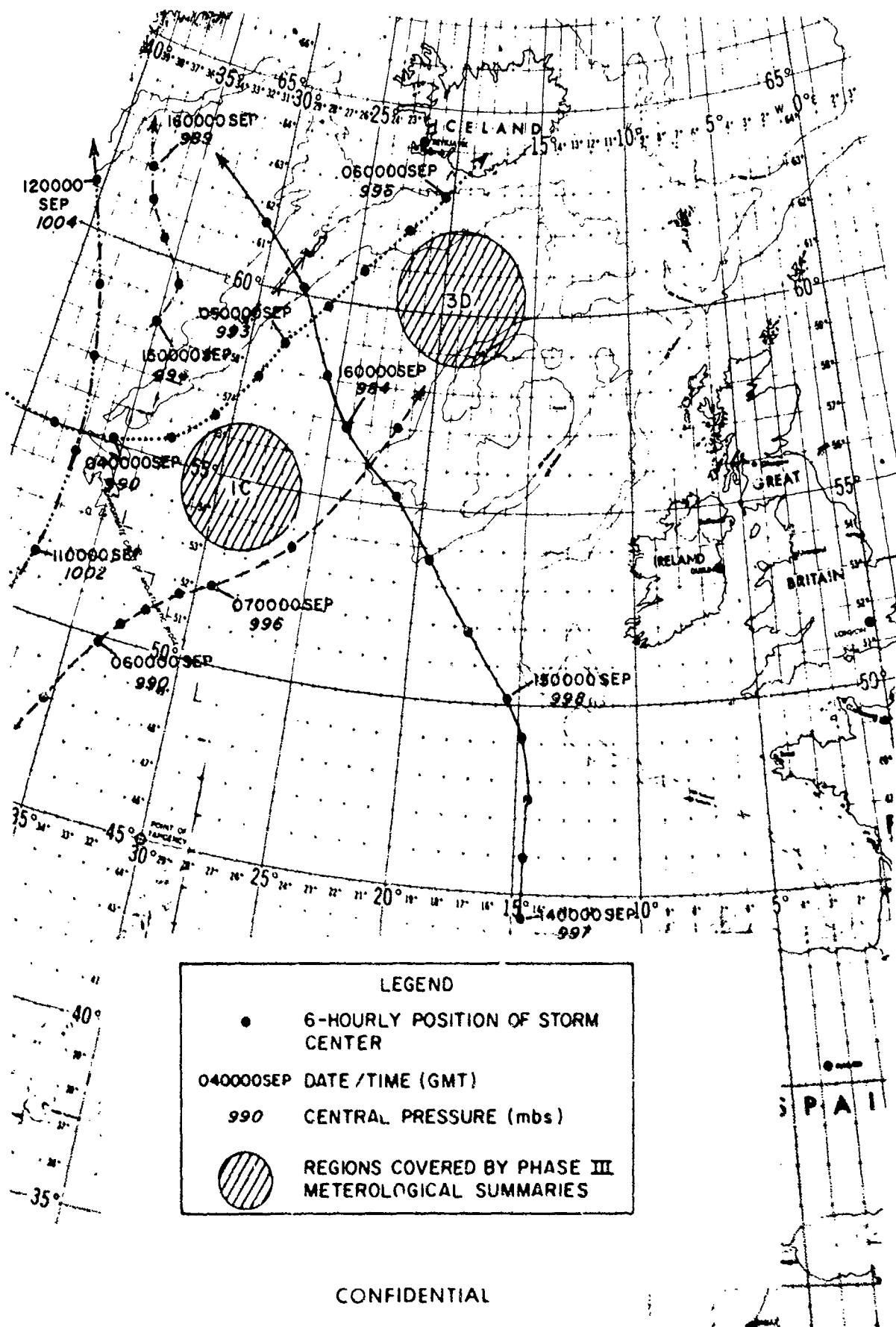


NOTES:  
 • ARROWS INDICATE DIRECTION WIND IS BLOWING  
 • C INDICATES CALM WIND CONDITIONS  
 • DASHED LINES AND ARROWS INDICATE HINDCASTS

UNCLASSIFIED

(U) Figure 46. Meteorological Conditions Near Phase II ACODAC Sites

CONFIDENTIAL

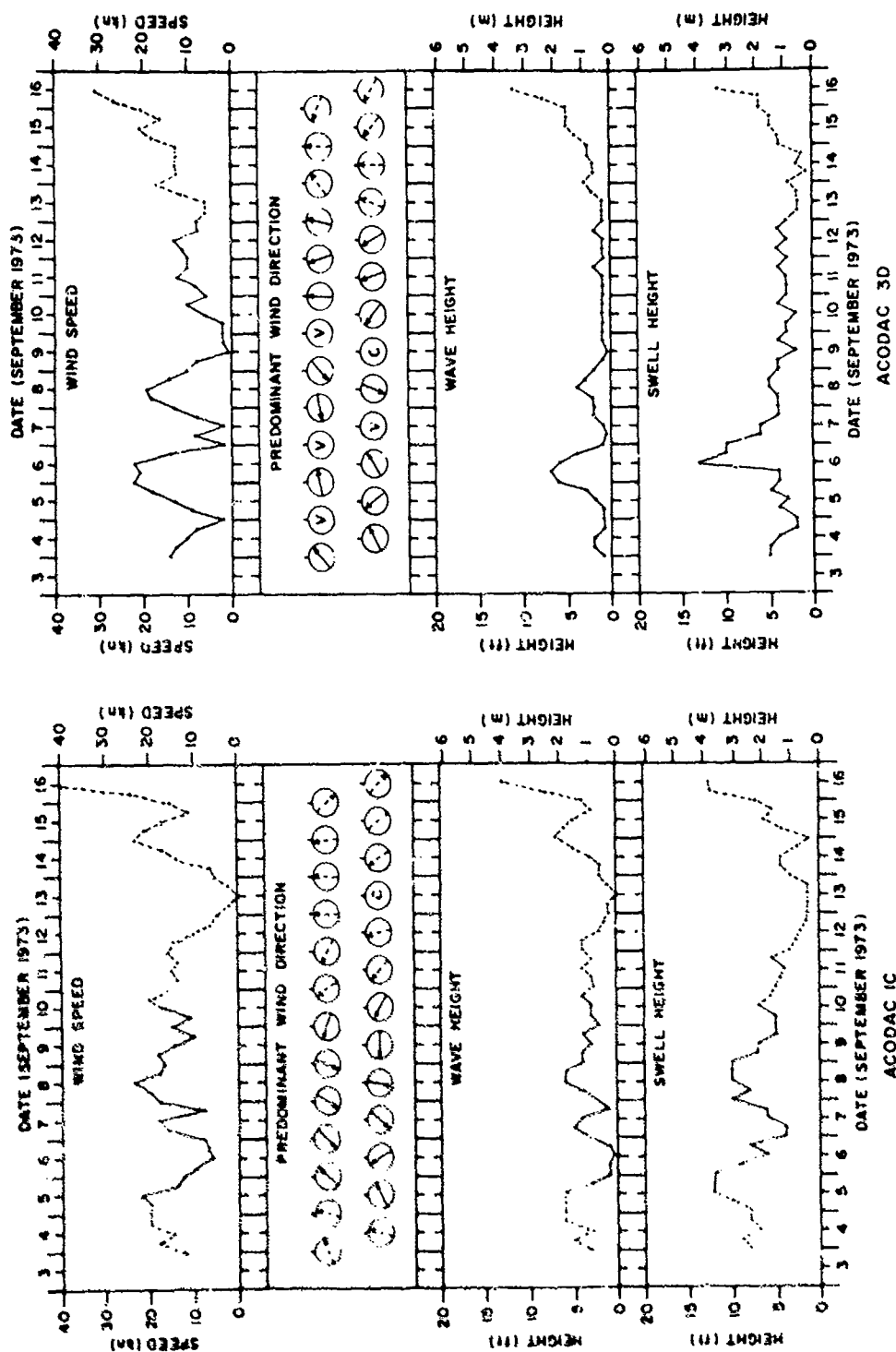


CONFIDENTIAL

(U) Figure 47. Major Storm Tracks During Phase III (2-16 Sep)

CONFIDENTIAL

CONFIDENTIAL



NOTES  
 • ARROWS INDICATE DIRECTION WIND IS BLOWING  
 • V INDICATES VARIABLE WIND DIRECTION  
 • C INDICATES CALM WIND CONDITIONS  
 • DASHED LINES AND ARROWS INDICATE HINDCASTS

UNCLASSIFIED

(U) Figure 48. Meteorological Conditions Near Phase III ACODAC Sites

CONFIDENTIAL



This storm diminished in the vicinity of ACODAC 3D on 8 September. Winds were near 20 kn from the northeast with waves near 5 ft at both sites. ACODAC 1C, however, experienced higher swells (about 10 ft) during this period.

(C) Between 10 and 12 September, a weak storm moved south to north 300 nm west of ACODAC 1C and resulted in southeast winds of 15-20 kn, 4 ft waves, and 5 ft swells. However, this storm had little effect on the ACODAC 3D site. A moderate storm that developed 200 nm north-west of ACODAC 1C on 15 September caused southerly winds of 20-25 kn, 6-8 ft waves, and 5-6 ft swells at both sites before moving rapidly north toward Greenland. On 16 September, a severe storm passed midway between the ACODAC 1C and 3D sites. This disturbance moved northwest from about 45°N, 15°W (off the Iberian Peninsula) during the period 14-16 September, and developed a central pressure of 984 mb by 160000Z September. In the exercise area, the storm caused 30-40 kn winds from the northwest at ACODAC 1C and similar winds from the southeast at ACODAC 3D. Both sites were affected by the 12-15 ft waves and 10-13 ft swells associated with this storm at the end of phase III. This final storm was the most intense observed during SQUARE DEAL and had stronger effects than the major storm that occurred during the second week of phase I (Fig. 44).

(C) The 30-40 kn winds (Beaufort force 7-8) at ACODAC 1C at the end of phase III theoretically should have had pronounced effects on ambient noise intensities in the higher frequency bands, at least for the shallower hydrophones. These relatively high winds may at least partially explain the increase in ambient noise intensities at this site on 15 September for frequencies of 160, 200, and 250 Hz (Maury Center for Ocean Science, 1974). Such increases were observed in the time-series plots of ambient noise intensity at ACODAC 1C for all hydrophones except that at the bottom. ACODAC 3D was not operational during the last three days of phase III.

Generally, the WECO Survey Array at point 3A and MABS II at point 3AA were under the influence of the same weather patterns as ACODAC 3D. However, both these receivers ceased operations on 11 September. Based on the storm tracks shown in Figure 47, the WECO Survey Array 3Z site was not markedly affected by major storms during phase III of the exercise.

## VIII. Summary (U)

(C) From July through September 1973, 258 SV/STDs, 27 SVDs, 21 CV/STDs, and 1045 XBTs were collected in the north-east Atlantic Ocean north of about 48°N as part of the SQUARE DEAL Exercise. In addition, 2383 surface meteorological observations and nearly 27,000 nm of bathymetric tracks were collected by participating ships. Sound velocity profiles were calculated for all XBTs using the equation of Wilson (1960) and salinities measured during the exercise. The total sound velocity data base formed a roughly rectilinear grid and was more complete and better distributed than that of any previous LRAPP exercise. These data were more than adequate to describe environmental effects on acoustic propagation and were sufficient for the following analyses:

- Time-series analyses at several reference points
- Average areal presentations of selected sound velocity parameters
- Sound velocity cross sections along four exercise baselines

Generally, sound velocities measured directly agreed within 0.2-0.5 m/sec of computed values.

(U) Sound velocity structures during SQUARE DEAL were affected by three major intrusive water masses: warm, high salinity Mediterranean Intermediate Water (MIW); cold, low salinity Labrador Sea Water (LSW); and very cold, low salinity Norwegian Sea Overflow Water (NSOW). All three of these water masses altered the basic sound velocity structure associated

with North Atlantic Central Water (NACW) carried by the North Atlantic and Irminger Currents. The interplay of various water masses frequently created a bichannel sound velocity profile where the upper sound channel (USC) axis was separated from the deep sound channel (DSC) axis by an intermediate-depth sound velocity maximum. The intermediate velocity maximum either coincided with the MIW salinity maximum or corresponded to the bottom of the North Atlantic Current. This latter case was more common in the SQUARE DEAL area. The USC axis generally corresponded to the maximum depth of summer warming.

(U) The relative concentrations of MIW, LSW, and NSOW had pronounced effects on the depth and sound velocity at the DSC axis throughout the exercise area. MIW was the primary control in regions where the deep axial depth was greater than 1200 m and deep axial velocity was greater than 1490 m/sec (southeast part of the exercise area and the Rockall Trough). LSW was the primary control where deep axial depth was less than 900 m and deep axial velocity was less than 1488 m/sec (western half of the exercise area). However, in the vicinity of the Faeroe-Iceland Ridge, NSOW caused a DSC just above the bottom with sound velocities that varied between about 1460 and 1488 m/sec. In the Maury Trough, NSOW caused a weakening of the near-bottom positive velocity gradient and even a reversal of this gradient.

(U) Mixing of NACW, MIW, and LSW created a series of horizontal and vertical fronts in the region west of Porcupine Bank and southwest of the Rockall Plateau that should have significantly affected underwater sound propagation. This frontal zone generally corresponds with the subsurface position of the Subarctic Convergence during summer (Rossov and Kislyakov, 1972). Surface frontal zones also were found along the north wall of the North Atlantic Current and over the Faeroe-Iceland Ridge. These latter frontal zones generally correspond to the

August position of the near-surface front shown by Baranov (1972) and the Polar Front, respectively. The Polar Front extended to at least 1000 m during the exercise, and separated the warmer waters of the northeast Atlantic from the colder waters of the Norwegian Sea.

(C) Meteorological observations collected during SQUARE DEAL were combined with hindcasted values to produce 6 hour averages of wind speed, predominant wind direction, wave height, and swell height within a 100 nm radius of the two ACODAC sites during each of the three exercise phases. In addition, track charts of major storms were produced for each exercise phase. During phase I, the frequency of low pressure systems was slightly greater than normal. A major storm (central pressure of 985 mb) caused 30 kn winds at point 1C on 4-5 August, and probably had pronounced effects on ambient noise intensities measured by ACODAC 1C and WECO Survey Array 1A. During phase II, no major storms passed close enough to affect markedly ACODAC 2C, ACODAC 2D, or any other phase II acoustic receiver. During phase III, the advent of winter storm patterns caused 50% more storms than normal. In addition, the phase III storms were more intense than those during phases I and II. Wind speeds of 30-40 kn were experienced at ACODACs 1C and 3D at the end of phase III during the most intense storm of the exercise. Relatively high winds from this storm may be at least partially responsible for the increase in ambient noise intensities at several frequencies observed at ACODAC 1C on 15 September. All other phase III acoustic receivers (including ACODAC 3D) were nonoperational during the passage of the final exercise storm.

(C) Significant temporal variability in sound velocity was detected throughout the exercise area. This variability was caused by internal waves with a semidiurnal period (similar to that of the tides) and by mixing of various water masses. At point 1C (54°52'N,

29°49'W), mixing of LCW and NACW and internal wave action caused a 3.9 m/sec variation in the sound velocity at the DSC axis over a period of four days. At point 2C (51°30'N, 19°38'W), internal waves and mixing between MIW and NACW caused a 2.7 m/sec variation in the sound velocity at the USC axis and a 3.1 m/sec variation in the sound velocity at the intermediate maximum in less than two days. At point 2D (55°13'N, 13°33'W), temporal variability was caused exclusively by internal waves, and was less than 1.8 m/sec throughout the water column (except in the near-surface layer).

(C) At point 3Z (63°10'N, 12°10'W), NSOW boluses mixing with NACW over the crest of the Faeroe-Iceland Ridge caused a 10.8 m/sec variation in near-bottom sound velocity over less than four days. This dramatic variation is even greater than that observed along the Subarctic Convergence during the NORLANT-72 Exercise (Fenner and Bucca, 1974). At point 3ZZ (64°28'N, 7°40'W) in the Norwegian Basin, temporal variability at the DSC axis was only 1.5 m/sec, and was caused primarily by internal waves.

(U) At the Porcupine Bank time-series station (53°00'N, 15°30'W), internal waves and mixing caused the disappearance of bichannel sound velocity structures sometime between 11 and 20 August (between phases I and II). This basic change in sound velocity structure probably was initiated by the migration of a cell of relatively cold, low salinity water from the west. This cell most likely contained upper-lobe LSW (as defined by Bubnov, 1968), and was similar to that observed 150 nm to the west in July 1965 (Howe and Tait, 1967). Changes from a bichannel to a single channel structure were also observed at points 2C and 3ZZ. At other locations, temporal variability produced significant changes in the "strength" of the USC and in the width of the DSC.

(C) Significant temporal variability in sound velocity was detected at the following acoustic measurement locations:

- ACODAC sites 1C, 2C, and 3D
- WECO Survey Array sites 2A, 2B, 3A, and 3Z
- MABS sites 2AA and 3AA
- ANB site 2BB

At these and other acoustic receiver sites, temporal variability probably had significant effects on acoustic propagation and may have been partially responsible for observed diurnal and semidiurnal periods in spectral ambient noise intensities. In addition, short-term temporal variability probably caused propagation anomalies throughout the SQUARE DEAL area.

(C) The sonic layer was quite sporadic during the exercise, owing to both diurnal effects and the passage of several storms. Generally, the sonic layer was shallower in the southern part of the exercise area and over the Faeroe-Iceland Ridge, but was never deeper than 60 m. Throughout most of the area, sonic layers occurred 20-80% of the time. However, they occurred greater than 80% of the time in a broken band that was oriented along the North Atlantic Current. Since all of the acoustic frequencies used during the exercise were lower than the theoretical minimum that could propagate within a 50 m sonic layer, surface duct paths probably were not a significant factor in SQUARE DEAL acoustic propagation.

(U) A USC and intermediate maximum were not uniformly present throughout the exercise area because of the variability in oceanographic conditions and bottom depths. Both parameters were present greater than 80% of the time in the eastern half of the exercise area, but were effectively absent west of 20°-25°W. In addition, an intermediate maximum was absent over Porcupine Bank and parts of the Faeroe Plateau and Wyville-Thomson Ridge due to topographic interference. Both features

disappeared near the subsurface position of the Subarctic Convergence during summer (Rossov and Kislyakov, 1972). Both features were present only 20-80% of the time in the region due west of Porcupine Bank. Here, transitory bichannel structures probably were caused by a cell of upper-lobe LSW that migrated into the area west of Porcupine Bank sometime near the end of phase I.

(U) When present, the USC axis had an average depth of about 100-250 m, and was generally shallower over Porcupine Bank and the Faeroe Plateau. Average upper axial velocities varied between about 1486 and 1501 m/sec, and were generally greater in the south. Standard deviations of these two parameters were generally less than 50 m and 1.0 m/sec, respectively. The average depth of the intermediate maximum varied between about 300 and 1100 m, and was greatest south of Porcupine Bank and in the Rockall Trough. Average sound velocities at the intermediate maximum varied between 1487 and 1505 m/sec, and were greater than 1500 m/sec south of Porcupine Bank and in the Rockall Trough. Standard deviations in the average depth and sound velocity at the intermediate maximum were generally less than 100 m and 1.5 m/sec, respectively.

(C) According to Hanna (1969), a well-developed USC can act as a sound propagation path for sources within the upper channel. Based on Hanna's findings and SQUARE DEAL data, it is safe to assume that some USC propagation was possible during the exercise in regions where the sound velocity at the intermediate maximum or at the bottom exceeded that at the USC axis by more than 3 m/sec (i.e., where the "strength" of the USC was greater than 3 m/sec). Such regions occurred throughout most of the eastern half of the exercise area except over the shallowest portions of Porcupine Bank, in the region due west of Porcupine Bank, and over the Faeroe-Iceland Ridge. USC propagation apparently was possible over Porcupine Bank, the

Faeroe Plateau, and throughout Rockall Trough.

(C) A DSC was present throughout the exercise area except in the shallow regions surrounding Rockall Trough and the Faeroe Islands. The average depth of the DSC axis varied from less than 100 m over the southern end of the Reykjanes Ridge to more than 1600 m in Rockall Trough and south of Porcupine Bank. Average deep axial velocity varied from less than 1455 m/sec over the Faeroe-Iceland Ridge to more than 1496 m/sec in the region south of Porcupine Bank. The DSC probably was the most efficient path for sound propagation in the SQUARE DEAL area, except over the Faeroe-Iceland Ridge and the Rockall Plateau. The subsurface Subarctic Convergence and the Polar Front compressed deep axial depth and velocity isopleths and caused horizontal gradients at the axis of 0.2-0.4 m/sec/nm. In the northern Rockall Trough, mixing between NACW, MIW, and NSOW caused a horizontal gradient at the DSC axis of nearly 0.5 m/sec/nm. Standard deviations in average deep axial velocity were similar to those for the USC and intermediate velocity maximum, while standard deviations in average deep axial depth were greater and more variable. This indicates that deep axial depth was more sensitive to environmental fluctuations than was deep axial velocity.

(C) Average critical depths varied from greater than 3400 m along about 47°N to less than 1500 m over the southern end of the Reykjanes Ridge and in the region surrounding the Faeroe Islands. Standard deviations in average critical depth were generally less than 100 m, except in the frontal zones along the north wall of the North Atlantic Current. Convergence zone propagation from a near-surface source probably was possible in large regions of the West European Basin and the Maury Trough where the bottom was more than 400 m deeper than critical depth (depth excess regions). However, the shallow bathymetry of Porcupine Bank, the

Scotland continental shelf, the Rockall Plateau, the northern Rockall Trough, and the Faeroe-Iceland Ridge caused substantial bottom-limited regions (regions of depth difference). A well-developed USC was present greater than 80% of the time in all bottom-limited regions except over the Faeroe-Iceland Ridge. Here, acoustic propagation was confined to less reliable bottom bounce paths.

(C) Oceanographic conditions along the 1E-3B track (West European Basin) were quite variable owing to disparate intermediate water masses at opposite ends of the track. Surface sound velocities varied from about 1513 m/sec at point 1E to about 1489 m/sec at point 3B. A continuous USC occurred along the first 270 nm of the track, but disappeared crossing the North Atlantic Current. The depth of the DSC varied between 1500 m at point 1E to less than 100 m at point 3B. Deep axial velocities varied from 1493 and 1476 m/sec between these same points. Since the DSC was uninterrupted, it probably was the most effective propagation path between points 1E and 3B. Depth excess was greater than 400 m along the entire track, and allowed for unimpeded convergence zone propagation from a near-surface source. However, the region of intense mixing associated with the North Atlantic Current probably had adverse effects on acoustic propagation in the region between ACODAC 1C and ACODAC 2C.

(C) Sound velocity structures along the 2L-2K track were quite complex, since the track crossed the North Atlantic Current several times and also crossed the intense mixing zone due west of Porcupine Bank. Surface sound velocities varied from about 1516 m/sec at point 2L to about 1502 m/sec at point 2FA. A USC occurred near point 2L, around point 2C, and over the Rockall Trough. In all three regions, the USC was extremely well developed ("strengths" greater than 6 m/sec), and probably acted as a supplementary sound transmission path for sources within the upper channel. Along the entire

track, the depth and sound velocity at the DSC axis were quite erratic, varying from 700 to 1700 m and from 1485 to 1496 m/sec, respectively. Maximum values for both parameters occurred near point 2K at the base of the Scotland continental shelf. Over most of the track, the DSC was uninterrupted and probably acted as the most effective sound propagation path. Over the Rockall Trough, depth excess was not adequate for convergence zone formation considering a near-surface source. Here, sound propagation was confined to USC and bottom bounce paths. All modes of acoustic propagation probably were degraded by the intense mixing that occurred due west of Porcupine Bank (between the ACODAC 2C and 2D sites).

(C) Except over Rockall Trough, the 2BB-3AB track was bottom-limited by the shallow topography of the Rockall Plateau. The Rockall Plateau extended above the DSC axis and even into the USC. However, a well developed USC ("strengths" greater than 4 m/sec) occurred over most of the track. This USC apparently acted as a reliable acoustic path as indicated by the relatively low propagation losses observed by ANB 2BB for the KINGSPORT CW tow (event 13a). This is significant, since Rockall Bank was only 400 m below the surface at mid-range. DSC propagation was possible only over the deeper parts of Rockall Trough.

(C) Oceanographic conditions along the 3F-3ZZ track were more complex and variable than those along any other SQUARE DEAL baseline due to the wide variety of surface and intermediate water masses. Surface sound velocities varied between 1508 m/sec at point 3F and 1482 m/sec at point 3ZZ, but were between 1495 and 1498 m/sec along most of the track. A USC occurred over most of Maury Trough, and was well-developed ("strengths" of 3-5 m/sec) between points 3D and 3Z. In the Maury Trough, the USC probably acted as a supplementary sound propagation path for sources located there. Both the depth and sound velocity at the DSC were extremely variable and erratic along the entire

track. Deep axial depth varied between about 130 and 1150 m and deep axial velocity varied between about 1439 and 1457 m/sec. Southwest of point 3Z, the Faeroe-Iceland Ridge extended into the DSC and the DSC axis coincided with the near-bottom NSOW core. However, over most of the track, the DSC was uninterrupted and probably acted as the most reliable acoustic path. Depth excess was greater than 400 m over much of the track, and was adequate for convergence zone formation for a near-surface source. However, the shallow topography of the Faeroe-Iceland Ridge and the intense Polar Front precluded significant sound transmission between points 3D and 3ZZ. In addition, all modes of propagation probably were degraded by the oceanographic mixing associated with the Irminger Current between the ACCODAC 1C and 3D sites.

(C) Near point 3D, sound velocity structures were extremely complex throughout the water column. Near-bottom variability may have caused the extreme fluctuations in ambient noise intensity observed at ACCODAC 3D. The unusually high ambient noise levels recorded by the bottom hydrophone at ACCODAC 3D might be explained by turbidity and strong bottom currents that have been associated with NSOW boluses in Maury Trough (Cherkis et al., 1973).

(U) Sound velocity variations along the 3F-3ZZ track were more extreme than those found along any other SQUARE DEAL baseline. Sound velocities varied by about 26 m/sec at the surface, 34 m/sec at 500 m, 26 m/sec at 1000 m, and 21 m/sec at 1500 m. Much of this variation was caused by the intense Polar Front that lay just northeast of point 3Z during phase III of the exercise. Along the southern flanks of the Faeroe-Iceland Ridge (southwest of point 3Z), the depth of the DSC axis decreased from 1150 to 320 m (gradient of about 8.8 m/nm) and deep axial velocity decreased from 1484.6 to 1456.8 m/sec (gradient of about 0.3 m/sec/nm). Across the Polar Front itself, the sound velocity at the DSC axis decreased by 13.2 m/sec over a distance

of 36 nm (gradient of nearly 0.4 m/sec/nm), nearly double that found south of Davis Strait during the NORLANT-72 Exercise (Fenner and Bucca, 1974). In this same region, NSOW caused a variation in deep axial velocity of 10.8 m/sec over a period of less than four days (point 3Z time-series station). These dramatic variations at the DSC axis indicate that sound velocity structures along the crest of the Faeroe-Iceland Ridge are more complex and variable than those found during any previous LRAPP exercise.

## IX. References (U)

- Baranov, Y.I. (1972). Average Monthly Positions of Oceanic Fronts in the North Atlantic. *Oceanology*, v. 12, no. 2, p. 187-193 (translated from Russian by Am. Geophys. Union).
- Bubnov, V.A. (1968). Intermediate Subarctic Waters in the Northern Part of the Atlantic Ocean. *Okeanologicheskkiye Issledovaniya*, v. 19, p. 136-153 (translated from Russian as Naval Oceanographic Office Translation 545, Washington, D.C., 1973, 26 p.).
- Carnvale, A., P. Bowe, M. Basileo, and J. Sprenke (1968). Absolute Sound Velocity Measurement in Distilled Water. *J. Acoust. Soc. Am.*, v. 44, n. 4, October, p. 1098-1102.
- Cherkis, N.Z., H.S. Fleming, and R.H. Feden (1973). Morphology and Structure of Maury Channel, Northeast Atlantic Ocean. *Bull. Geol. Soc. Am.*, v. 84, May, p. 1601-1606.
- Defant, A. (1961). *Physical Oceanography*, Volume 1. New York, Pergamon, 729 p.
- Dietrich, G. (1967). The International "Overflow" Expedition (ICES) of the Iceland-Faeroe Ridge, May-June 1960, A Review. *Rapports et Proces-Verbaux des Reunions Conseil Permanent International pour l'Exploration de la Mer*, v. 157, July, p. 268-274.

# CONFIDENTIAL

Ellet, D.J. and D.G. Roberts (1973). The Overflow of Norwegian Sea Deep Water Across the Wyville-Thomson Ridge. Deep Sea Res., v. 20, p. 819-835.

Fenner, D.F. and P.J. Bucca (1971). The Sound Velocity Structure of the North Atlantic Ocean. Naval Oceanographic Office, Washington, D.C., November, 86 p. (NAVOCEANO IR No. 71-13).

Fenner, D.F. and P.J. Bucca (1973). CHURCH GABBRO Sound Velocity Analysis and Environmental Data Summary. Naval Oceanographic Office, Washington, D.C., May, 57 p. (NAVOCEANO Tech. Note No. 7005-3-73).

Fenner, D.F. and P.J. Bucca (1974). Sound Velocity Structure of the Labrador Sea, Irminger Sea, and Baffin Bay During the NORLANT-72 Exercise (U). Naval Oceanographic Office, Washington, D.C., November, 97 p. (NAVOCEANO Provisional TR-245). CONFIDENTIAL

Guthrie, R.C. (1964). Sound Velocity Distribution in the Irminger Sea. Proc. First U.S. Navy Symposium on Military Oceanography, Naval Oceanographic Office, Washington, D.C., v. 1, p. 97-111.

Hanna, J.S. (1969). Sound Propagation in the Presence of a Strongly-Developed Secondary Sound Channel (U). Proc. 27th Navy Symposium on Underwater Acoustics, Naval Undersea Research and Development Center (now Naval Ocean Systems Center), San Diego, Calif., v. 1, p. 262-270. CONFIDENTIAL

Herman, F. (1967). The T-S Diagram Analysis of the Water Masses Over the Iceland-Faeroe Ridge and in the Faeroe Bank Channel. Rapports et Proces-Verbaux des Reunions Conseil Permanent International pour l'Exploration de la Mer, v. 157, July, p. 139-159.

Howe, M.R. and R.I. Tait (1967). A Subsurface Cold-Core Cyclonic Eddy. Deep Sea Res., v. 14, p. 373-378.

Lee, A. and D. Ellet (1965). On the Contribution of Overflow Water from the Norwegian Sea on the Hydrographic Structure of the North Atlantic Ocean. Deep Sea Res., v. 12, p. 129-142.

Magaard, I. and W. Krauss (1967). Internal Waves at Diamond Stations During the International Iceland-Faeroe Ridge Expedition. May-June 1960. Rapports et Proces-Verbaux des Reunions Conseil Permanent International pour l'Exploration de la Mer, v. 157, July, p. 173-183.

Maury Center for Ocean Science (1973). SQUARE DEAL Exercise Plan (U). Washington, D.C., May, MC Plan 012. CONFIDENTIAL

Maury Center for Ocean Science (1974). SQUARE DEAL Synopsis Report (U). Washington, D.C., February, MC Rep. 0015. SECRET

Maury Center for Ocean Science (1975). SQUARE DEAL Environmental Acoustics Summary (U). Washington, D.C., October (revised November 1977), MC Rep. 111. SECRET

Naval Oceanographic Office (1965). Oceanographic Atlas of the North Atlantic Ocean, Section 1, Tides and Currents. H.O. Pub. No. 700, Washington, D.C., 75 p.

Rossov, V.V. and A.G. Kislyakov (1972). The Polar Front in the North Atlantic in 1968-1969. Rapports et Proces-Verbaux des Reunions Conseil International pour l'Exploration de la Mer, v. 162, October, p. 220-226.

Sverdrup, H.U., M.W. Johnson, and R.H. Fleming (1966). The Oceans, Their Physics, Chemistry, and General Biology. Englewood Cliffs, N.J., Prentice-Hall, 1087 p.

Wilson, W.D. (1960). Equation for the Speed of Sound in Sea Water. J. Acoust. Soc. Am., v. 32, n. 10, October, p. 1357-1358.

## Appendix A: Temperature-Salinity-Sound Velocity Relations at Selected SQUARE DEAL Reference Points (U)

(U) This appendix contains temperature, salinity, and sound velocity profiles along with T-S diagrams for 13 selected SQUARE DEAL reference points, including the two occupations of the Porcupine Bank time-series station. Locations of the various reference points are shown in Figure 6. All data used in constructing Figures 49-61 were collected during the exercise.

(U) At point 1C (Fig. 49), Labrador Sea Water (LSW) was the predominant water mass throughout the water column. This water mass caused a shallow, low velocity deep sound channel (DSC) just above the depth of the salinity minimum for the upper LSW lobe. The lower LSW lobe (1600 m) did not appreciably affect the positive velocity gradient below the DSC axis.

(U) At point 1E (Fig. 50), the interplay of various water masses created a bichannel sound velocity profile, where the upper sound channel (USC) was separated from the DSC by an intermediate-depth sound velocity maximum that coincided with the Mediterranean Intermediate Water (MIW) salinity maximum. The USC axis occurred at the maximum depth of summer warming, and various secondary T-S maxima in the MIW core caused sound velocity perturbations above the DSC axis. The DSC axis at point 1E was considerably deeper and of higher velocity than that at point 1C, due to the presence of MIW. The 56% unmixed MIW concentration at point 1E was the highest found at any SQUARE DEAL reference point. The single lobe of LSW at about 1760 m was too diluted by mixing and occurred too deep in the water column to affect sound velocity structures at point 1E.

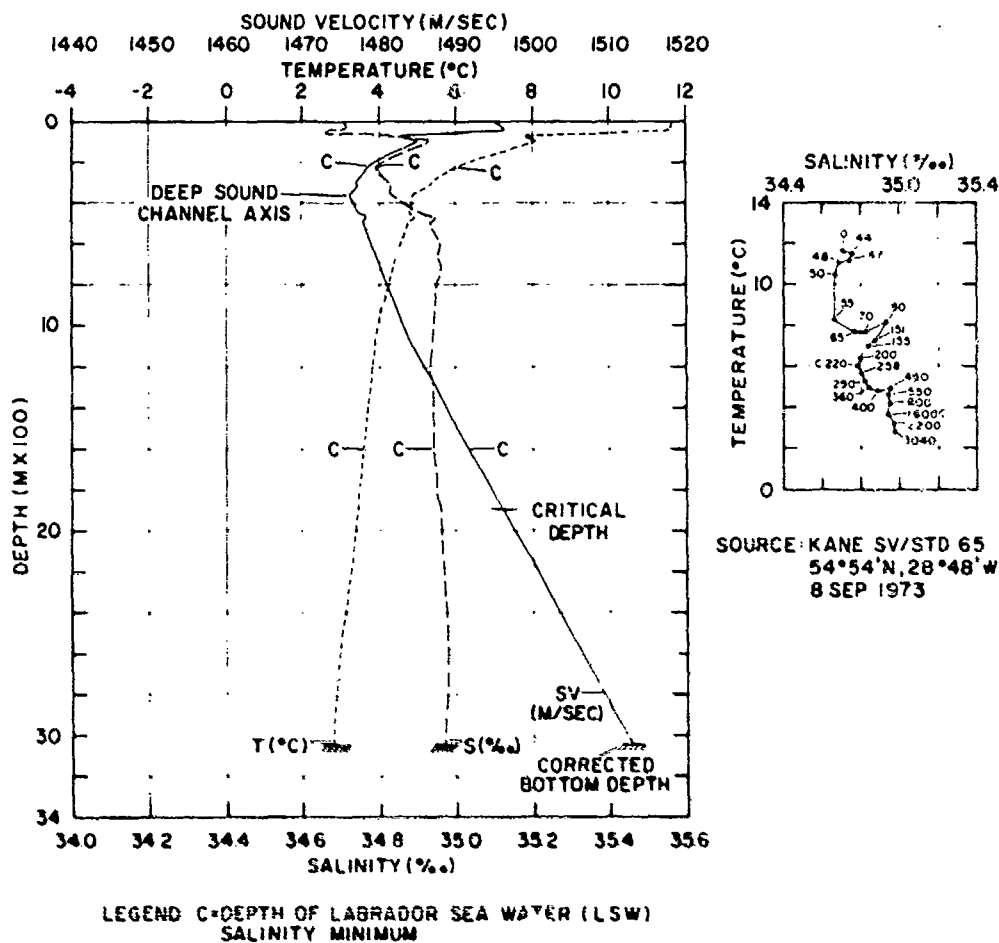
(U) At points 2C, 2D, 2F, and 2L (Figs. 51, 52, 53, and 54, respectively), the overall sound velocity structure was

quite similar to that at point 1E with one notable exception: the intermediate sound velocity maximum lay at depths well above those of the MIW salinity maximum. At these sites, the intermediate sound velocity maximum apparently corresponded to the maximum depth of winter cooling and roughly coincided with the bottom of the North Atlantic Current. This situation applied throughout much of the SQUARE DEAL area. At points 2D and 2F (Figs. 52 and 53), the USC was particularly well-developed, and the sound velocity at the intermediate maximum was more than 6 m/sec greater than that at the USC axis. In addition, Norwegian Sea Overflow Water (NSOW) was present at point 2F just above the bottom. This water mass emanated from the north across the Wyville-Thomson Ridge (Ellet and Roberts, 1973) and caused lower sound velocities in the near-bottom layer throughout Rockall Trough.

(U) At point 3B (Fig. 55), LSW was the predominant water mass, and the sound velocity structure was similar to that at point 1C (Fig. 49). However, both LSW lobes at point 3B lay higher in the water column due to the proximity of the Reykjanes Ridge. The lower LSW lobe caused a deflection in the sound velocity profile at about 1060 m depth. Both MIW and NSOW were present at point 3B, but neither water mass affected the positive sound velocity gradient below the DSC axis.

(U) At point 3D (Fig. 56), the sound velocity profile was basically isovelocity between about 100 and 1000 m. The sound velocity at the USC axis was less than that at the DSC axis, and the intermediate maximum lay only 100 m above deep axial depth. This type of sound velocity profile was common throughout northern Maury Trough and



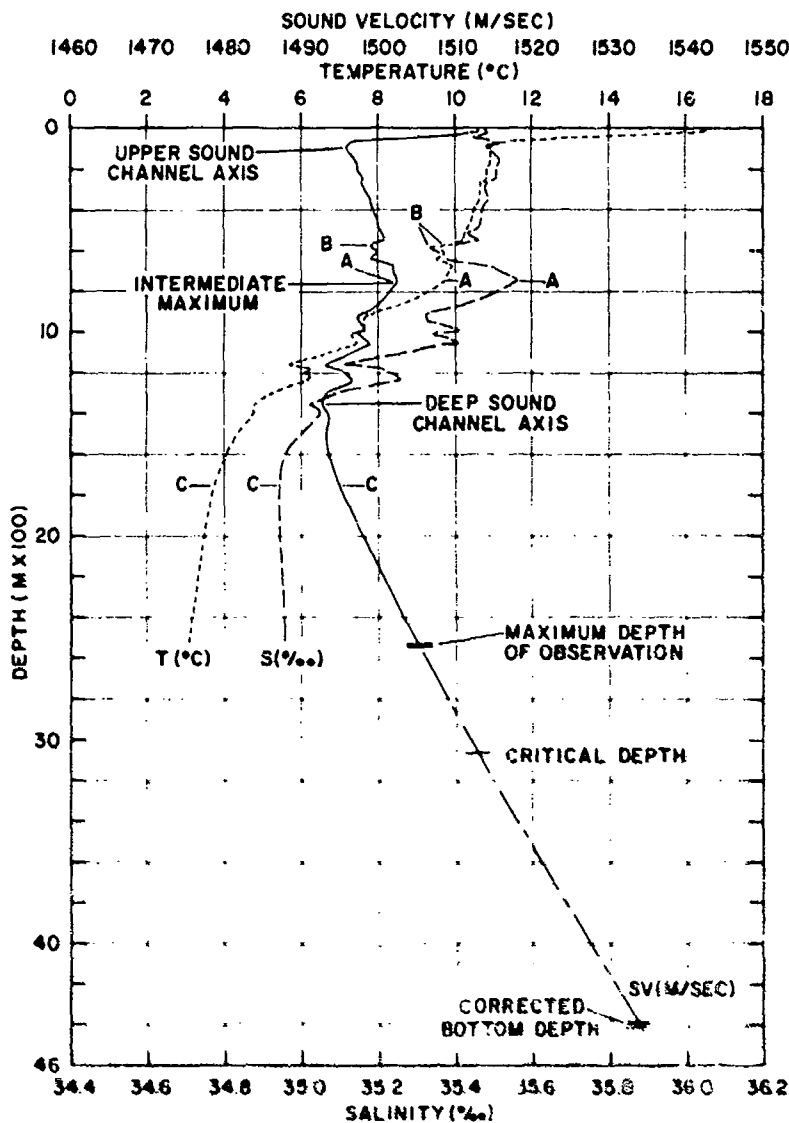


**CONFIDENTIAL**

(U) Figure 49. Temperature-Salinity-Sound Velocity Profiles and T-S Diagram at Point 1C

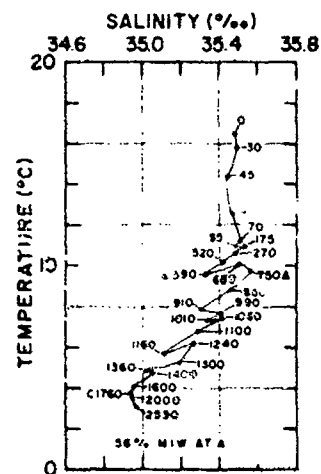
**CONFIDENTIAL**

CONFIDENTIAL



LEGEND A-DEPTH OF MEDITERRANEAN INTERMEDIATE WATER (MIW) SALINITY MAXIMUM  
B-BOTTOM OF NORTH ATLANTIC CENTRAL WATER (NACW) LAYER  
C-DEPTH OF LABRADOR SEA WATER (LSW) SALINITY MINIMUM

CONFIDENTIAL

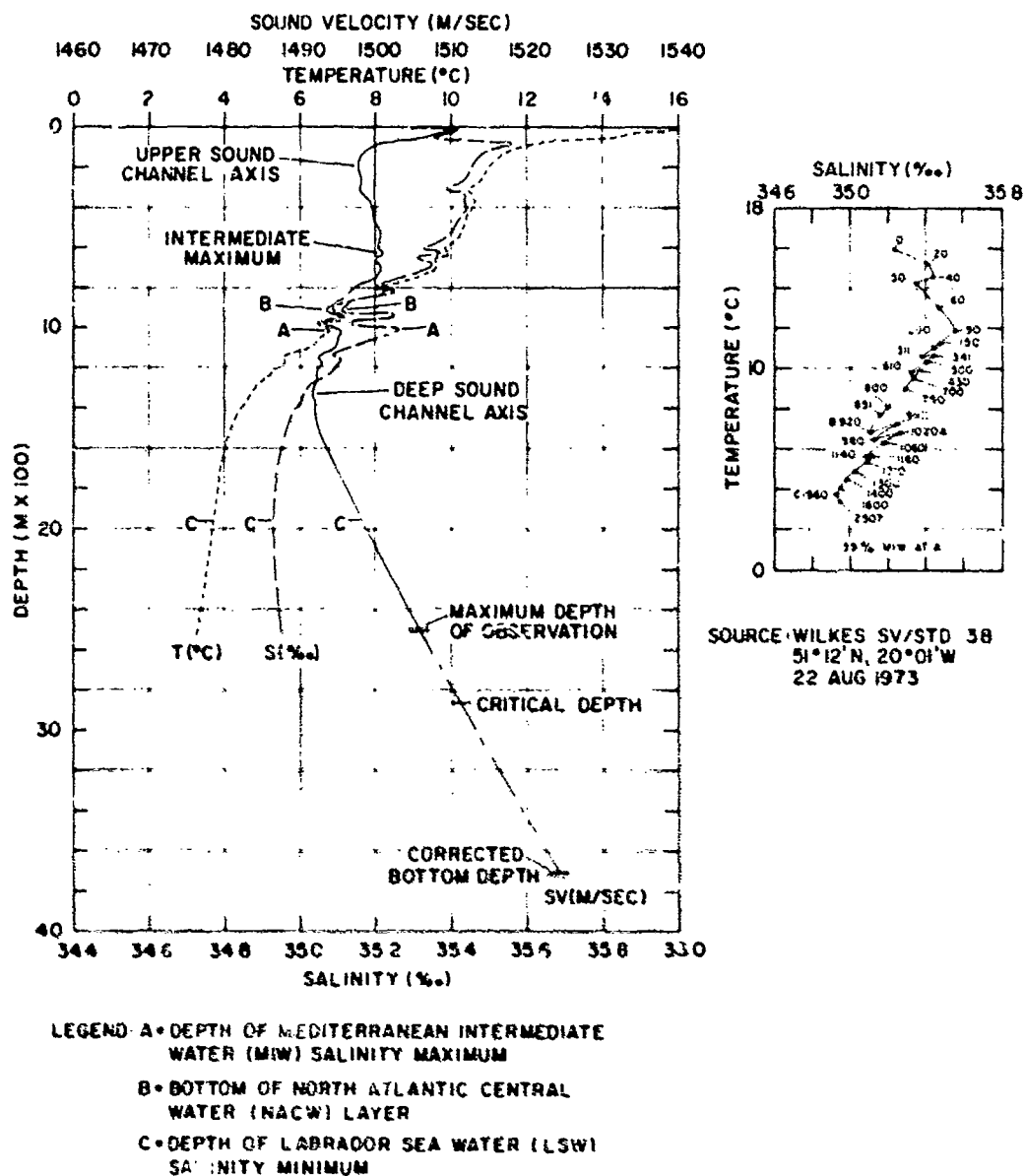


SOURCE: KANE SV/STD 32  
49°34'N, 14°32'W  
18 AUG 1973

(U) Figure 50. Temperature-Salinity-Sound Velocity Profiles and T-S Diagram at Point 1E

CONFIDENTIAL

CONFIDENTIAL

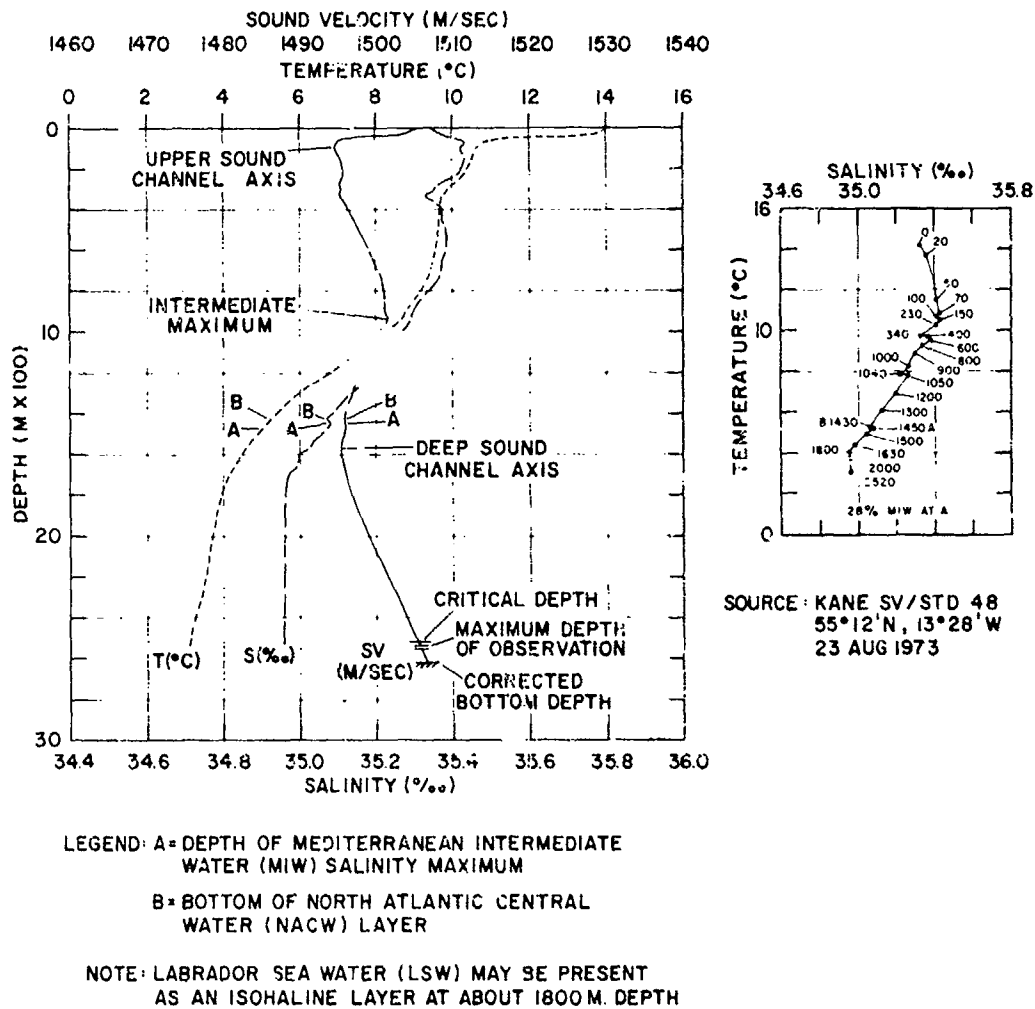


CONFIDENTIAL

(U) Figure 51 Temperature-Salinity-Sound Velocity Profiles and T-S Diagram of Point 2C

CONFIDENTIAL

CONFIDENTIAL

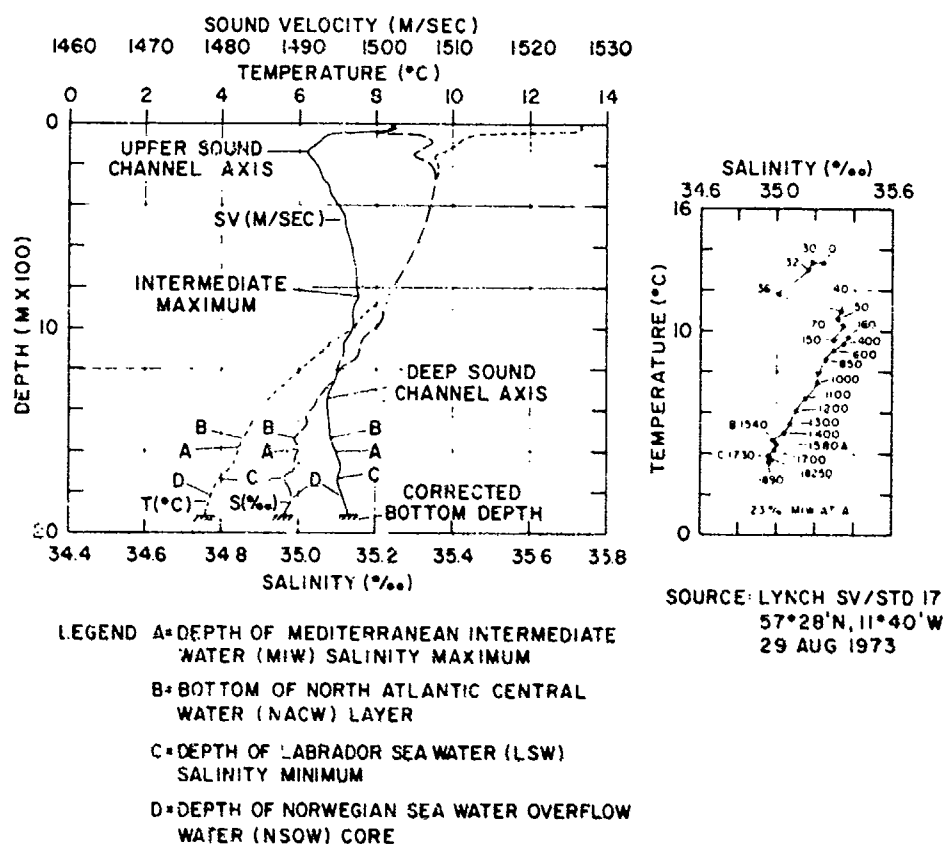


CONFIDENTIAL

(U) Figure 52. Temperature-Salinity-Sound Velocity Profiles and T-S Diagram at Point 2D

CONFIDENTIAL

CONFIDENTIAL

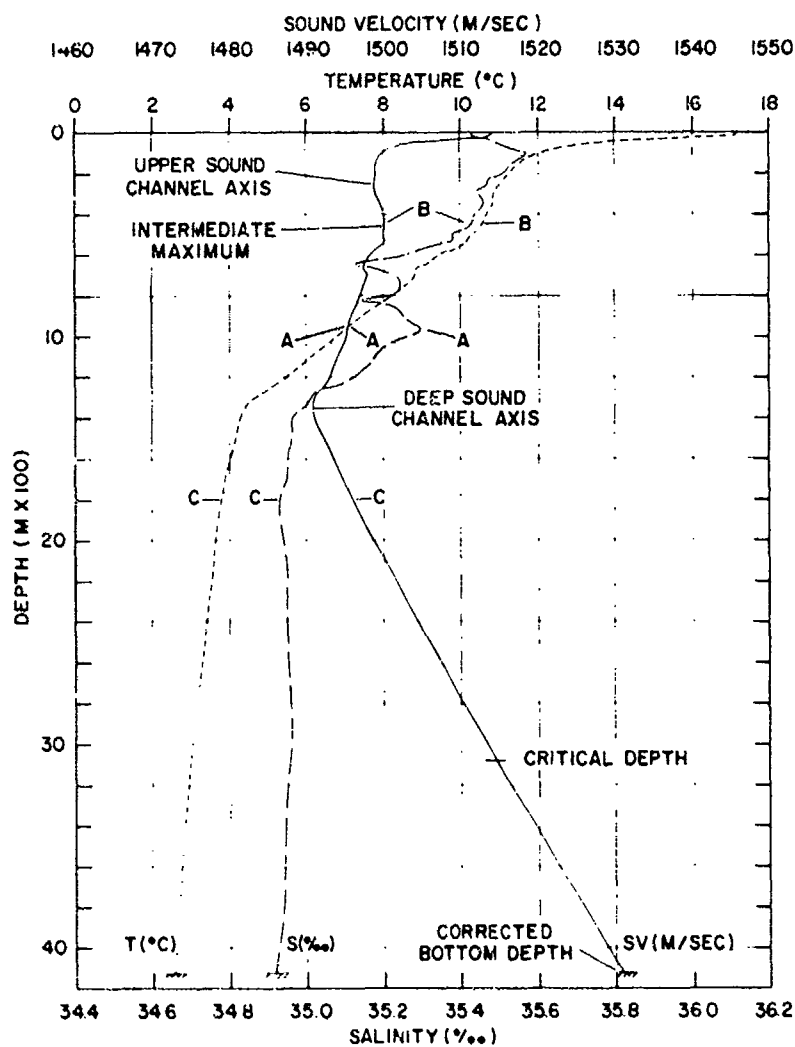


CONFIDENTIAL

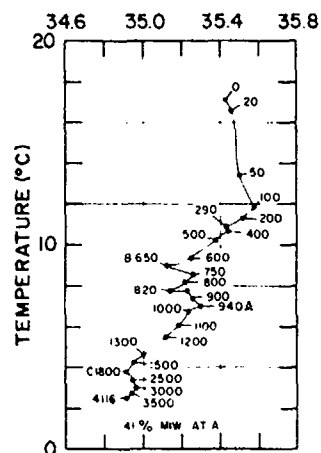
(U) Figure 52. Temperature-Salinity-Sound Velocity Profiles and T-S Diagram at Point 2F

CONFIDENTIAL

CONFIDENTIAL



LEGEND: A = DEPTH OF MEDITERRANEAN INTERMEDIATE WATER (MIW) SALINITY MAXIMUM  
 B = BOTTOM OF NORTH ATLANTIC CENTRAL WATER (NACW) LAYER  
 C = DEPTH OF LABRADOR SEA WATER (LSW) SALINITY MINIMUM



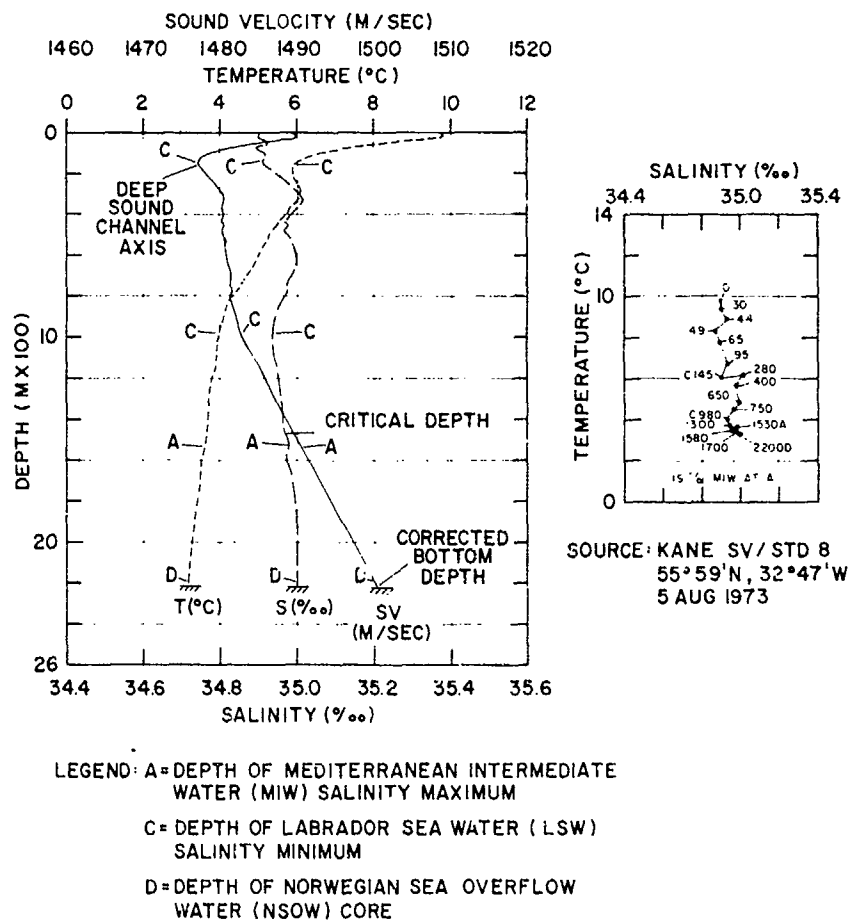
SOURCE: WILKES SV/STD 33  
 48°10'N, 23°57'W  
 20 AUG 1973

CONFIDENTIAL

(U) Figure 54. Temperature-Salinity-Sound Velocity Profiles and T-S Diagram at Point 2L

CONFIDENTIAL

CONFIDENTIAL

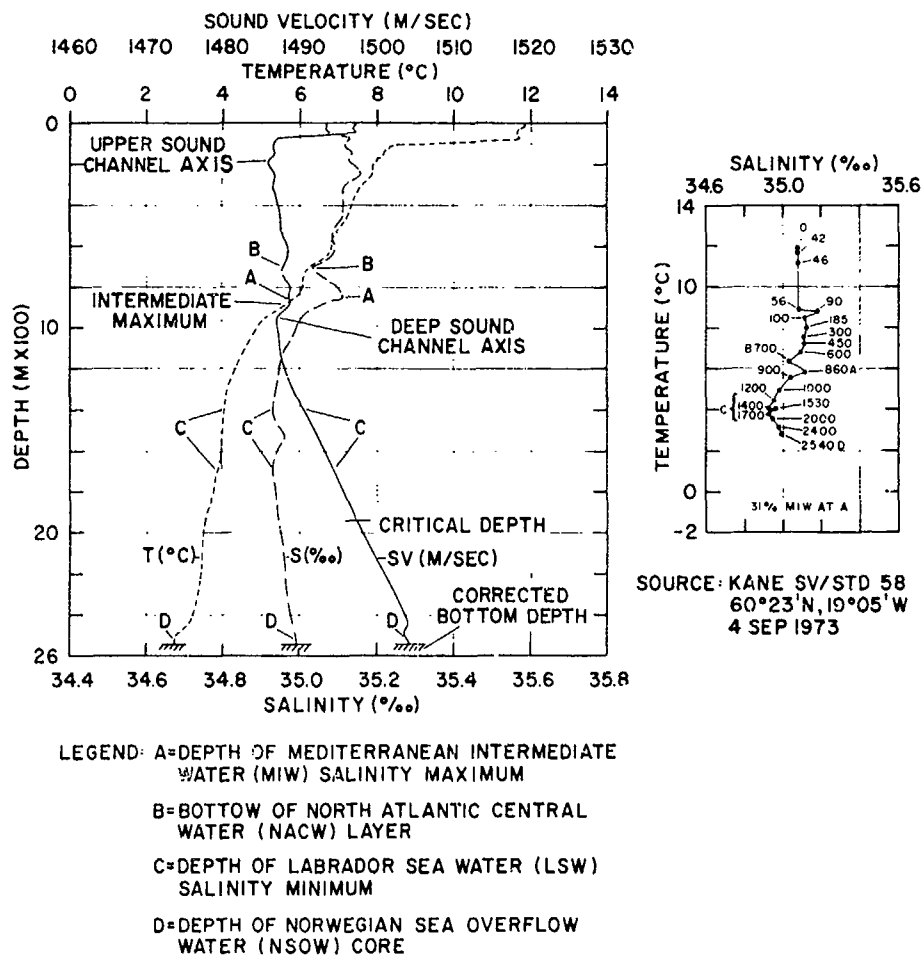


CONFIDENTIAL

(U) Figure 55. Temperature-Salinity-Sound Velocity Profiles and T-S Diagram at Point 3B

CONFIDENTIAL

CONFIDENTIAL



CONFIDENTIAL

(U) Figure 56. Temperature-Salinity-Sound Velocity Profiles and T-S Diagram at Point 3D

CONFIDENTIAL



was caused by mixing of MIW with North Atlantic Central Water carried by the Irminger Current. Two LSW lobes occurred at point 3D, both below the DSC axis. In the near-bottom layer, very cold, low salinity NSOW descending into the Maury Trough from the north caused a small sound channel just above the bottom. Throughout the Maury Trough, NSOW caused a weakening of the near-bottom positive velocity gradient and resulted in lower sound velocities than those found in either Rockall Trough or the West European Basin. Similar near-bottom sound velocity structures have been observed west of the Reykjanes Ridge in the Irminger Sea by Guthrie (1964).

(U) At point 3F (Fig. 57), the sound velocity structure was somewhat different from that found throughout most of the exercise area. Although LSW was present at point 3F, it did not result in as shallow or low velocity a DSC axis as would be expected for a location west of the Mid-Atlantic Ridge. This was due to both the presence of MIW and the proximity of point 3F to the North Atlantic Current (Fig. 6).

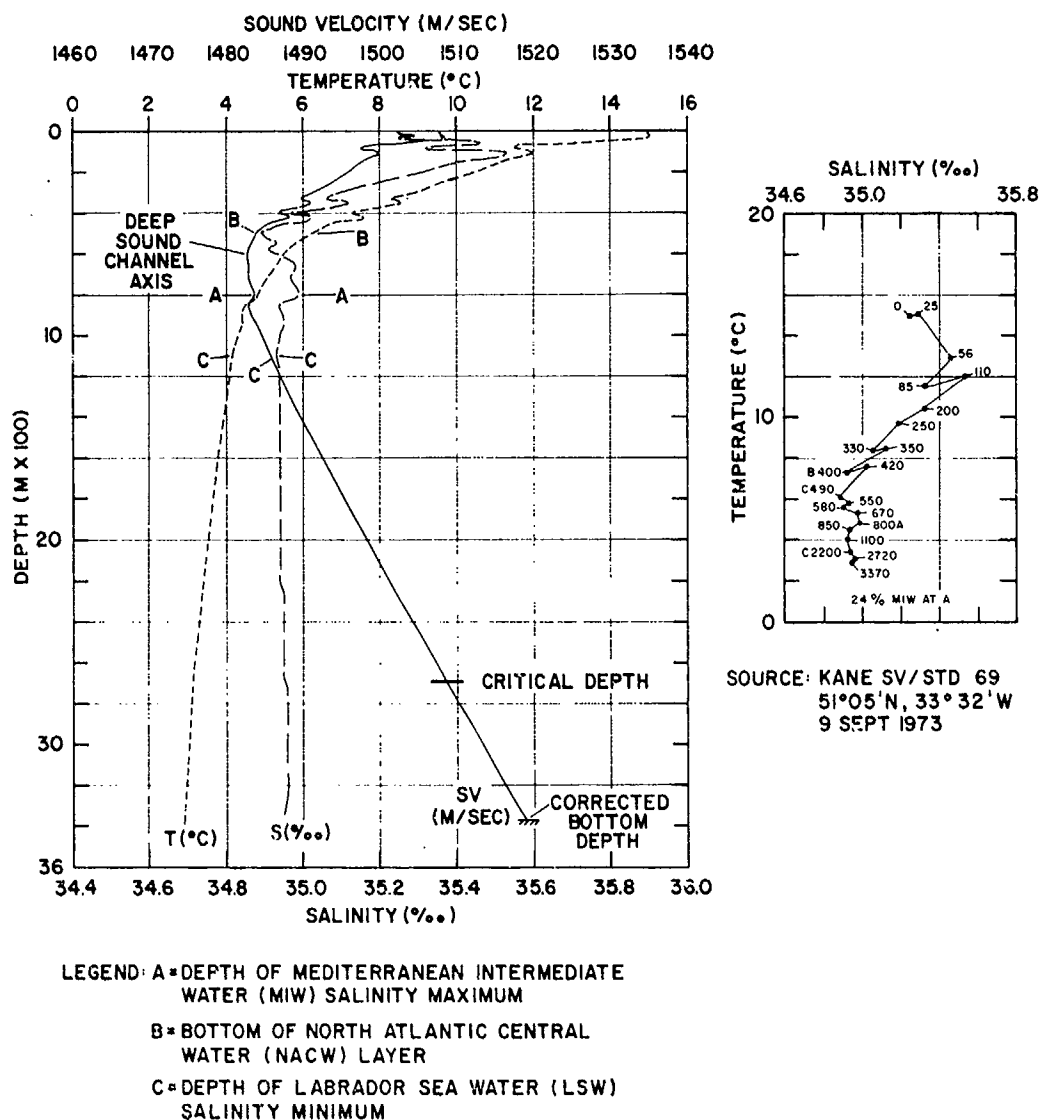
(U) Figure 58 demonstrates oceanographic conditions along the crest of the Faeroe-Iceland Ridge, and is typical of conditions farther west at point 3Z. Here, the minimum sound velocity in the water column occurred at the bottom and coincided with the depth of the NSOW core. Along the southern flanks of the Faeroe-Iceland Ridge (i.e., between points 3D and 3Z), the sound velocity minimum produced a narrow sound channel just above the bottom. At point 3ZZ in the Norwegian Basin (Fig. 59), extremely cold Norwegian Sea Deep Water caused sound velocities to be 25-30 m/sec lower than those at the same depth south of the Faeroe-Iceland Ridge. This large difference indicates that points 3D and 3ZZ were separated by an intense frontal zone (Polar Front) that extended to depths greater than 1000 m. During SQUARE DEAL, point 3Z lay just south of the meandering Polar Front (Fig. 6).

(U) Two temperature-salinity-sound velocity comparisons are presented for the Porcupine Bank time-series station, one for phase I (Fig. 60) and one for phase II (Fig. 61). The phase I station was occupied about 9 days prior to the phase II station. Both figures show the presence of MIW at depths between 750 and 800 m and LSW at depths between 1600 and 1750 m. However, the weak USC present during phase I was replaced by intense sound velocity perturbations during phase II. In addition, the DSC axis was nearly 200 m deeper in the water column during phase I than during phase II. Such variability was caused by internal waves, the passage of MIW boluses, and the migration of a LSW cell into the region west of Porcupine Bank between phases I and II. The T-S diagram in Figure 61 shows several T-S perturbations between depths of about 400 and 1000 m that were caused by mixing between MIW and the upper LSW lobe. Such mixing would be expected throughout the southern part of Rockall Trough.

#### References (U)

- Ellet, D.J. and D.G. Roberts (1973). The Overflow of Norwegian Sea Deep Water Across the Wyville-Thomson Ridge. *Deep Sea Res.*, v. 20, p. 819-835.
- Guthrie, R.C. (1964). Sound Velocity Distribution in the Irminger Sea. *Proc. First U.S. Navy Symposium on Military Oceanography*, Naval Oceanographic Office, Washington, D.C., v. 1, p. 97-111.

CONFIDENTIAL

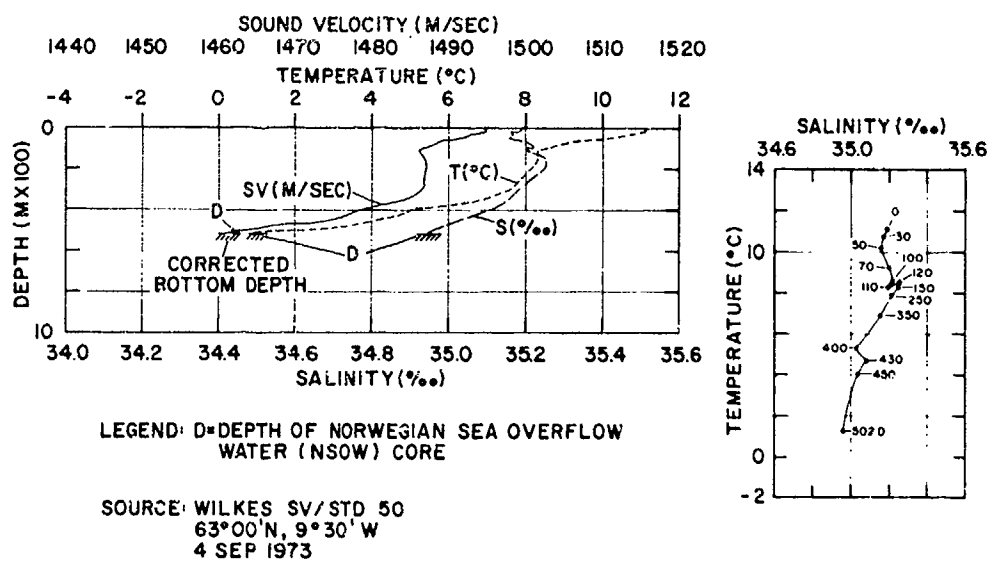


CONFIDENTIAL

(U) Figure 57. Temperature-Salinity-Sound Velocity Profiles and T-S Diagram at Point 3F

CONFIDENTIAL

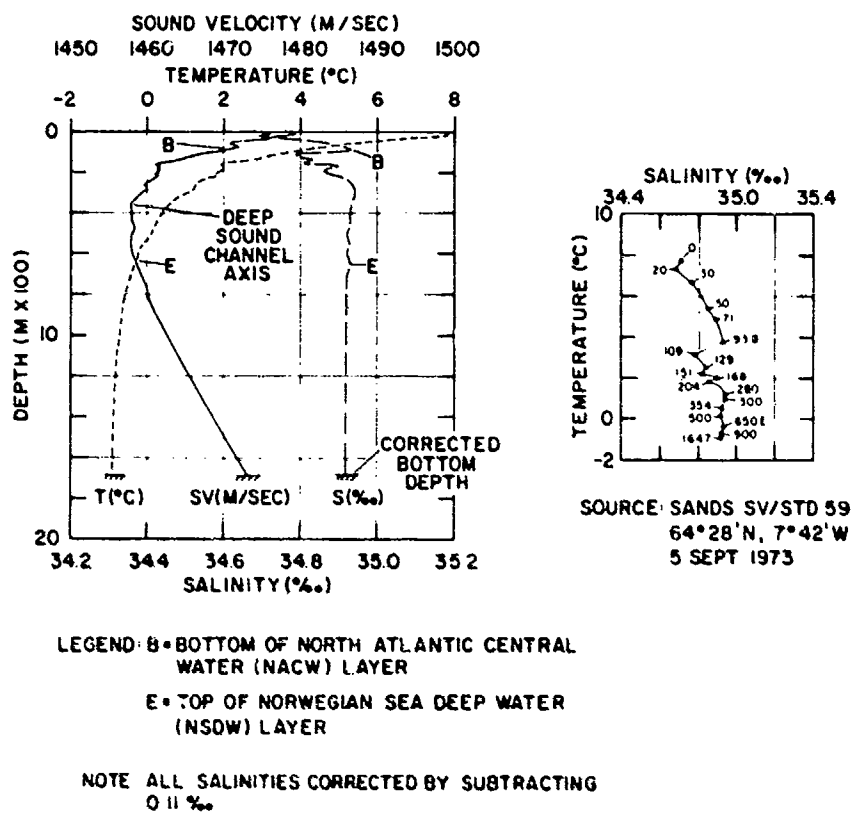
CONFIDENTIAL



CONFIDENTIAL

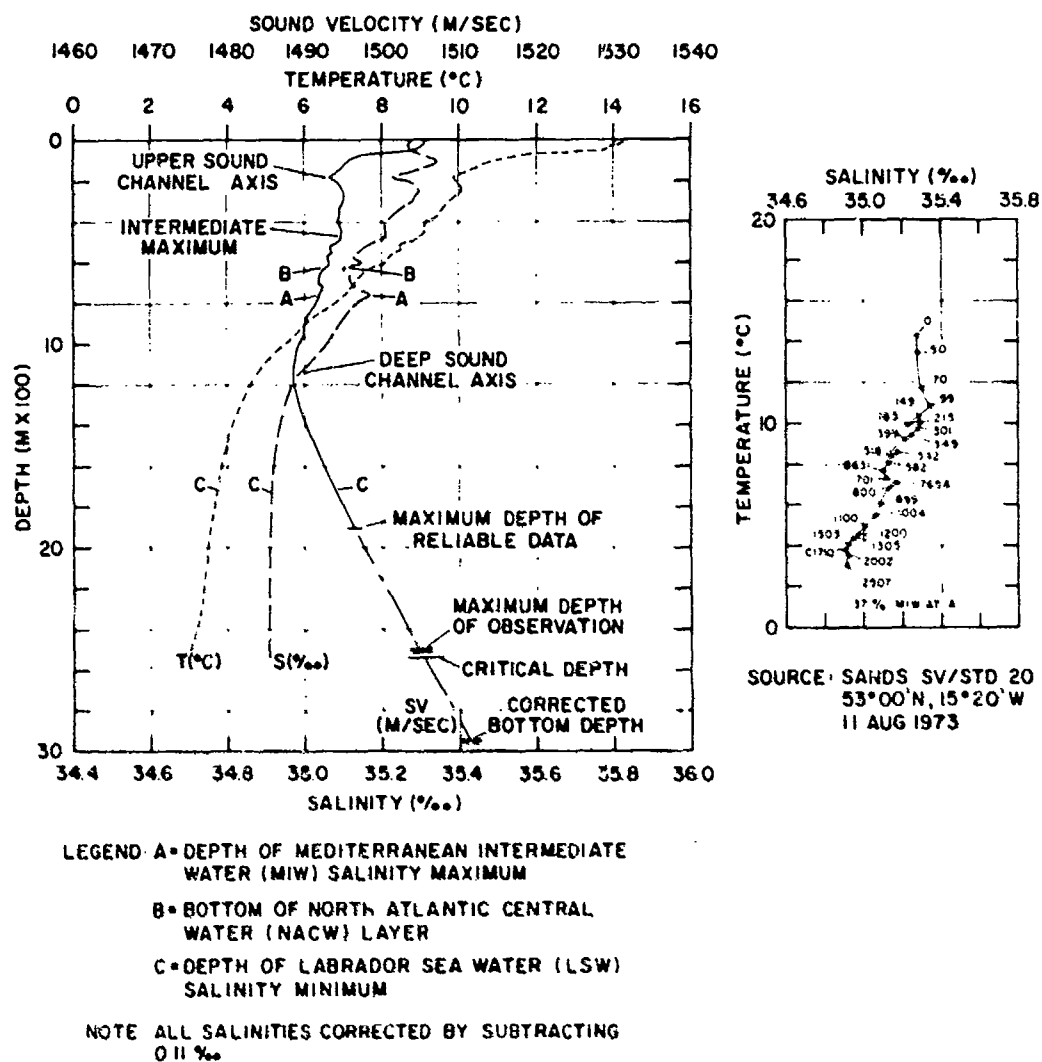
(U) Figure 58. Temperature-Salinity-Sound Velocity Profiles and T-S Diagram on Faeroe-Iceland Ridge Near Point 32

CONFIDENTIAL



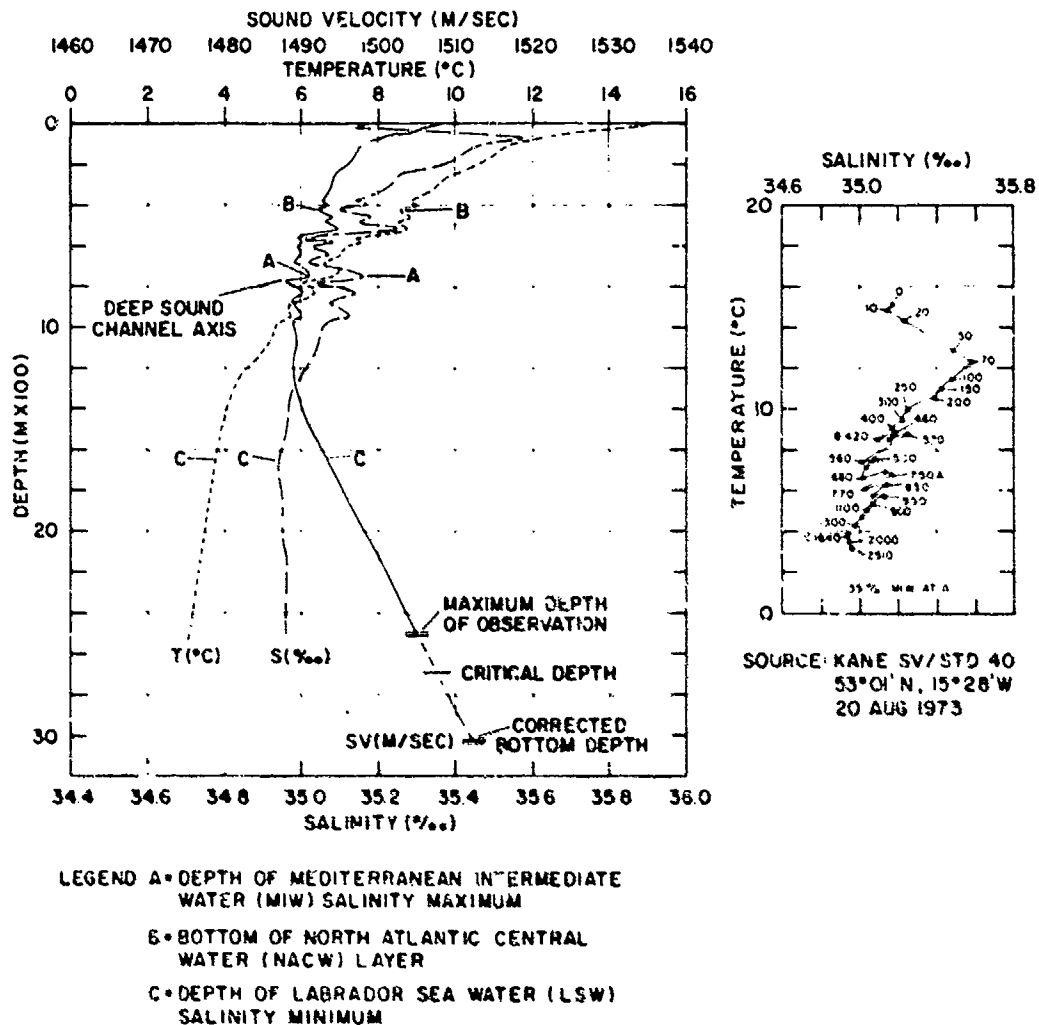
CONFIDENTIAL

(U) Figure 59. Temperature-Salinity-Sound Velocity Profiles and T-S Diagram at Point 322



UNCLASSIFIED

(U) Figure 60. Temperature-Salinity-Sound Velocity Profiles and T-S Diagram Off Porcupine Bank (Phase I)



UNCLASSIFIED

(U) Figure 61. Temperature-Salinity-Sound Velocity Profiles and T-S Diagram Off Porcupine Bank (Phase II)

CONFIDENTIAL

THIS PAGE INTENTIONALLY  
LEFT BLANK

# CONFIDENTIAL

## Appendix B: Data Identification Tables (U)

REFERENCE POINT	SV/STD OR SVD OBSERVATION	DATE (1973)	TIME (GMT)	Phase	LAT (°N)	LONG (°W)
1A/1AA	WI 1	5 Aug	2231	I	54°49'	25°21'
	AR 8	12 Aug	2045	I	54°54'	24°57'
1C	KN 5	4 Aug	1300	I	54°54'	28°53'
	KN 65	8 Sep	0316	III	54°54'	28°48'
1E	SD 1	1 Aug	1530	I	49°18'	14°51'
	KN 32	18 Aug	0900	II	49°34'	14°32'
2A/2AA	AR 10	16 Aug	1040	II	56°09'	13°58'
	AR 17	26 Aug	0850	II	56°09'	13°59'
2BA/2BB	AR 9	14 Aug	1330	I	54°16'	13°12'
	SD 34	17 Aug	1929	II	53°56'	12°56'
	AR 16	25 Aug	1600	II	54°18'	13°03'
2C/2CA	SD 5	3 Aug	1000	I	51°20'	19°39'
	WI 39	22 Aug	2100	II	51°47'	19°08'
2D	SD 30	16 Aug	0050	II	55°11'	13°52'
	SD 50(U)	23 Aug	2310	II	55°14'	13°28'
2FA/3QB	AR 11	22 Aug	1710	II	56°38'	10°45'
	LY 16	29 Aug	0430	II	56°31'	10°14'
	WI 43	31 Aug	2014	III	56°41'	11°07'
3A/3AA	LY 8	26 Aug	1808	II	59°07'	18°39'
	KN 57	4 Sep	0618	III	59°07'	18°37'
	AR 1(RAE)	15 Sep	1800	—	59°07'	18°08'
3D	KN 58	4 Sep	1811	III	60°23'	19°05'
	SD 79	10 Sep	0832	III	60°27'	19°05'
3F	WI 14	11 Aug	1753	I	51°06'	33°36'
	KN 69	9 Sep	2339	III	51°05'	33°32'
3Z	AR 18	7 Sep	1510	III	63°11'	12°21'
	AR 27(U)	13 Sep	0845	III	63°16'	12°19'
3ZZ	SD 59	5 Sep	0843	III	64°28'	7°42'
	SD 8(RAE)	15 Sep	2257	—	64°28'	7°42'
Porcupine Bank	SD 17	10 Aug	1000	I	52°58'	15°14'
	SD 44(U)	21 Aug	1529	II	53°02'	15°32'

NOTES: \* (U) indicates upcast, all other data from downcasts.

\* (RAE) indicates data from the Ridge Acoustics Exercise.

CONFIDENTIAL

(U) Table 2. Identification of Temporal Sound Velocity Comparison Data



# CONFIDENTIAL

PROFILE	OBSERVATION	DATE (1973)	TIME (GMT)	LAT (°N)	LONG (°W)
1	AR XBT 1	5 Aug	2030	54°55'	29°03'
2	AR XBT 2	6 Aug	0415	54°55'	28°41'
3	AR XBT 3	6 Aug	0800	54°54'	28°37'
4	AR SVD 1(D)	6 Aug	1342	54°52'	28°37'
5	AR XBT 5	6 Aug	2000	54°51'	28°27'
6	AR SVD 2(D)	7 Aug	0035	54°48'	28°18'
7	AR XBT 6	7 Aug	0300	54°46'	28°15'
8	AR XBT 7	7 Aug	0800	54°45'	28°09'
9	AR SVD 3(D)	7 Aug	1445	54°41'	28°29'
10	AR XBT 9	7 Aug	2000	54°49'	28°26'
11	AR SVD 4(D)	8 Aug	0050	54°54'	28°42'
12	AR XBT 11	8 Aug	0400	54°53'	28°40'
13	AR SVD 5(D)	8 Aug	1232	54°51'	28°36'
14	KP XBT 32	9 Aug	0400	54°53'	29°08'
15	KP XBT 34	9 Aug	0800	54°53'	28°24'
16	KN SV/STD 5(D)	9 Aug	1330	54°53'	28°53'
17	KN XBT 51	9 Aug	1610	54°53'	28°52'

- NOTES:
- All SVD and SV/STD times are means of total elapsed cast time.
  - (D) indicates downcast.
  - Nominal position of Point 1C is 54°52'N, 28°49'W.

## CONFIDENTIAL

(U) Table 3. Identification of Data Used in Phase I Time-Series Study at Point 1C

PROFILE	OBSERVATION	DATE (1973)	TIME (GMT)	LAT (°N)	LONG (°W)
1	WI SV/STD 38(D)	22 Aug	1038	51°12'	20°00'
2	OL XBT 9	22 Aug	1600	51°14'	20°00'
3	OL XBT 10	22 Aug	1800	51°35'	19°38'
4	KP XBT 133	22 Aug	2000	51°40'	19°45'
5	KP XBT 134	22 Aug	2200	51°37'	19°28'
6	CH XBT 29	23 Aug	0230	51°41'	20°10'
7	CH SV/CTD 14(D)	23 Aug	0530	51°31'	20°09'
8	CH SV/CTD 14(U)	23 Aug	0656	51°34'	20°09'
9	CH XBT 30	23 Aug	0900	51°22'	20°08'
10	CH XBT 31	23 Aug	1600	51°23'	19°42'
11	CH SV/CTD 16(D)	24 Aug	0240	51°26'	19°33'

- NOTES:
- All SV/STD and SV/CTD times are means of total elapsed cast time.
  - (U) indicates upcast, (D) indicates downcast.
  - Nominal position of Point 2C is 51°30'N, 19°38'W.

## CONFIDENTIAL

(U) Table 4. Identification of Data Used in Phase II Time-Series Study at Point 2C

# CONFIDENTIAL

PROFILE	SANDS OBSERVATION	DATE (1973)	TIME (GMT)	LAT (°N)	LONG (°W)
1	SV/STD 41(D)	22 Aug	0415	55°11'	13°30'
2	SV/STD 41(U)	22 Aug	0545	55°11'	13°30'
3	SV/STD 42(D)	22 Aug	0900	55°14'	13°31'
4	SV/STD 42(U)	22 Aug	1030	55°14'	13°31'
5	SV/STD 43(D)	22 Aug	1402	55°14'	13°34'
6	SV/STD 43(U)	22 Aug	1547	55°14'	13°34'
7	SV/STD 44(D)	22 Aug	1856	55°16'	13°36'
8	XBT 102	22 Aug	2055	55°16'	13°35'
9	SV/STD 45(D)	22 Aug	2351	55°13'	13°34'
10	SV/STD 45(U)	23 Aug	0013	55°13'	13°34'
11	SV/STD 46(D)	23 Aug	0422	55°14'	13°34'
12	SV/STD 46(U)	23 Aug	0557	55°14'	13°34'
13	SV/STD 47(D)	23 Aug	0900	55°15'	13°33'
14	SV/STD 47(U)	23 Aug	1015	55°15'	13°33'
15	SV/STD 48(D)	23 Aug	1355	55°12'	13°32'
16	SV/STD 48(U)	23 Aug	1519	55°12'	13°32'
17	SV/STD 49(D)	23 Aug	1843	55°13'	13°29'
18	SV/STD 49(U)	23 Aug	2006	55°13'	13°29'
19	SV/STD 50(D)	23 Aug	2242	55°14'	13°28'
20	SV/STD 50(U)	23 Aug	2337	55°14'	13°28'

- NOTES:
- All SV/STD times are means of total elapsed cast time.
  - (U) indicates upcast, (D) indicates downcast.
  - Nominal position of Point 2D is 55°13'N, 13°33'W.

## CONFIDENTIAL

(U) Table 5. Identification of Data Used in Phase II Time-Series Study at Point 2D

PROFILE	OBSERVATION	DATE (1973)	TIME (GMT)	LAT (°N)	LONG (°W)
1	AR XBT 32	22 Aug	1720	56°38'	10°44'
2	AR SVD 11(U)	22 Aug	1834	56°38'	10°45'
3	AR SVD 12(D)	23 Aug	0700	56°38'	10°45'
4	AR SVD 13(D)	23 Aug	1930	56°38'	10°45'
5	OL XBT 23	23 Aug	2200	56°26'	11°08'
6	OL XBT 24	24 Aug	0000	56°46'	10°27'
7	AR SVD 14(D)	24 Aug	0640	56°38'	10°45'
8	KP XBT 156	24 Aug	1600	56°34'	10°54'
9	AR SVD 15(D)	24 Aug	1836	56°38'	10°45'

- NOTES:
- All SVD times are means of total elapsed cast time.
  - (U) indicates upcast, (D) indicates downcast.
  - Nominal position of Point 2FA is 56°38'N, 10°45'W

## CONFIDENTIAL

(U) Table 6. Identification of Data Used in Phase II Time-Series Study at Point 2FA

# CONFIDENTIAL

PROFILE	OBSERVATION	DATE 1973)	TIME (GMT)	LAT (°N)	LONG (°W)
1	AR XBT 53	7 Sep	1200	63°15'	11°59'
2	AR SVD 18(D)	7 Sep	1547	63°11'	12°21'
3	AR SVD 18(U)	7 Sep	1707	63°11'	12°21'
4	SD XBT 147	7 Sep	1957	63°10'	11°56'
5	SD SV/STD 74(D)	7 Sep	2133	63°04'	12°18'
6	AR SVD 19(D)	8 Sep	0032	63°11'	12°15'
7	AR SVD 20(D)	9 Sep	0415	63°16'	12°18'
8	AR XBT 54A	9 Sep	0505	63°17'	12°18'
9	KP XBT 265	9 Sep	1200	63°10'	12°00'
10	AR SVD 21(U)	9 Sep	1250	63°19'	12°25'
11	AR XBT 55	9 Sep	1555	63°14'	12°32'
12	AR XBT 57	9 Sep	2105	63°21'	12°11'
13	AR SVD 22(D)	9 Sep	0040	63°16'	12°21'
14	AR XBT 60	10 Sep	0810	63°16'	12°18'
15	AR SVD 23(D)	10 Sep	1216	63°17'	12°16'
16	AR XBT 61	10 Sep	1605	63°16'	12°20'
17	AR XBT 62	10 Sep	2000	63°16'	12°21'
18	AR SVD 24(D)	11 Sep	0022	63°16'	12°19'
19	AR XBT 63	11 Sep	0115	63°16'	12°19'
20	AR XBT 64	11 Sep	0400	63°15'	12°18'

- NOTES:
- All SVD and SV/STD times are means of total elapsed cast time.
  - (U) indicates upcast, (D) indicates downcast.
  - Nominal position of Point 3Z is 63°10'N, 12°10'W

## CONFIDENTIAL

(U) Table 7. Identification of Data Used in Phase II Time-Series Study at Point 3Z

# CONFIDENTIAL

PROFILE	SANDS SV/STD OBSERVATION	DATE (1973)	TIME (GMT)	LAT (°N)	LONG (°W)
1	61(D)	5 Sep	2047	64°27'	7°41'
2	61(U)	5 Sep	2158	64°26'	7°41'
3	62(D)	5 Sep	2317	64°26'	7°40'
4	62(U)	6 Sep	0025	64°26'	7°40'
5	63(D)	6 Sep	0132	64°26'	7°40'
6	63(U)	6 Sep	0311	64°26'	7°41'
7	64(D)	6 Sep	0508	64°25'	7°43'
8	64(U)	6 Sep	0641	64°25'	7°44'
9	65(D)	6 Sep	0810	64°31'	7°36'
10	65(U)	6 Sep	0941	64°31'	7°35'
11	66(D)	6 Sep	1104	64°28'	7°40'
12	66(U)	6 Sep	1209	64°28'	7°40'
13	67(D)	6 Sep	1305	64°28'	7°39'
14	67(U)	6 Sep	1414	64°28'	7°39'
15	68(D)	6 Sep	1527	64°27'	7°39'
16	68(U)	6 Sep	1633	64°27'	7°39'
17	69(D)	6 Sep	1739	64°27'	7°39'
18	69(U)	6 Sep	1844	64°27'	7°37'
19	70(D)	6 Sep	1942	64°27'	7°37'
20	70(U)	6 Sep	2041	64°28'	7°38'
21	71(D)	6 Sep	2152	64°28'	7°38'
22	71(U)	6 Sep	2310	64°38'	7°38'

- NOTES:
- All SV/STD times are means of total elapsed cast time.
  - (U) indicates upcast, (D) indicates downcast.
  - Nominal position of Point 3ZZ is 64°28'N, 7°40'W.

## CONFIDENTIAL

(U) Table 8. Identification of Data Used in Phase III Time-Series Study at Point 3ZZ

# CONFIDENTIAL

PROFILE	SANDS OBSERVATION	DATE (1973)	TIME (GMT)	LAT (°N)	LONG (°W)
1	SV/STD 17(D)	10 Aug	1045	52°58'	15°34'
2	SV/STD 17(U)	10 Aug	1215	52°58'	15°34'
3	XBT 43	10 Aug	1325	52°58'	15°34'
4	SV/STD 18(D)	10 Aug	1505	52°58'	15°34'
5	SV/STD 19(D)	10 Aug	2222	52°59'	15°19'
6	SV/STD 19(U)	10 Aug	2355	52°59'	15°20'
7	SV/STD 20(D)	11 Aug	0320	53°00'	15°20'
8	SV/STD 20(U)	11 Aug	0430	53°00'	15°20'
9	SV/STD 21(D)	11 Aug	0729	53°02'	15°23'
10	SV/STD 21(U)	11 Aug	0911	53°02'	15°23'
11	SV/STD 22(D)	11 Aug	1151	53°02'	15°20'
12	SV/STD 22(U)	11 Aug	1313	53°02'	15°20'
13	SV/STD 23(D)	11 Aug	1947	53°01'	15°27'
14	SV/STD 23(U)	11 Aug	2118	53°01'	15°27'
15	XBT 49	11 Aug	2215	53°03'	15°31'

- NOTES: • All SV/STD times are means of total elapsed cast time.  
• (U) indicates upcast, (D) indicates downcast.

## CONFIDENTIAL

(U) Table 9. Identification of Data Used in Phase I Porcupine Bank Time-Series Study

PROFILE	KANE OBSERVATION	DATE (1973)	TIME (GMT)	LAT (°N)	LONG (°W)
1	SV/STD 37(D)	20 Aug	0934	53°00'	15°30'
2	SV/STD 37 (U)	20 Aug	1115	53°00'	15°31'
3	SV/STD 38(D)	20 Aug	1326	53°00'	15°31'
4	SV/STD 38 (U)	20 Aug	1450	53°00'	15°33'
5	SV/STD 39 (D)	20 Aug	1643	53°00'	15°33'
6	SV/STD 39 (U)	20 Aug	1823	53°02'	15°34'
7	SV/STD 40 (D)	20 Aug	2026	53°01'	15°28'
8	XBT 128	20 Aug	2140	53°00'	15°30'
9	SV/STD 40 (U)	20 Aug	2222	53°01'	15°29'
10	SV/STD 41 (D)	21 Aug	0045	53°02'	15°27'
11	XBT 129	21 Aug	0128	53°03'	15°28'
12	SV/STD 41 (U)	21 Aug	0222	53°02'	15°29'
13	SV/STD 42 (D)	21 Aug	0522	53°03'	15°29'
14	XBT 130	21 Aug	0613	53°02'	15°29'
15	SV/STD 42 (U)	21 Aug	0706	53°04'	15°32'
16	SV/STD 43 (D)	21 Aug	1026	53°01'	15°29'
17	SV/STD 43 (U)	21 Aug	1210	53°02'	15°29'
18	SV/STD 44 (D)	21 Aug	1459	53°00'	15°30'
19	SV/STD 44 (U)	21 Aug	1610	53°02'	15°32'

- NOTES: • All SV/STD times are means of total elapsed cast time.  
• (U) indicates upcast, (D) indicates downcast.

## CONFIDENTIAL

(U) Table 10. Identification of Data Used in Phase II Porcupine Bank Time-Series Study

# CONFIDENTIAL

PROFILE	OBSERVATION	DATE (12/3)	TIME (GMT)	LAT (°N)	LONG (°W)
1	SD SV/STD 1	1 Aug	1530	49°18'	14°51'
2	SD XBT 3	1 Aug	2335	49°33'	15°32'
3	SD SV/STD 2	2 Aug	0255	49°47'	16°01'
4	WI XBT 5	2 Aug	1100	49°51'	16°11'
5	SD XBT 5	2 Aug	0912	50°14'	16°45'
6	SV/SV STD 3	2 Aug	1205	50°22'	17°16'
7	SD XBT 9	2 Aug	1815	50°40'	17°49'
8	SD SV/STD	2 Aug	2145	50°56'	18°23'
9	WI XBT 10	2 Aug	2100	51°08'	18°46'
10	SD XBT 11	3 Aug	0345	51°18'	18°59'
11	WI XBT 11	2 Aug	2300	51°21'	19°20'
12	SD SV/STD 5	3 Aug	1000	51°28'	19°39'
13	WI XBT 13	3 Aug	0100	51°35'	19°53'
14	SD XBT 13	3 Aug	1555	51°43'	20°10'
15	WI XBT 14	3 Aug	0300	51°48'	20°26'
16	SD SV/STD 6	3 Aug	2130	51°56'	20°35'
17	WI XBT 15	3 Aug	0500	52°02'	20°58'
18	KN XBT 11	2 Aug	1800	52°12'	21°04'
19	WI XBT 16	3 Aug	0705	52°17'	21°29'
20	SD SV/STD 7	4 Aug	1355	52°24'	21°56'
21	SD XBT 17	4 Aug	1934	52°36'	22°22'
22	KN SV/STD 1	2 Aug	2302	52°42'	22°36'
23	SD SV/STD 8	4 Aug	2350	52°54'	22°58'
24	KN XBT 14	3 Aug	0436	52°58'	23°16'
25	WI XBT 20	3 Aug	1500	53°06'	23°33'
26	KN SV/STD 2	3 Aug	0800	53°16'	24°02'
27	KN XBT 17	3 Aug	1345	53°31'	24°48'
28	WI XBT 23	3 Aug	2100	53°41'	25°10'
29	KN SV/STD 3	3 Aug	1729	53°50'	25°35'
30	KN XBT 19	3 Aug	2303	54°06'	26°22'
31	WI XBT 26	4 Aug	0300	54°16'	26°52'
32	KN SV/STD 4	4 Aug	0247	54°23'	27°12'
33	WI XBT 27	4 Aug	0500	54°27'	27°27'
34	KN XBT 21	4 Aug	0815	54°37'	27°59'
35	WI XBT 29	4 Aug	0900	54°49'	28°36'
36	KN SV/STD 5	4 Aug	1300	54°54'	28°53'
37	WI XBT 33	4 Aug	1100	54°58'	29°07'
38	KN XBT 26	4 Aug	1908	55°05'	29°30'
39	KN SV/STD 6	4 Aug	2309	55°16'	30°06'
40	KN XBT 31	5 Aug	0524	55°26'	30°50'
41	KN SV/STD 7	5 Aug	0921	55°38'	31°26'
42	WI XBT 40	5 Aug	0000	55°47'	31°52'
43	KN XBT 34	5 Aug	1517	55°49'	32°06'
44	KN SV/STD 8	5 Aug	1832	55°59'	32°47'
45	KN XBT 37	6 Aug	0030	56°09'	33°28'

NOTE: All SV/STD observations are downcasts.

CONFIDENTIAL

(U) Table 11. Identification of Data Used in Point 1E to Point 3B Cross Section

# CONFIDENTIAL

PROFILE	OBSERVATION	DATE (1973)	TIME (GMT)	LAT (°N)	LONG (°W)
1	WI SV/STD 33	20 Aug	0715	48°09'	23°57'
2	WI XBT 129	20 Aug	1325	48°27'	23°40'
3	WI SV/STD 34	20 Aug	1740	48°47'	23°16'
4	WI XBT 131	20 Aug	2300	49°06'	22°52'
5	WI SV/STD 35	21 Aug	0355	49°22'	22°26'
6	OL XBT 4	22 Aug	0600	49°35'	22°18'
7	WI XBT 133	21 Aug	1032	49°48'	22°00'
8	WI SV/STD 36	21 Aug	1406	50°01'	21°42'
9	WI XBT 135	21 Aug	1924	50°23'	21°18'
10	OL XBT 7	22 Aug	1200	50°29'	21°05'
11	WI SV/STD 37	22 Aug	0006	50°37'	20°54'
12	WI XBT 139	22 Aug	0600	50°55'	20°27'
13	WI SV/STD 38	22 Aug	1008	51°12'	20°01'
14	CH XBT 31	23 Aug	1600	51°23'	19°42'
15	OL XBT 10	22 Aug	1800	51°35'	19°28'
16	WI SV/STD 39	22 Aug	2100	51°47'	19°08'
17	OL XBT 10A	22 Aug	2000	51°58'	18°55'
18	WI XBT 143	23 Aug	0315	52°03'	18°40'
19	WI SV/STD 40	23 Aug	0704	52°25'	18°18'
20	WI XBT 145	23 Aug	1247	52°44'	17°51'
21	KP XBT 139	23 Aug	0800	52°50'	17°37'
22	WI SV/STD 41	23 Aug	1724	53°02'	17°28'
23	WI XBT 147	23 Aug	2215	53°18'	17°01'
24	KN SV/STD 45	21 Aug	2336	53°25'	16°44'
25	WI SV/STD 42	24 Aug	0107	53°34'	16°32'
26	OL XBT 15	23 Aug	0600	53°46'	16°10'
27	KN SV/STD 46	22 Aug	0111	54°02'	15°43'
28	KP XBT 146	23 Aug	2000	54°16'	15°15'
29	OL XBT 17	23 Aug	1000	54°26'	14°58'
30	KN SV/STD 47	22 Aug	2110	54°37'	14°37'
31	OL XBT 18	23 Aug	1200	54°47'	14°20'
32	KN XBT 143	23 Aug	0330	54°54'	14°04'
33	OL XBT 19	23 Aug	1400	55°08'	13°43'
34	KN SV/STD 48	23 Aug	0805	55°12'	13°28'
35	LY SV/STD 2	25 Aug	0116	55°30'	13°23'
36	KP XBT 152	24 Aug	0800	55°38'	12°45'
37	OL XBT 21	24 Aug	1800	55°48'	12°28'
38	OL XBT 22	23 Aug	2000	56°07'	11°48'
39	KP XBT 155	24 Aug	1400	56°19'	11°24'
40	KP XBT 156	24 Aug	2200	56°34'	10°54'
41	AR SVD 15	24 Aug	1810	56°38'	10°45'
42	OL XBT 24	24 Aug	0000	56°46'	10°27'
43	OL XBT 25	24 Aug	0200	57°06'	9°44'
44	KP XBT 159	24 Aug	2200	57°11'	9°34'
45	OL XBT 26	24 Aug	0400	57°26'	9°02'
46	KP XBT 161	25 Aug	0200	57°36'	8°36'
47	KP XBT 162	25 Aug	0400	57°45'	8°02'
48	KP XBT 164	25 Aug	0630	58°04'	7°31'

NOTE: All SV/STD and SVD observations are downcasts.

CONFIDENTIAL

(U) Table 12. Identification of Data Used in Point 2L to Point 2K Cross Section

# CONFIDENTIAL

PROFILE	OBSERVATION	DATE (1973)	TIME (GMT)	LAT (°N)	LONG (°W)
1	SD SV/STD 34	17 Aug	1939	53°56'	12°56'
2	KP XBT 84	19 Aug	0000	54°11'	13°17'
3	SD XBT 74	17 Aug	2345	54°16'	13°30'
4	KP XBT 85	19 Aug	0240	54°25'	13°42'
5	SD SV/STD 35	18 Aug	1010	54°39'	14°04'
6	SD XBT 77	18 Aug	1556	54°56'	14°44'
7	SD SV/STD 36	18 Aug	2010	55°12'	15°21'
8	SD XBT 81	19 Aug	0230	55°23'	16°01'
9	KP XBT 92	19 Aug	1400	55°42'	16°22'
10	SD SV/STD 37	19 Aug	1015	55°49'	16°36'
11	KP XBT 93	19 Aug	1600	55°55'	16°50'
12	SD XBT 83	19 Aug	1415	56°09'	17°19'
13	SD SV/STD 38	19 Aug	2003	56°24'	17°52'
14	KP XBT 97	19 Aug	2200	56°33'	18°16'
15	SD XBT 87	20 Aug	0205	56°41'	18°33'
16	KP XBT 98	20 Aug	0000	56°49'	18°49'
17	SD SV/STD 39	20 Aug	0505	56°57'	19°19'
18	KP XBT 100	20 Aug	0400	57°09'	19°43'
19	SD XBT 89	20 Aug	0900	57°14'	19°56'
20	KP XBT 101	20 Aug	0600	57°21'	20°13'
21	SD SV/STD 40	20 Aug	1410	57°31'	20°34'
22	KP XBT 111	21 Aug	0200	57°37'	20°58'

NOTE: All SV/STD observations are downcasts.

## CONFIDENTIAL

(U) Table 33. Identification of Data Used in Point 288 to Point 3AB Cross Section



# CONFIDENTIAL

PROFILE	OBSERVATION	DATE (1973)	TIME (GMT)	LAT (°N)	LONG (°W)
1	KN SV/STD 69	9 Sep	2333	51°05'	33°32'
2	OL XBT 73	10 Sep	1900	51°12'	33°28'
3	OL XBT 72	10 Sep	1800	51°24'	33°14'
4	KN XBT 202	9 Sep	1919	51°36'	33°03'
5	OL XBT 70	10 Sep	1600	51°44'	32°49'
6	KN SV/STD 68	9 Sep	1212	52°03'	32°26'
7	KN XBT 200	9 Sep	0820	52°26'	31°59'
8	OL XBT 65	10 Sep	1100	52°46'	31°38'
9	KN SV/STD 67	9 Sep	0118	53°01'	31°19'
10	OL XBT 63	10 Sep	0900	53°10'	31°08'
11	OL XBT 62	10 Sep	0800	53°22'	30°52'
12	KN XBT 197	8 Sep	2009	53°29'	30°42'
13	OL XBT 60	10 Sep	0600	53°46'	30°21'
14	KN SV/STD 66	8 Sep	1404	53°56'	30°06'
15	OL XBT 59	10 Sep	0400	54°08'	29°50'
16	KN XBT 194	8 Sep	0940	54°25'	29°30'
17	OL XBT 58	10 Sep	0200	54°32'	29°18'
18	KN SV/STD 65	8 Sep	0316	54°54'	28°48'
19	OL XBT 56	9 Sep	2200	55°20'	28°16'
20	KN SV/STD 64	7 Sep	1624	55°42'	27°34'
21	OL XBT 54	9 Sep	1800	56°03'	27°07'
22	KN XBT 188	7 Sep	1102	56°09'	26°59'
23	OL XBT 53	9 Sep	1600	56°26'	26°29'
24	KN SV/STD 63	7 Sep	0434	56°32'	26°19'
25	OL XBT 52	9 Sep	1400	56°48'	25°53'
26	KN XBT 185	7 Sep	0024	56°54'	25°44'
27	OL XBT 51	9 Sep	1200	57°12'	25°16'
28	KN SV/STD 62	6 Sep	1817	57°20'	24°59'
29	OL XBT 50	9 Sep	1000	57°34'	24°38'
30	KN XBT 183	6 Sep	1445	57°44'	24°19'
31	OL XBT 49	9 Sep	0800	57°55'	23°59'
32	KN SV/STD 61	6 Sep	0913	58°08'	23°36'
33	OL XBT 48	9 Sep	0600	58°17'	23°19'
34	OL XBT 47	9 Sep	0400	58°42'	22°45'
35	KN SV/STD 60	5 Sep	1842	58°54'	22°09'
36	OL XBT 46	9 Sep	0200	59°00'	21°59'
37	KN XBT 175	5 Sep	1302	59°19'	21°17'
38	KN SV/STD 59	5 Sep	0614	59°40'	20°39'
39	SD SV/STD 80	10 Sep	1642	59°50'	20°19'
40	KN XBT 172	5 Sep	0028	60°00'	19°54'
41	SD XBT 165	10 Sep	1357	60°10'	19°41'
42	KN SV/STD 58	4 Sep	1811	60°23'	19°05'
43	SD XBT 162	9 Sep	2130	60°39'	18°25'
44	KP XBT 255	8 Sep	1600	60°53'	18°00'
45	SD SV/STD 78	9 Sep	1619	60°59'	17°49'
46	KP XBT 256	8 Sep	1800	61°07'	17°28'
47	SD XBT 160	9 Sep	1333	61°15'	17°08'
48	OL XBT 39	8 Sep	1200	61°20'	16°55'
49	SD SV/STD 77	9 Sep	0839	61°30'	16°30'

CONFIDENTIAL

(U) Table 14. Identification of Data Used in Point 3F to Point 32Z Cross Section

# CONFIDENTIAL

(Continued)

50	OL XBT 38	8 Sep	1000	61°41'	16°07'
51	SD XBT 157	8 Sep	2100	61°49'	15°45'
52	SD SV/STD 76	8 Sep	1615	62°01'	15°08'
53	SD XBT 152	8 Sep	1315	62°17'	14°26'
54	KP XBT 262	9 Sep	0600	62°30'	13°54'
55	SD SV/STD 75	8 Sep	0841	62°36'	13°43'
56	SD XBT 149	8 Sep	0100	62°45'	13°12'
57	OL XBT 34	8 Sep	0200	62°53'	12°49'
58	KP XBT 264	9 Sep	1000	62°57'	12°37'
59	SD SV/STD 74	7 Sep	2123	63°04'	12°18'
60	SD XBT 147	7 Sep	1957	63°09'	11°56'
61	SD SV/STD 73	7 Sep	1513	63°32'	10°48'
62	SD XBT 144	7 Sep	1200	63°52'	9°50'
63	SD SV/STD 72	7 Sep	0845	64°01'	9°16'
64	KP XBT 272	11 Sep	0800	64°07'	8°54'
65	SD SV/STD 71	6 Sep	2108	64°28'	7°38'

NOTE: All SV/STD observations are downcasts.

CONFIDENTIAL

CONFIDENTIAL

THIS PAGE INTENTIONALLY  
LEFT BLANK

# CONFIDENTIAL

## Appendix C: Glossary (U)

ACODAC: Acoustic Data Capsule.

ANB: Ambient Noise Buoy.

Bottom bounce: An acoustic propagation path where underwater sound is reflected off the bottom one or more times before reaching the receiver or target.

CHURCH GABBRO: A LRAPP acoustic/environmental exercise in the Cayman Trough and adjacent regions of the Caribbean Sea during November-December 1972.

Convergence zone: A region where sound rays arrive at the surface in successive intervals; an underwater sound propagation path.

Critical depth: That depth where the maximum sound velocity at the surface or in the near-surface layer recurs; bottom of the DSC.

CW: Continuous wave; a continuous underwater sound source.

Depth difference: The amount of sea floor topography that protrudes above critical depth into the DSC (leads to bottom limited conditions).

Depth excess: The depth interval between critical depth and the seafloor (necessary for convergence zone formation).

DSC: Deep sound channel, generally the absolute sound velocity minimum; an underwater sound propagation path.

GMT: Greenwich Mean Time.

Intermediate sound velocity maximum: The sound velocity inflection point lying between the depths of the USC and DSC axes.

LRAPP: Long Range Acoustic Propagation Project.

LSW: Labrador Sea Water (low salinity).

MABS: Moored Acoustic Buoy System.

MIW: Mediterranean Intermediate Water (high salinity).

NACW: North Atlantic Central Water (carried by the North Atlantic and Irminger Currents).

NAVOCEANO: Naval Oceanographic Office, NSTL Station, Mississippi.

NORDA: Naval Ocean Research and Development Activity, NSTL Station, Mississippi.

NORLANT-72: A LRAPP acoustic/environmental exercise in the western North Atlantic Ocean during July-September 1972.

NSDW: Norwegian Sea Deep Water.

NSTL: National Space Technology Laboratories.

NSOW: Norwegian Sea Overflow Water (near-bottom, low salinity).

RAE: Ridge Acoustics Exercise; a LRAPP acoustic exercise over and north of the Faeroe-Iceland Ridge during September-October 1973.

Sigma-t: An abbreviated value of sea water density.

Sonic layer depth: Depth of near-surface sound velocity maximum (not necessarily the same as thermal layer depth).

# CONFIDENTIAL

"Strength" of USC: The difference between the sound velocity at the intermediate maximum (or at the bottom) and the sound velocity at the USC axis.

Surface duct: The zone immediately below the sea surface where sound rays are refracted toward the surface and then reflected; an underwater sound propagation path.

SUS: Signals underwater sound; a high explosive underwater sound source.

S/CTD: An oceanographic instrument that measures sound velocity, salinity, and temperature as a function of depth.

T-S: Temperature-salinity.

USC: Upper sound channel, a sound velocity minimum lying above the DSC and separated from it by an intermediate-depth sound velocity maximum; an underwater sound propagation path.

WECO: Western Electric Company, Winston-Salem, North Carolina.

XBT: Expendable bathythermographs; an oceanographic instrument that measures temperature as a function of depth to either 460 m (Sippican model T-4 probe), 760 m (T-7 probe), or 1830 m (T-5 probe).

# CONFIDENTIAL

## Distribution List

### CHIEF OF NAVAL OPERATIONS

DEPARTMENT OF THE NAVY

WASHINGTON, DC 20350

ATTN: OP-095 1  
OP-951 1  
OP-952 1  
OP-951F 1  
OP-952D 1

### HEADQUARTERS

NAVAL MATERIAL COMMAND

WASHINGTON, DC 20360

ATTN: CODE MAT-08T245 2

### PROJECT MANAGER

ANTISUBMARINE WARFARE SYSTEM PROJ

DEPARTMENT OF THE NAVY

WASHINGTON, DC 20360

ATTN: A. V. BERNARD, PM-4 2

### DIRECTOR

STRATEGIC SYSTEM PROJECTS OFFICE

DEPARTMENT OF THE NAVY

WASHINGTON, DC 20360

ATTN: PM-1 1

### OFFICE OF NAVAL RESEARCH

800 NORTH QUINCY STREET

ARLINGTON, VA 22217

ATTN: CODE 102A 1  
CODE 102B 1  
CODE 222 1  
CODE 230 1  
CODE 460 1  
CODE 480 1

### COMMANDER

NAVAL ELECTRONIC SYSTEMS COMMAND

NAVAL ELECTRONIC SYS COMMAND HDQRS

WASHINGTON, DC 20360

ATTN: PME-124 1  
PME-124TA 1  
PME-124/30 1  
PME-124/40 1  
PME-124/60 1  
ELEX-320 2

### COMMANDER

NAVAL SEA SYSTEMS COMMAND

NAVAL SEA SYSTEMS COMMAND HDQRS

WASHINGTON, DC 20362

ATTN: NSEA-06H1 1

### COMMANDER

NAVAL AIR SYSTEMS COMMAND

NAVAL AIR SYSTEMS COMMAND HDQRS

WASHINGTON, DC 20361

ATTN: NAIR-370 1  
PMA-264 1

### DEFENSE ADV RESEARCH PROJ AGENCY

1400 WILSON BOULEVARD

ARLINGTON, VA 22209

ATTN: R. G. COOK 1  
DR. T. KOOLJ 1  
CDR V. E. SIMMONS 1

### COMMANDER

NAVAL OCEANOGRAPHY COMMAND

NSTL STATION, MS 39529 1

### COMMANDER IN CHIEF

U.S. ATLANTIC FLEET 1

NORFOLK, VA 23511

### COMMANDER

SECOND FLEET

FPO NEW YORK, NY 09501 1

### COMMANDER

SIXTH FLEET

FPO NEW YORK, NY 09501 1

### COMMANDER

SUBMARINE DEVELOPMENT GROUP 12

BOX 70 NAV SUP BASE, N LONDON

GROTON, CT 06340 1

### COMMANDER

OPERATIONAL TEST AND EVAL. FORCE

NAVAL BASE

NORFOLK, VA 23511 1

### COMMANDER

OCEANOGRAPHIC SYSTEM, ATLANTIC

BOX 100

NORFOLK, VA 23511 2

### COMMANDING OFFICER

FLEET NUMERICAL WEATHER CENTRAL

MONTEREY, CA 93940 2

### COMMANDING OFFICER

FLEET WEATHER CENTRAL

MCADIE BUILDING (U-117)

NSA NORFOLK, VA 23511 1

# CONFIDENTIAL

OCEANOGRAPHIC DEVELOPMENT SQD 8  
NAVAL AIR STATION  
PATUXENT RIVER, MD 20670 1

ACOUSTIC RESEARCH CENTER DARPA  
NAVAL AIR STATION  
MOFFETT FIELD, CA 94035  
ATTN: E. L. SMITH 2

COMMANDING OFFICER  
NAVAL RESEARCH LABORATORY  
WASHINGTON, DC 20375  
ATTN: CODE 8100 1  
CODE 8160 1  
CODE 2627 1

COMMANDER  
NAVAL OCEANOGRAPHIC OFFICE  
NSTL STATION, MS 39529  
ATTN: CODE 3000 1  
CODE 7000 1  
CODE 7200 1  
CODE 7200 1  
CODE 7300 1  
CODE 9100 1  
LIBRARY 1

COMMANDING OFFICER  
NAVAL OCEAN RESEARCH & DEVELOPMENT  
ACTIVITY  
NSTL STATION, MS 39529  
ATTN: CODE 110 1  
CODE 125 1  
CODE 200 1  
CODE 300 1  
CODE 320 1  
CODE 330 1  
CODE 340 1  
CODE 500 1  
CODE 520 1  
CLASSIFIED LIBRARY 3

NAVAL OCEAN RESEARCH & DEVELOPMENT  
ACTIVITY  
LIAISON OFFICE  
800 NORTH QUINCY STREET  
ARLINGTON, VA 22217  
ATTN: CODE 130 1

OFFICER IN CHARGE  
NEW LONDON LABORATORY  
NAVAL UNDERWATER SYSTEMS CENTER  
NEW LONDON, CT 06320  
ATTN: CODE 311 1  
CODE 312 1  
CODE 542 1

OFFICER IN CHARGE  
NEWPORT LABORATORY  
NAVAL UNDERWATER  
SYSTEMS CENTER  
NEWPORT, RI 06320  
ATTN: CODE 311 1

COMMANDER  
NAVAL OCEAN SYSTEMS CENTER  
SAN DIEGO, CA 92152  
ATTN: CODE 5301 1  
CODE 714 1  
CODE 7143 1

COMMANDER  
NAVAL AIR DEVELOPMENT CENTER  
WARMINSTER, PA 18974  
ATTN: CODE 303 1  
CODE 3032 1

COMMANDING OFFICER  
NAVAL COASTAL SYSTEMS LABORATORY  
PANAMA CITY, FL 32407 1

OFFICER IN CHARGE  
WHITE OAK LABORATORY  
NAVAL SURFACE WEAPONS CENTER  
SILVER SPRING, MD 20910 1

OFFICER IN CHARGE CARDEROCK LAB  
DAVID W. TAYLOR NAVAL SHIP RES &  
DEVELOPMENT CENTER  
BETHESDA, MD 20084 1

DIRECTOR  
NAVAL OCEAN SURVEILLANCE INFO CENT  
4301 SUITLAND ROAD  
WASHINGTON, DC 20390 1

COMMANDING OFFICER  
NAVAL INTELLIGENCE SUPPORT CENTER  
4301 SUITLAND ROAD  
WASHINGTON, DC 20390 1

SUPERINTENDENT  
NAVAL POSTGRADUATE SCHOOL  
MONTEREY, CA 93940  
ATTN: LIBRARY 1

CHIEF DEF. RES. EST. ATLANTIC  
P. O. BOX 1012  
DARTMOUTH, NOVA SCOTIA B2Y 3Z7 1

# CONFIDENTIAL

JOHN HOPKINS UNIVERSITY  
APPLIED RESEARCH LABORATORY  
JOHN HOPKINS ROAD  
LAUREL, MD 20910  
ATTN: W. L. MAY 1  
G. L. SMITH 1

PALISADES GEOPHYSICAL INST. INC.  
131 ERIE STREET  
P. O. BOX 396  
BLAUVELT, NY 10913 1

UNIVERSITY OF TEXAS  
APPLIED RESEARCH LABORATORIES  
P. O. BOX 8029  
AUSTIN, TX 78712  
ATTN: G. E. ELLIS 1  
DR. L. D. HAMPTON 1  
DR. K. E. HAWKER 1

WOODS HOLE OCEANOGRAPHIC INST.  
WOODS HOLE, MA 02543  
ATTN: DR. E. E. HAYS 2

ANALYSIS AND TECHNOLOGY, INC.  
ROUTE 2  
NORTH STONINGTON, CT 06359  
ATTN: S. ELAM 1

B-K DYNAMICS  
15825 SHADY GROVE ROAD  
ROCKVILLE, MD 20850  
ATTN: P. G. BERNARD 1

BELL TELEPHONE LABORATORIES  
1 WHIPPANY, NJ 07981  
ATTN: DR. J. GOLDMAN 1  
DR. L. FRETWELL 1

BOLT, BERANEK AND NEWMAN  
1701 N. FORT MYER DRIVE  
SUITE 1001  
ARLINGTON, VA 22209 1

DANIEL ANALYTICAL SERVICES CORP.  
16821 BUCCANEER LANE  
CLEAR LAKE CITY  
HOUSTON, TX 77058  
ATTN: E. D. GRAHAM 1

DAUBIN SYSTEMS CORP.  
104 CRANFORD BOULEVARD  
SUITE 315  
KEY BISCAYNE, FL 33149  
ATTN: DR. S. C. DAUBIN 1

OCEAN DATA SYSTEMS, INC.  
6000 EXECUTIVE BOULEVARD  
ROCKVILLE, MD 20852  
ATTN: G. JACOBS 1  
DR. E. MORENOFF 1  
J. H. LOCKLIN 1

OCEAN DATA SYSTEMS, INC.  
2400 GARDEN ROAD  
MONTEREY, CA 93940 1

OCEAN DATA SYSTEMS, INC.  
3581 KENYON ST.  
SAN DIEGO, CA 92110 1

OPERATIONS RESEARCH, INC.  
1400 SPRING STREET  
SILVER SPRINGS, MD 20910  
ATTN: DR. J. I. BOWEN 1

PLANNING SYSTEMS INC.  
7900 WESTPARK DRIVE  
SUITE 600  
MCLEAN, VA 22101  
ATTN: R. KLINKNER 1  
DR. L. P. SOLOMON 1

PURVIS SYSTEMS, INC.  
3420 KENYON ST.  
SUITE 130  
SAN DIEGO, CA 92110  
ATTN: T. R. FITZGERALD 1

SANDERS ASSOCIATES, INC.  
95 CANAL STREET  
NASHUA, NH 03060  
ATTN: L. E. GAGNE 1  
R. P. WHITE 1

SCIENCE APPLICATIONS, INC.  
8400 WESTPARK DRIVE  
MCLEAN, VA 22101  
ATTN: DR. J. S. HANNA 1  
C. W. SPOFFORD 1

SCIENCE APPLICATIONS, INC.  
21133 VICTORY BLVD.  
SUITE 216  
CANOGA PARK, CA 91303  
ATTN: DR. J. H. WILSON 1

SUTHRON CORP.  
1925 N. LYNN STREET  
SUITE 700  
ARLINGTON, VA 22209  
ATTN: C. H. DABNEY 1



# CONFIDENTIAL

TRACOR, INC.  
1601 RESEARCH BOULEVARD  
ROCKVILLE, MD 20850  
ATTN: J. T. GOTTWALD 1  
DR. A. F. WITTENBORN 1

TRW SYSTEMS GROUP  
7600 COLSHIRE DRIVE  
MCLEAN VA 22101  
ATTN: R. T. BROWN 1  
I. P. GEREBEN 1

UNDERWATER SYSTEMS, INC.  
8101 GEORGIA AVE.  
SILVER SPRING, MD 20910  
ATTN: DR. M.S. WEINSTEIN 1

WESTERN ELECTRIC COMPANY  
P. O. BOX 25000  
GREENSBORO, NC 27420 2

XONICS, INC.  
6837 HAYVENHURST AVENUE  
VALLEJO, CA 94606 1

DEFENSE DOCUMENTATION CENTER  
CAMERON STATION  
ALEXANDRIA, VA 22314 10

UNCLASSIFIED

(This page is unclassified)

SECURITY CLASSIFICATION OF THIS PAGE (When Data Entered)

REPORT DOCUMENTATION PAGE		READ INSTRUCTIONS BEFORE COMPLETING FORM
1. REPORT NUMBER NORDA Report 23	2. GOVT ACCESSION NO. AD-C029 5461	3. RECIPIENT'S CATALOG NUMBER
4. TITLE (and Subtitle) SOUND SPEED STRUCTURE OF THE NORTHEAST ATLANTIC OCEAN IN SUMMER 1973 DURING THE SQUARE DEAL EXERCISE (U)		5. TYPE OF REPORT & PERIOD COVERED FINAL
7. AUTHOR(s) Don F. Fenner		6. PERFORMING ORG REPORT NUMBER
9. PERFORMING ORGANIZATION NAME AND ADDRESS Naval Ocean Research and Development Activity NSTL Station, Mississippi 39529		8. CONTRACT OR GRANT NUMBER(s)
11. CONTROLLING OFFICE NAME AND ADDRESS Long Range Acoustic Propagation Project NSTL Station, Mississippi 39529		10. PROGRAM ELEMENT, PROJECT, TASK AREA & WORK UNIT NUMBERS 63795N/AR0119/300/13412100
14. MONITORING AGENCY NAME & ADDRESS (if different from Controlling Office) N/A		12. REPORT DATE January 1979
Further dissemination is directed by or higher DoD authority.		13. NUMBER OF PAGES 111
16. DISTRIBUTION STATEMENT (of this Report) In addition to the security requirements which apply to this document and must be met, it may be further distributed by the holder only with the specific prior approval of the Director, Long Range Acoustic Propagation Project, NSTL Station, Mississippi 39529		15. SECURITY CLASS. (of this report) CONFIDENTIAL
17. DISTRIBUTION STATEMENT (of the abstract entered in Block 20, if different from Report)		
18. SUPPLEMENTARY NOTES		
19. KEY WORDS (Continue on reverse side if necessary and identify by block number) SQUARE DEAL Exercise, sound velocity data, temperature-salinity data, bathymetric tracks, meteorological data, bichannel sound velocity profiles, northeast Atlantic Ocean, Mediterranean Intermediate Water, Polar Front, interleaving, microstructure, internal waves, propagation loss, ambient noise.		
20. ABSTRACT (Continue on reverse side if necessary and identify by block number) During July-September 1973, 1351 oceanographic observations were taken in the northeast Atlantic Ocean during the SQUARE DEAL Exercise. Three-quarters of these data were expendable bathythermographs (XBTs) that were converted to sound velocity using the equation of Wilson (1960) and a salinity field derived from exercise deep ocean station data. Sound velocity profiles were extremely complex and variable throughout the exercise area owing to internal waves and mixing between various intrusive water masses (including high-salinity Mediterranean Intermediate Water). Frequently, intense		

DD FORM 1 JAN 73 1473

EDITION OF 1 NOV 65 IS OBSOLETE  
(NATIONAL SECURITY AGENCY)

CONFIDENTIAL UNCLASSIFIED

SECURITY CLASSIFICATION OF THIS PAGE (When Data Entered)  
(This page is unclassified)

**CONFIDENTIAL**  
(This page is unclassified)  
**UNCLASSIFIED**

SECURITY CLASSIFICATION OF THIS PAGE (When Data Entered)

mixing caused microstructures that masked the major features of the sound velocity profile. The interplay of various water masses caused bichannel sound velocity structure east of 20-25°W, and exerted a strong control on the deep sound channel (DSC) axis. Atop the Faeroe-Iceland Ridge, boluses of Norwegian Sea Overflow Water caused a 10.8 m/sec variation at the DSC axis over less than four days. Nearby, the intense Polar Front caused a 13.2 m/sec variation at the axis over 36 nm (gradient of about 0.4 m/sec/nm). West of Porcupine Bank, a migrating cell of Labrador Sea Water caused the disappearance of bichannel sound velocity structures in less than 10 days. Several possible effects of extreme sound velocity and meteorological variability on propagation loss and ambient noise are discussed.

**CONFIDENTIAL**  
(This page is unclassified)

**UNCLASSIFIED**

SECURITY CLASSIFICATION OF THIS PAGE (When Data Entered)



**DEPARTMENT OF THE NAVY**

OFFICE OF NAVAL RESEARCH  
875 NORTH RANDOLPH STREET  
SUITE 1425  
ARLINGTON VA 22203-1995

IN REPLY REFER TO:

5510/1  
Ser 321OA/011/06  
31 Jan 06

**MEMORANDUM FOR DISTRIBUTION LIST**

**Subj: DECLASSIFICATION OF LONG RANGE ACOUSTIC PROPAGATION PROJECT (LRAPP) DOCUMENTS**

**Ref: (a) SECNAVINST 5510.36**

**Encl: (1) List of DECLASSIFIED LRAPP Documents**

1. In accordance with reference (a), a declassification review has been conducted on a number of classified LRAPP documents.
2. The LRAPP documents listed in enclosure (1) have been downgraded to UNCLASSIFIED and have been approved for public release. These documents should be remarked as follows:

Classification changed to UNCLASSIFIED by authority of the Chief of Naval Operations (N772) letter N772A/6U875630, 20 January 2006.

DISTRIBUTION STATEMENT A: Approved for Public Release; Distribution is unlimited.

3. Questions may be directed to the undersigned on (703) 696-4619, DSN 426-4619.

A handwritten signature in black ink, appearing to read "B. F. Link", is positioned above the typed name.

BRIAN LINK  
By direction

Subj: DECLASSIFICATION OF LONG RANGE ACOUSTIC PROPAGATION PROJECT  
(LRAPP) DOCUMENTS

DISTRIBUTION LIST:

NAVOCEANO (Code N121LC – Jaime Ratliff)  
NRL Washington (Code 5596.3 – Mary Templeman)  
PEO LMW Det San Diego (PMS 181)  
DTIC-OCQ (Larry Downing)  
ARL, U of Texas  
Blue Sea Corporation (Dr. Roy Gaul)  
ONR 32B (CAPT Paul Stewart)  
ONR 321OA (Dr. Ellen Livingston)  
APL, U of Washington  
APL, Johns Hopkins University  
ARL, Penn State University  
MPL of Scripps Institution of Oceanography  
WHOI  
NAVSEA  
NAVAIR  
NUWC  
SAIC

# Declassified LRAPP Documents

Report Number	Personal Author	Title	Publication Source (Originator)	Pub. Date	Current Availability	Class.
ARLTR7952	Focke, K. C., et al.	CHURCH STROKE 2 CRUISE 5 PAR/ACODAC ENVIRONMENTAL ACOUSTIC MEASUREMENTS AND ANALYSIS (U)	University of Texas, Applied Research Laboratories	791029	ADC025102; NS; AU; ND	C
Unavailable	Van Wyckhouse, R. J.	SYNBAPS. VOLUME I. DATA BASE SOURCES AND DATA PREPARATION	Naval Ocean R&D Activity	791201	ADC025193	C
NORDATN63	Brunson, B. A., et al.	ENVIRONMENTAL EFFECTS ON LOW FREQUENCY TRANSMISSION LOSS IN THE GULF OF MEXICO (U)	Naval Ocean R&D Activity	800901	ADC029543; ND	C
NORDATN80C	Gereben, I. B.	ACOUSTIC SIGNAL CHARACTERISTICS MEASURED WITH THE LAMBDA III DURING CHURCH STROKE III (U)	Naval Ocean R&D Activity	800915	ADC023527; NS; AU; ND	C
NOSCTR664	Gordon, D. F.	ARRAY SIMULATION AT THE BEARING STAKE SITES	Naval Ocean Systems Center	810401	ADC025992; NS; AU; ND	C
NOSCTR703	Gordon, D. F.	NORMAL MODE ANALYSIS OF PROPAGATION LOSS AT THE BEARING STAKE SITES (U)	Naval Ocean Systems Center	810801	ADC026872; NS; AU; ND	C
NOSCTR680	Neubert, J. A.	COHERENCE VARIABILITY OF ARRAYS DURING BEARING STAKE (U)	Naval Ocean Systems Center	810801	ADC028075; NS; ND	C
HSECO735	Luehrmann, W. H.	SQUARE DEAL R/V SEISMIC EXPLORER FIELD OPERATIONS REPORT (U)	Seismic Engineering Co.	731121	AD0530744; NS; ND	C; U
MPL-C-42/76	Morris, G. B.	CHURCH ANCHOR EXPLOSIVE SOURCE (SUS) PROPAGATION MEASUREMENTS FROM R/P FLIP (U)	Marine Physical Laboratory	760701	ADC010072; AU; ND	C; U
ARLTR7637	Mitchell, S. K., et al.	SQUARE DEAL EXPLOSIVE SOURCE (SUS) PROPAGATION MEASUREMENTS. (U)	University of Texas, Applied Research Laboratories	760719	ADC014196; NS; AU; ND	C; U
NORDAR23	Fenner, D. F.	SOUND SPEED STRUCTURE OF THE NORTHEAST ATLANTIC OCEAN IN SUMMER 1973 DURING THE SOUND VELOCITY CONDITIONS DURING THE CHURCH ANCHOR EXERCISE (U)	Naval Ocean R&D Activity	800301	ADC029546; NS; ND	C; U
NOOTR230	Bucca, P. J.	PARKA II EXPERIMENT UTILIZING SEA SPIDER, ONR SCIENTIFIC PLAN 2-69 (U)	Naval Oceanographic Office	751201	NS; AU; ND	C; U
ONR SP 2-69; MC PLAN-01	Unavailable	PARKA I EXPERIMENT	Maury Center for Ocean Science	690626	ADB020846; ND	U
Unavailable	Unavailable	SEA SPIDER TRANSPONDER TRANSDUCER	Maury Center for Ocean Science	691101	AD0506209	U
USRD CR 3105	Unavailable	ATLANTIC TEST BED MEASUREMENT PROGRAM (U)	Naval Research Laboratory	700505	ND	U
MC PLAN 05; ONR Scientific Plan 1-71	Unavailable	PROJECT NEAT- A COLLABORATIVE LONG RANGE PROPAGATION EXPERIMENT IN THE NORTHEAST ATLANTIC, PART I (U)	Maury Center for Ocean Science	701020	ND	U
ACR-170 VOL.1	Hurdle, B. G.	THE PARKA I EXPERIMENT. APPENDICES- PACIFIC ACOUSTIC RESEARCH KANOEHE-ALASKA (U)	Naval Research Laboratory	701118	ND	U
MC-003-VOL-2	Unavailable		Maury Center for Ocean Science	710101	ND	U